FACULTY OF ELECTRICAL ENGINEERING
UNIVERSITY OF BANJA LUKA

ELECTRONICS

VOLUME 22, NUMBER 1, JUNE 2018

FACULTY OF ELECTRICAL ENGINEERING
UNIVERSITY OF BANJA LUKA

Address: Patre 5, 78000 Banja Luka, Bosnia and Herzegovina
Phone: +387 51 211824
Fax: +387 51 211408
Web: www.etf.unibl.org

E L E C T R O N I C S

Web: www.els-journal.etf.unibl.org
E-mail: els-journal@etf.unibl.org

Publisher:

Faculty of Electrical Engineering, University of Banja Luka, Bosnia and Herzegovina

Number of printed copies: 100

Editor's Column

Mladen Knezic

> In any moment of decision, the best thing you can do is the right thing, the next best thing is the wrong thing, and the worst thing you can do is nothing.
>
> *Theodore Roosevelt*

Editorial Letter
DOI: 10.7251/ELS1822001K

WHEN I was offered an opportunity to act as an Editor-in-Chief of the Electronics journal, I knew it would be a challenging task and, honestly, I hesitated to accept such a high-responsibility role in the early stage of my academic career. Obviously, my biggest concern was whether I would be able to quickly grasp the whole process and do the things in a right way. However, some decisions, no matter how hard they may look to us and how much effort they might require from us, should not be made so that our own comfort zone stays untouched. Therefore, I decided to make a step out of the comfort zone and *do the things*, in a right or wrong way, leaving time to witness whether this decision was the good or bad one in honest believe that doing nothing is certainly the worst thing I can do under the given circumstances.

This decision was strongly supported by the current team of the Electronics journal, our Managing Editors, Aleksandar Pajkanovic and Mitar Simic, who selflessly devoted a significant amount of their available time for maintaining and even improving the publication process of the journal. One of the major improvements is certainly the introduction of web-based manuscript submission tracking system. It did not only enable better control over the whole review process, but also helped us to better understand and adequately address the issues related to the delays in reaching the first decision regarding the paper status. In the following years, we will continue to improve the technical aspects of the journal aiming at increasing its scope and global recognition.

The current state of the journal, in terms of the publication metrics, is improved. Both CiteScore and SJR of the journal in 2017 has been increased to 0.68 and 0.12, respectively. The value of CiteScore has reached its maximum since the journal is covered by Scopus, whereas SJR experience the growing trend after a small drop in 2016. We can promise that we will do our best to maintain this progress and keep the positive trend of the journal.

The current issue contains papers that belong to a special issue devoted to advances in power electronics and Internet of Things. The special issue has been managed and edited by Akhtar Kalam, Anand R, and G. R. Kanagachidambaresan, whom I would like to thank for making a significant effort during the review and paper selection process.

I thank Aleksandar and Mitar for assisting me during the first months of my work as Editor-in-Chief of the journal. They really did a great job in terms of communication with the authors and setting up the online submission system. Finally, I would like to express my gratitude to the past Editor-in-Chief, Prof. Branko Dokic, for giving me the opportunity to become a part of this great project. I sincerely hope I will not fail the expectations.

Guest Editorial
Special Issue on Recent Advances in Power Electronics and Internet of Things

Akhtar Kalam, Anand R, and G. R. Kanagachidambaresan

Editorial Letter
DOI: 10.7251/ELS1822003K

POWER management and the Internet of Things (IoT) are essential parts of the modern cyber physical system. This field is in rapid change in terms of technology, devices and future trends. Nowadays, the IoT and power management are prevalent in daily life, from cell phone to household applications. An individual's quality of life mainly depends on the amount of electrical power consumption. The energy resource usage has been considered as the most important and ubiquitous issue of the present era. This special issue focuses on improving the aspects of renewable energy generation using power electronic devices and better computational algorithms. *Artificial Intelligence* (AI) based switching algorithms are commonly used in DC/DC converters and the *Maximum Power Point Tracking* (MPPT) algorithm found its way into the solar energy conversion systems. The AI also has the capability to understand and react to faults in hybrid systems. The capability of a remote monitoring and surveillance is achieved with tiny wireless embedded systems commonly referred to as *sensor nodes*. The mobility of such sensor nodes is enabled thorugh wireless connectivity protocols such as Bluetooth, ZigBee, WiFi, WiMAX, etc. This special issue includes the papers that bring enhancements to the lifetime of a network through the AI based intelligent algorithms. It mainly focuses on solutions to problems identified in smart grid, renewable energy supplies, power electronics and the IoT applications.

The paper "A Study of Inverter Drives and Its Ride Through Capabilities in Industrial Applications" provides a study view about the inverter drives and their capabilities in industrial applications. The industrial operating drives provide wide disturbances and, hence, a study on controlling and providing better results is discussed in this article.

The paper "An Enhanced Incremental Conductance Algorithm for Photovoltaic System" considers the incremental conductance of a photovoltaic cell. The renewable energy is the major upcoming research area. In that regard, the efficiency improvement of such systems is considered and an algorithm to address this issue is framed in this article.

In the paper "Drift Free Variable Step Size Perturb and Observe MPPT Algorithm for Photovoltaic Systems Under Rapidly Increasing Insolation", the Perturb and Observe based MPPT algorithm is investigated. The algorithm concentrates on obtaining maximum power from limited input power supply. It also investigates the operation during rapidly increasing insolation.

Energy efficient and load balancing routing is necessary in *Mobile Ad Hoc Networks* (MANETs). An intelligent hybrid routing protocol is designed in the paper "An Intelligent Hybrid Protocol for Effective Load Balancing and Energy Efficient Routing for MANETs". The algorithm provides better load balancing and serves to be energy efficient in nature.

Monitoring of patients with remote sensors using wireless networks has become more famous. The paper "Epilepsy Detecting and Halting Mechanism Using Wireless Sensor Networks" provides an efficient epilepsy detection mechanism for patients in a hospital. The application could provide better care to patients in developing countries.

DFIG (*Doubly Fed Induction Generator*) is mainly used in wind based power plants. The paper "Research Issues in DFIG Based Wind Energy System" investigates the issues persisting in DFIG wind energy systems in different approaches.

The wireless smart metering concepts have got its own role in modern smart power system. The increased usage of smart meters and, consequently, the interference created due to the dense nodes distribution are thoroughly studied in the paper "A Collaborative Framework for Avoiding Interference Between Zigbee and Wifi for Effective Smart Metering Applications."

We would like to thank Editor-in-Chief of the *Electronics* journal for providing us an opportunity to edit a special issue in this esteemed journal.

Akhtar Kalam has been at Victoria University since 1985 and was a former Deputy Dean of the Faculty of Health, Engineering and Science for 7 years. He has wide experience in educational institutions and industry across four continents.

He received his B.Sc. and B.Sc. Engineering from Calcutta University and Aligarh Muslim University, India in 1969 and 1973, respectively. He completed his M.S. and Ph.D. at the University of Oklahoma, USA and the University of Bath, UK in 1975 and 1981, respectively.

He has worked with Ingersoll Rand and other electrical manufacturers. He has held teaching appointments at the University of Technology, Baghdad, Iraq and Capricornia Institute of Advanced Education, Rockhampton, Queensland. He is regularly invited to deliver lectures, work on industrial projects and examine external thesis overseas.

His major areas of interests are power system analysis, communication, control, protection and co-generation systems. He has been actively engaged in the teaching of Energy Systems to undergraduates, postgraduates and providing professional courses to the industry both in Australia and overseas. He regularly offers professional development courses on Power System Protection, Renewable Energy and Cogeneration and Gas Turbine Operation to the Energy Supply Association of Australia (ESAA) and Australian Power Institute (API).

Anand R currently serves as an Assistant Professor (Senior Grade) at the Department of Electrical and Electronics Engineering at Amrita School of Engineering, Bengaluru. His area of interest in research includes Power Electronics, Electrical Drives, Renewable Energy Systems and Soft Computing.

He completed his B.E. (Electrical and Electronics Engineering) from Velalar College of Engineering and Technology, Erode, India. He then completed his M.E. (Power Electronics and Drives) from AMS Engineering College, Namakkal, India. He completed his Ph.D. in Electrical Engineering from Anna University, Chennai, India.

He has 11 years of teaching and research experience. He has published his research works in 5 national conferences, 10 international conferences and 10 international journals, out of which majority of the papers are indexed in Scopus, SCI and Web of Science. He has filed and published 3 patents. He has membership in professional bodies like IEEE and IAENG. He has guided many B. Tech. and M. Tech. student projects.

G. R. Kanagachidambaresan received his B.E. degree in Electrical and Electronics Engineering in 2010, and M.E. Pervasive Computing Technologies in 2012, both from Anna University, Chennai, India. He completed his Ph.D. in Information and Communication Engineering from Anna University. He is currently an Associate Professor in Department of Computer Science Engineering, "Veltech Rangarajan Dr. Sagunthala" R&D Institute of Science and Technology, Chennai, India. His main research interests include IoT and fault tolerant system design.

A Study of Inverter Drives and Its Ride Through Capabilities in Industrial Applications

Vishnu Murthy K, Ashok Kumar L and Dhayaneswaran Y

Abstract—**In modern industry, majority of the mechanical elements are driven by either induction motors or special motors like servo motors, synchronous motors, BLDC motors. In order to drive the motors and to vary the speed of the motors, electronics drives are required. Since the drives are powered with three phase AC, if the power grid has power quality issue, which directly reflects on to the power electronics drives. As per Indian grid standards, power quality is defined as harmonics, surge, sag, swell, which was formulated in the year of 2003 and further revision was done in 2010. But in the recent day's majority of the industries are constructed in same place (special economic zone), unpredicted industrial loads are increased and inserted in to existing running load, so eventually the power quality definition also changes and even sometimes connections are made as temporary for certain loads. Although these motors typically tolerate variations in utilization voltage, power quality professionals continue to spend a great deal of time answering questions about proper utilization voltage for a given motor. The voltage quality factors that create the most serious problems and confusion in the field include nominal utilization voltage that does not match the motor nameplate, proper voltage sag ride-through protection for the motor control circuitry, and phase-to-phase voltage imbalance. In review article, modern industry premises failure of components list and condition of power quality will be surveyed in various segments. Various failure of inverter drives namely, switching failure, commutation failure, common mode voltage problem, bearing current issues, harmonics etc., are discussed in details from various research article and presented in this review.**

Index Terms—**Power Quality, Industrial Drives, Inverter Drive Failures, VFD.**

Original Research Paper
DOI: 10.7251/ELS1822005V

Manuscript received 18 December 2017. Received in revised form 9 April 2018 and 15 May 2018. Accepted for publication 5 June 2018.

F. A. Vishnu Murthy K is Assistant Professor with the Department of Electrical & Electronics Engineering, Sri Krishna College of Technology, Coimbatore, India (phone: +91- 9486008600; e-mail: drkvm25@gmail.com).

S. B. Ashok Kumar L is Professor and Associate Head, Department of Electrical & Electronics Engineering, PSG College of Technology, Coimbatore, India (e-mail: askipsg@gmail.com).

T. C. Dhayaneswaran Y is R&D Team Head, LMW Machines Work Pt Ltd, Coimbatore, TamilNadu, India (e-mail: dhayaneswaran.y@gmail.com).

I. Introduction

With the invention of Tesla's AC machines, the Thomas Edison's counterfeit of the same become unpopular as it was in the post AC invention. Though it was the case, AC motor requires varying magnetic field or number of poles to be changed for their speed control in order to use for industrial applications. Even though AC machines gaining popularity, alteration of frequency remained undaunted task for particular speed control application in industrial process. Also, with respect to manufacturer side, the same has limited to produce the machine with two speed application design for consumers. By late 1980s, AC machine speed control drive technology has reached remarkable changes with cost effectiveness to compete with traditional DC technique. By taking over the AC speed control (Variable Frequency Drives VFD) the said action will be performed in more precisely and with high degree of accuracy. It can able to perform the control 0 r.p.m through full speed at rated torque of the machine, and if situations require super synchronous condition even at reduced torque. In these VFDs, the conventional CSI and VSI inverter get transformed into PWM VFDs due to its very good input PF, higher efficiencies, and lower cost. Although it is having numerous advantages over the drives, harmonics contents ejected from the same is of major concern with regard to VFD drives. Since the drive carried both rectifier and inverter, the two-step conversion leads to additional losses in the system.

Since the industrial processes are very diverse, the need of the same also differs accordingly as shown in Fig. 1. Every process demands required materials and energy to be outfitted to produce the desired task. Even this energy and materials may be processed by thermal, magnetic, electromagnetic, mechanical or even nuclear. During every process, the waste output in energy form is collected, the material process may also be controlled by VFDs. So, the process must be prepared to be well-defined shape and processed. Fig. 2 shows the potential possible level of sped control in industrial drives. In this figure, there are different components exists, energy, motor, transmission, and working machine. The energy, motor, and power together form the drive system and this systems performs the operation and send the energy to working machine for further load process. During these process, there will be one variable which needs to be confirmed so that the desired level of output may be obtained at the load as in Fig. 3. So, drive system, therefore, should ensure this variable must be given different methods of control to meet the desired output.

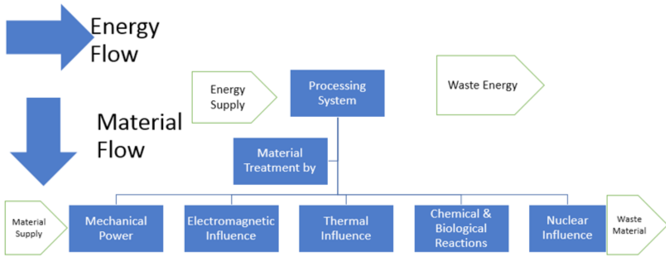

Fig. 1. Process involved in Industrial Drives.

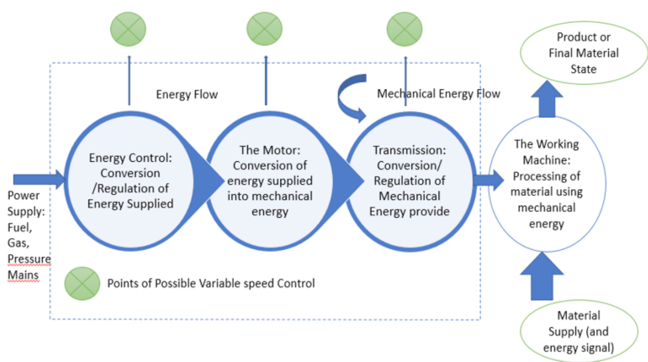

Fig. 2. Energy flow process of Industrial Drives.

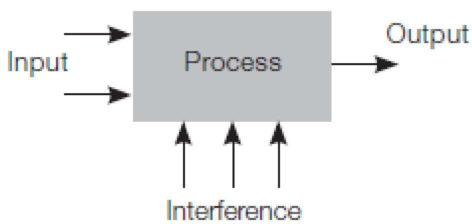

Fig. 3. Control of Variables in Industrial Drives.

II. Performance Analysis of Industrial Drives

Being AC drives machines, inverter drives has become heart of the industry process over the years, in particular with regard to precise control of machine speed is of utmost care. Almost all the machines use variable frequency drives as their preferred choice of the same, and reason behind the choice is it delivers high efficiency with great energy saving, higher degree of accuracy in controlling the speed, also to have inbuilt protection of the drives. Of all other drives that are currently used, the power electronic drives play a vital role in industrial market since it has ease of operation at desired level of control without any ride through capability by the operator. The manufacturer is trying to develop the drives with greater ride through capabilities and find herculean task in doing so. Also, the Integrated Motor Drive (IMD) takes a giant leap in current scenario and it have very high advantage over conventional drives like reduce mass, volume, lower cost, improved manufacturability, and much on ride through capability [1]. Manufacturers are trying to put their R&D in both spacing saving as well as integrated drive concept for effectual use of drives in productivity chain. Toyota prius adopted hybrid powertrain electronics control in their design aspect so that fuel efficiency can be even better over conventional types. Even now with greater advent of technology in electrical drives, there are key challenges still prevalent due to unhealthy power quality issues and they remain unattended. [2] The key challenges are power electrics cost reduction, to overcome thermal limit on drives, reliability.

III. Review of Electrical Drives and Its Recent Scenario

Sita Ram et al. [1] illustrated a in-depth review of slip power recovery drives, their performance analysis and control techniques employed for the same. Thomas M. Jahns et al. [2] gives the overall view of the past and present state of electrical drives available in the market and their state of art of technologies employed. Also, he draw attention to emphasize bottlenecks that has to be overcome and examine the the integrated motor drives feasibility and future scope of the same. This paper illustrated almost half century old drive system from past to future and their desideratum of electrical drives (IMD) in years to come to have better maneuverability and cross major technical problems that supress the future growth of the same. Piotr Sobanski et al. [3] deals about the single and multiple power switch failures when fed with drive system with shorter period of time. In this paper, field oriented control (FOC) type of drive technology employed test cases are considered and fault has been analysed. With the fault detection technique, the diagnostic methods been simplified and the versatility of the drives system. Masoud Farhadi et al. [4] discusses about the mean time failure of the inverter drives used in industry. The components failure rate, switching loses employed in different control strategies in wind up the reliability in loss through switches. It gives out the key feature of reliable modulation technique that should be employed in drive system. Based on this work, rating of switch, PF and capacitor may be the key fault parameter in inverter drives applications.

Chunyi Gu et al. [5] emphasizes the commutation failure in industrial drives based on stress due to voltage and current and capacitor parameter. Also the effects due to these faults directly related to capital cost and power loss is been discussed. by adopting suitable control strategy, the commutation failure can be greatly reduced and good performance curves can be observed. Md. Habibull et al. [6] discussed about the cause and effects of inverter drive system due to different switching frequency over the wide range. In this paper, because of finite element analysis of the same, the speed control regime steady state and transient state performance has been improved, switching frequency, torque characteristics has seen improved performance. THD, ripples in flux and torque, load side disturbances, also has significant reduction by using average switching frequency by having more number of voltage vectors in drive system. Aurelien Prudhom et al. [7] underlined the inverter drive motor failure due t bearing current issues over the years. The drives used for industrial purpose is being of VFDs, it lead to common mode voltage in turn results in currents discharged in bearing of the driven motor. The damages caused due to bearing currents has been analysed using time-frequency analysis and identified the potential problems and being monitored continuously to detect the same. Hadeed A. Sher et al. [8] coined the capacitor link failure in industrial drives because of open circuit condition and due to DC link failure or fault, the quality of the inverter is greatly affected. This literature underlines the ripple in frequency gives ride through capability during this fault scenarios. Mohamed Trabelsi et al. [9] literature gives the idea of open switch fault occurring in inverter and due to this effect, unfaulty switch gets changed because of freewheel diodes. By using of normalized values of inverter current from the output of the same, feedback has to be given and the potential problem may be eliminated. Gerard-Andre Capolino et al. [10] discussed elaborately about the diagnosis of recent advancements in electrical machines and its drive system under various fault condition. The failure identification in electrical machines due to bearing currents, short circuits, power interruption, inverter open circuit, power system fault etc are discussed for the mean cause of various issues in industrial drives. Based on the analysis, various novel techniques to deteriorating losses.

Seyed Kazem Hoseini et al. [11] discussed about the lowering of common mode voltage in AC drives and by doing so, the circulating currents in bearing of electrical machines reduced to greater extent there by saving the motor. It describes the various techniques been used and comparative model is prepared to sort out the best possible solution to the said problem in drives. By adopting the techniques, THD of the inverter drives also reduced to such ah extent and efficiency of the drives is improved to next level. P. P. Rajeevan et al. [12] also sketch out the possible solution for common mode voltage due to inverter drives having single voltage source. Using muti level inverter topology, the said problem can be eliminated in the drive applications. Sang Bin Lee et al. [13] emphasizes the VFD system with condition monitoring capability which determines the quality assessment in offline over the unsafe inverter components. The offline quality assessment includes the DC link, connections, cable insulation, and rotor and stator parameter. It also pitched the rank based overhauling of machines to be made in precise manner. Pawan Garg et al. [14] discussed about the fault phase of the VFDs and its tolerance capability. This paper gives out the common mode distortion ratio of the inverter drives and isolating the same will results in mitigating the foresaid problem in drive system. Romero de Souza Araujo et al. [15] provides the persisting failures on bearings in inverter drives induction motor system. The potential problems are analysed by theoretical aspects and then the practical issues are considered and comparative study been made sort out the possible solution in inverter drive system. Romero de Souza Araujo et al. [16] in his continued research article, the author gives the solution for the previously literature article for the same problem as stated above. Because of leakage currents through the motor bearings the problem of motor being temporarily halted or even permanently. The proposed topology in this paper suggest to use the high frequency drives to eliminate the circulating currents in motor bearing thereby protecting the same from prior deterioration. N. Bianchi et al. [17] literature possible strategies for inverter drive faults in synchronous motor systems. PMSM are used in wide range in industries and their reliability is very uncertain. To avoid the fault and to have the ride through capability, the defective inverter is being isolated electrically as a first prime task and made the inverter to obtain their necessary parameter from remaining phases till the faulty inverter is being restored. Tada Comedang et al. [18] discusses the typical PID controller for any feedback system having current control loop. Since the conventional current control operational amplifier is of not controllable electronically, the said can be controlled electronically by adding current mirror into the same using DT technology. From the authors claim, it is evident that, the use of proposed controller feedback mechanism will limit the maximum overshoot, quick rise time, fast settling time, and reduced steady state error in the system. So, by adopting these controller block in the feedback mechanism, the inverter drives can be made to precise the performance in well manner.

IV. Power Quality Issues and Its Potential Effects on Industrial Drives

From the literature above it is seen that, the major fault causing parameter for the industrial drives is due to unhealthy voltage, current, power factor, harmonics, transients. Because of all these issues either one form or combined together it leads to very adverse effects on drive system that in turn will have a slough drive motor performance. Based on the literature conclusion, to cross check the said problems, the power quality of electrical supply system is required for further analysis. So, in order to get the said power quality issues, the power quality analyzer is being used to capture the data of Indian grid supply quality and is figured out below. The power quality analyzer is kept for testing the same at one textile mills using industrial drives for their manufacturing process. Based on the data, Fig. 4 and Fig. 5 show the flicker on power instantaneous values and cumulative probability of the same. By inference this snapshot, it is understood that, the power instantaneous has experienced the flicker for significant duration of time period and the cumulative probability is between the ranges of 50% to 95%.

Fig 5. tells the line to line voltage disturbances over the 24 hours duration and it emphasizes, average RMS values of voltage per cycle. The orange shades indicate the value below 372.4 V and the average value is 412.4 V. Due to this fact, when the inverter drives runs continuously for stipulated duration of time, some sudden disturbances in any one parameter will lead to adverse effect on the inverter drives. Fig. 6 gives the cumulative probability of the line to line voltage. It shows only 50% the drives are getting rated voltage levels and remain 40%, the drives been supplied with voltage levels of 400 V. So, by inferring this data, the power quality is of major concern with regard to industrial drives.

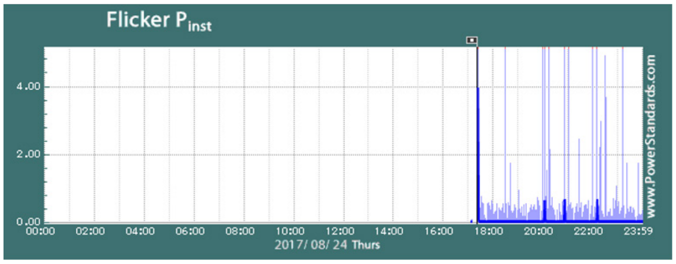

Fig. 4. Flicker on Industrial Drives.

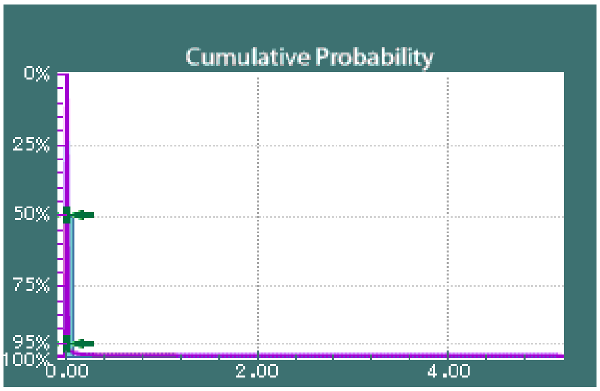

Fig. 5. Cumulative Flicker Probability of Industrial Drives.

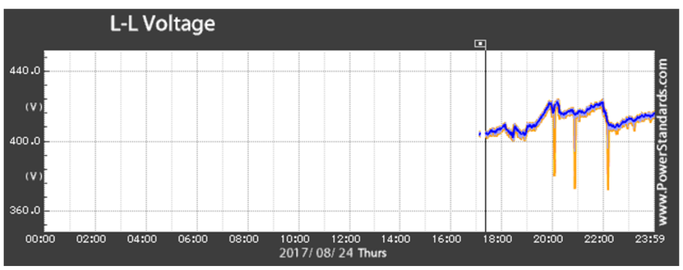

Fig. 6. Line - Line Voltage Disturbance Graph.

Apart from this, the THD analysis also been collected to and it reveals, THD levels of voltage are within the permissible limits, but with regard to current is concerned, the levels are exceeding the determined values. Fig. 7 and Fig. 8 shows the THD of voltage and current parameter. The zero-sequence unbalance voltage parameter reached maximum of 999.90% and minimum of 0.80% and average range of 6.60% and the graph of the same is showed in Fig. 9. With that of the current values the ranges from 7.10% to 82.90% and the average values cloaked at 44.90%. THD of current levels are given in Table I. IEC zero sequence Voltage level data are given in Table II to cross check the values recorded vs. graph snapshot obtained from the power quality analyzer. The line to line voltage cycles counting for the particular period of time is been given for further reference in Fig. 11.

V. Industrial Drive Topology and Its Mitigating Effects – A Review

With the advent of IMD, almost most of the day to day application becomes very cost effective and convenient to operate at better performance. Automotive industry, fan, water pump, industrial grade motor drives, servo drives, compressor etc. are having state of art in this technology and experiencing the convenient of advanced technology. With the rapid developments of the same as it is finding applications in small size device to electric vehicles and even in most advanced strategic importance equipment's, the future of this drive is more prominent and it is of further performance, cost as well as compactness be improved and packed in single module to meet the customer requirement with wireless technology. In near future, the wideband gap semiconductor by using silicon carbide or gallium nitride. This technology is in nourishing stage, and after the development of the same, it may give equal significance to the conventional IMDs. This is due to the better operating characteristics in temperature, efficiency, and switching frequencies. Due to the wide band gap, the leakage current may be low and it results in increased temperature limit. The on-state resistance of the SiC or GaN is 3000 times comparatively less than the silicon devices, gives better thermal conductivity. Also, at the reduction of its mass and volume, the wideband gap devices provide higher switching frequencies at faster rate will tend to shift the application areas to its favor's [2].

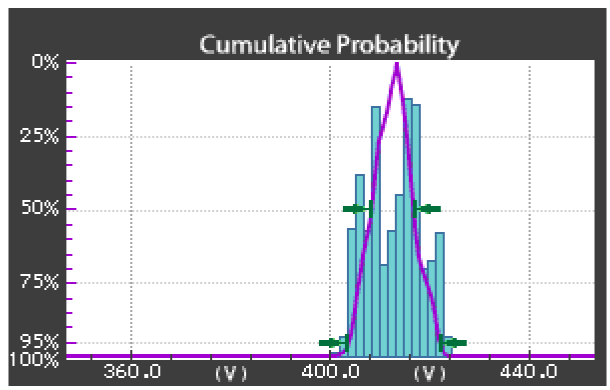

Fig. 7. Line - Line Voltage Disturbance Cumulative Graph.

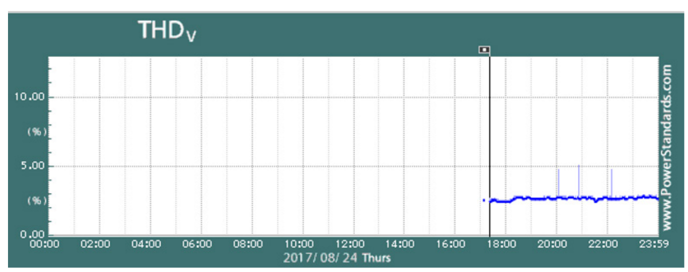

Fig. 7. THD level of Voltage.

TABLE I
THD Level – Current Parameter in %

TDD-A (%)	
Summary	
Median	3.25%
Mode	3.45%
Mean	3.20%
Range - min	-0.05%
Range - max	25.55%

TABLE II
IEC ZERO SEQUENCE VOLTAGE (IN %)

IEC Zero Sequence Voltage	Percent of Duration
Coverage	28.06%
Uncovered	71.94%
UnderRange	0.00%
OverRange	6.06%

The importance of THD and zero sequence voltage is inferred from the Table I and II. Since the said parameter is unbalanced current flow in the faulty circuit, it adds up the fuel into the system. From the table it has been observed that, the zero sequence voltage and THD limits are getting over ranged during the loading times.

Since the table depicts zero sequence voltage and current majority in the uncovered region, the power quality problems prevails much higher than the normal scenarios in the incoming supply of the drive system. Piotr Sobanski et al. [3] elaborates the operation of induction motor drive, the open circuit fault diagnosis is being considered for the analysis purpose. This fault detection cinches the power failures in very minimal time span. In this paper, the author discusses power converter faults related to power devices and its circuit damages, since this account majority of the fault types almost about 60%. So, to diagnosis this frequent occurring fault, the voltage source inverter needs to be tested and bring it to foreseen picture. To do the fault diagnosis model, the author concentrated on voltage space vectors topology is being implemented. By based on the rotation of space vector against the motor direction, the space vectors are keeps on changed by its numbers as shown in Fig. 12. So, by going for direct torque control schemes with SV PWM technique, the fault diagnosis transistor also gets reduced and to narrow down the faulted transistor rule base is being implemented.

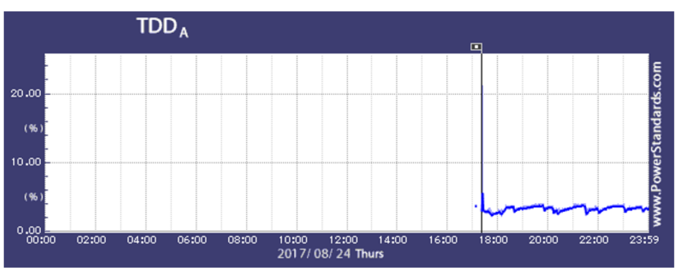

Fig. 8. THD Level of Current.

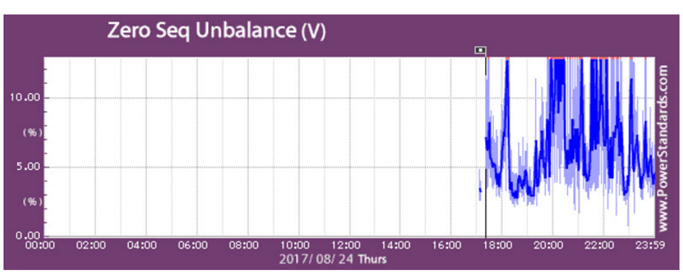

Fig. 9. Zero Sequence Unbalance Voltage.

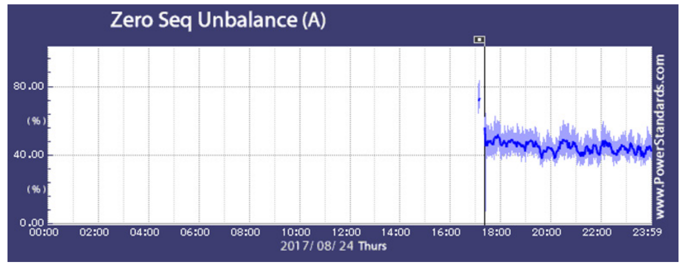

Fig. 10. Zero Sequence Unbalance Current.

In this paper [4], author described the general methodology for failure analysis and evaluation of the inverters configuration, their switching losses, rate of failure, temperature and their conduction losses and determined reliable control strategies. A three-phase three-level NPC inverter have been built for verifying the theoretical analysis and the experimental setup has been made and compared with simulation and results and author found out both simulation and experimental results are same. The author analysed the thermal image of the NPC topology converter configuration during their evaluation strategies. This article gives the comprehensive reliability analysis between the SPWM, THIPWM and SVPWM. NPC converter control strategy and their life time and based on the results obtained SVPWM becomes most feasible control strategy for Inverter drives configurations. This articles also confirms the power switches most assailable components and leads to loss distribution. Author [5] cites the commutation failure in inverter drives and the mitigating the same using thyristor based full bridge module (TFBM). The proposed topology by the author presents evolutional line commutated converter operates with thyristor in each arm in full bridge scheme and using TFBM the mitigating efforts is being performed in stage wise manner. Commutation support performance has been enhanced using this topology and to evaluate the susceptibility of CFs the immunity index is adopted which is given by

$$CFII = V^2/(\omega * L_{min} * P_{dc}) * 100.$$

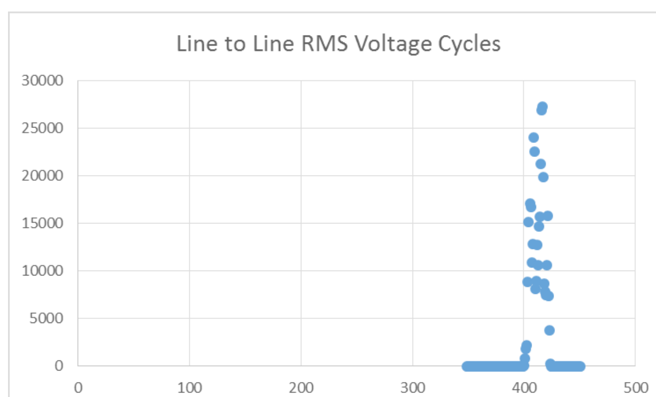

Fig. 11. Line line RMS Voltage Cycles.

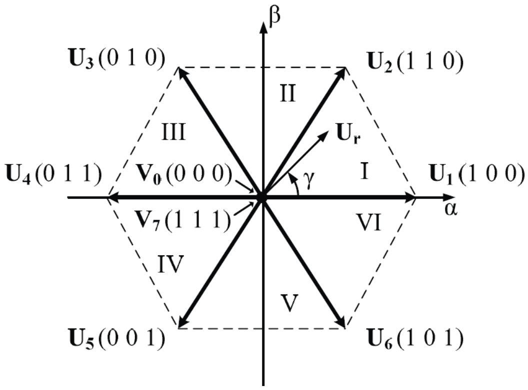

Fig. 12. Vector Control scheme of voltage space vectors to diagnosis of open circuit fault.

Md. Habibullah et al. [6], discusses the torque control of inverter drive suffering from high and variable switching frequencies in a wide range of inverter applications. To make stator currents with low harmonics, low torque ripple, the authors integrates the finite state predictive schemes of torque control in this article. Using this topology, the torque and flux ripples are reasonably good from the experimental results. Since the dead time incorporated in the inverter circuits, the higher order harmonics are relatively low compared to other methodology. Hadeed A. Sher et al. [8] discussed the experimental study of DC link capacitor failure in induction motor drive. Open circuit of the same has been discussed and analysis possible causes and effects for the said fault. From the analysis, it has been found out that, higher ripple frequencies will enable us to give better ride through capabilities to this particular fault. The three-phase induction machine model is created for the simulation and compared with single phase system, based on the simulation output the experimental setup was performed to validate the results obtained in simulation. The simulation block is presented in Fig. 13 which is used for ride through capabilities of DC link capacitor fault failure.

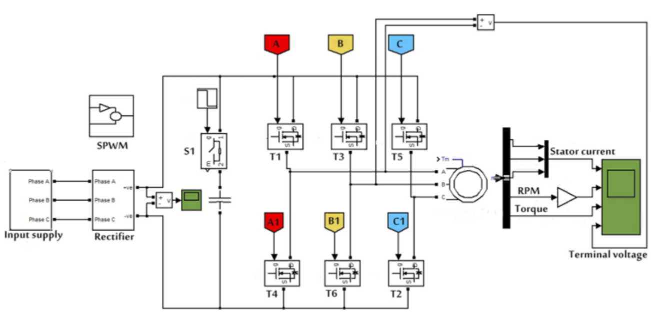

Fig. 13. Analysis of Inverter fed Induction Motor Drive under DC Link Capacitor Failure Scheme.

VI. Conclusion

Based on all the literature survey and testing of the industrial drives, it reveals the fact that the major prime factors for inverter drive failure or fault is due to the poor power quality issues from the supply side or intermittent side from grid supply to load through industry process as said early in introduction. Since the grid is having their own set of standards and rules to address these power quality issues, and even after taking lots of efforts to control the same to permissible levels, a sudden abnormality arises either in supply side or load side to inject disturbance in equipment's used for the process. Because of these sudden disturbances for very short time duration turned to be vulnerable to load as well as driving system associated with the load. Due to these vulnerabilities, the load parameter may get altered and accordingly the feedback systems get deviated from the prescribed limits there by affecting the inverter drives often. So, the possible solution for the same may be use of IOT integrated with the supply system as well as end customer equipment, so that any vulnerability arises, the necessary steps to ease out from the system will be carried out. From this literature survey article, the new and novel techniques have to be developed for making the industrial drives to ride through these vulnerabilities and having higher degree of operation performance with health monitoring system and predictive data maintenance systems (PDM). Because of the PDM, the manufacturer as well as customer can able to analysis the performance of a machine then and there, thereby the failure and health of the particular drive system is monitored regularly.

References

[1] S. Ram, O.P. Rahi, V. Sharma, "A Comprehensive Literature Review On Slip Power Recovery Drives," *Renewable And Sustainable Energy Reviews* 73 (2017) 922–934.

[2] T. M. Jahns And H. Dai "The Past, Present, And Future Of Power Electronics Integration Technology In Motor Drives," *CPSS Transactions On Power Electronics And Applications*, Vol. 2, No. 3, September 2017

[3] P. Sobański, T. Orłowska-Kowalska, "Detection Of Single And Multiple Igbts Open-Circuit Faults In A Field-Oriented Controlled Induction Motor Drive," *Archives Of Electrical Engineering* VOL. 66(1), Pp. 89-104 (2017)

[4] M. Farhadi, M. Abapour, M. Sabahi, "Failure Analysis And Reliability Evaluation Of Modulation Techniques For Neutral Point Clamped Inverters—A Usage Model Approach," *Engineering Failure Analysis*, EFA-02933, 28-06-2016

[5] C. Guo, C. Li, C. Zhao, X. Ni, K. Zha, W. Xu, "An Evolutional Line Commutated Converter Integrated With Thyristor Based Full-Bridge Module To Mitigate The Commutation Failure," *IEEE Transactions On Power Electronics*, 2016.

[6] M. Habibullah, D. Dah-Chuan Lu, D. Xiao, and M. F. Rahman, "Finite-State Predictive Torque Control Of Induction Motor Supplied From A Three-Level NPC Voltage Source Inverter," *IEEE Transactions On Power Electronics*, 2016

[7] A. Prudhom, J. Antonino-Daviu, H. Razik, V. Climente-Alarcon, "Time-Frequency Vibration Analysis For The Detection Of Motor Damages Caused By Bearing Currents," *Mechanical Systems And Signal Processing*, 24-05-2015

[8] H. A. Sher, K. E. Addoweesh, Z. Khalid, Y. Khan, "Theoretical And Experimental Analysis Of Inverter Fed Induction Motor System Under DC Link Capacitor Failure," *Journal Of King Saud University – Engineering Sciences* (2015)

[9] Mohamedtrabelsi, Mohamedboussak, Mohamedbenbouzid, "Multiple, Criteria For High Performance Real-Time Diagnostic Of Single And Multiple Open-Switch Faults In Ac-Motor Drives: Application To IGBT-Based Voltage Source Inverter," *Electric Power Systems Research* 144 (2017) 136–149.

[10] G. A. Capolino, F. Filippetti, "Introduction To The Special Section On Advances In Diagnosis For Electrical Machines," *Power Electronics,*

And Drives—Part I, IEEE Transactions On Industrial Electronics, Vol. 60, No. 8, August 2013

[11] S. K. Hoseini, J. Adabi, A. Sheikholeslami, "Predictive Modulation Schemes To Reduce Common-Mode Voltage In Three-Phase Inverters-Fed AC Drive Systems," *IET Power Electronics,* 26th October 2013.

[12] P. P. Rajeevan And K. Gopakumar, "A Hybrid Five-Level Inverter With Common-Mode Voltage Elimination Having Single Voltage Source For IM Drive Applications," *IEEE Transactions On Industry Applications*, Vol. 48, No. 6, November/December 2012

[13] S. B. Lee, Ji-Yoon, Jinkyuyang, J. Hong, "A New Strategy For Condition Monitoring Of Adjustable Speed Induction Machine Drive Systems," *IEEE Transactions On Power Electronics*, Vol. 26, No. 2, February 2011.

[14] P. Garg, S. Essakiappan, H. S. Krishnamoorthy, P. Enjeti, "A Fault Tolerant 3-Phase Adjustable Speed Drive Topology With Active Common Mode Voltage Suppression," *IEEE Transactions On Power Electronics*, 2014.

[15] R. De S. Araújo, H. De Paula, "Premature Wear And Recurring Bearing Failures In An Inverter-Driven Induction Motor—Part I: Investigation Of The Problem," *IEEE Transactions On Industry Applications,* Vol. 51, No. 6, November/December 2015.

[16] R. De S. Araújo, H. De Paula, "Premature Wear And Recurring Bearing Failures In An Inverter-Driven Induction Motor—Part II : The Proposed Solution," *IEEE Transactions On Industry Applications*, Vol. 51, No. 1, January/February 2015.

[17] N. Bianchi, S. Bolognani M. Zigliotto, "Innovative Remedial Strategies For Inverter Faults In IPM Synchronous Motor Drives," *IEEE Transactions On Energy Conversion,* Vol. 18, No. 2, June 2003.

[18] T. Comedang, P. Intani, "CFOA-Based Fractional Order PIλDδ Controller," *Electronics Journal,* Vol.21, No.1, June 2017.

[19] *ABB Drives,* Technical Guide No. 4 Guide To Variable Speed Drives.

An Enhanced Incremental Conductance Algorithm for Photovoltaic System

K. Ramesh, R. Giri Ganesh, Sri Lakshmi Vineela Reddy, K. Mahalakshmi and S. Suganya

***Abstract*—The energy obtained from the photovoltaic array is dependent on the available solar insolation, the panel tilt angle and the power point tracking algorithm of the system. Some of the Conventional MPPT methods are developed by considering uniform solar irradiance. During partial shading conditions, solar panel may produce multiple Local Maximum Power Points (LMPPs) in its power voltage characteristic curve. A new algorithm has been developed in this paper by using sequential sampling embedded with existing incremental conductance procedure in order to predict the Global Maximum Power Point (GMPP). The tracking capability of proposed algorithm is verified with simulation works carried out in MATLAB/SIMULINK. The results of proposed algorithm are likened with the results classical Perturb and Observe (P&O) and Incremental Conductance algorithms.**

***Index Terms* — Global Peak (GP), Photovoltaic (PV), Maximum Power Point Tracking (MPPT), Incremental Conductance, Single Ended Primary Inductor Converter (SPEIC).**

Original Research Paper
DOI: 10.7251/ELS1822012R

I. Introduction

Power demand is increasing nowadays because of increase in population and to satisfy their needs. Along with conventional energy sources, other energy sources such as the solar energy, bio-mass energy, wind energy etc. contribute to meet out the power demand conditions. These additional energy sources have gained huge interest due to environmental issues and looking for low-cost energy. [1-3] Solar energy is the united with the power and heat of the sun's rays. Solar energy is clean and available in most of the places. Photovoltaic energy conversion is the simple process and a smart method of converting the incident sun irradiance into an electrical energy [23] with the help of solar cells. As like other energy generation units, it won't produce any noise, pollution and it is robust and reliable. These PV panels consist of semiconductor materials and it producing electrical energy when it is subjected to sunlight and its output depends on forbidden energy gap level of semiconductor material used in PV panel. PV cell's output efficiency characteristics depends on solar intensity, temperature and resistance [17]. To achieve the maximum output efficiency condition, a control strategy known as maximum power point tracking (MPPT) is needed to identify the PV operating point that allows extraction of maximum power from the array.

In literature, many MPPT methods have been reported, including current mode model, [5] voltage operating mode, [25] Peak converter with Predictive Digital Current Control, [27] Hill Climbing, [2], [7] Incremental Conductance, [4], [20], [23] Perturb and Observe, [3] Particle Swarm Optimization, [13] and Neural Network [11]. These algorithms give better result when the PV modules are subjected to uniform solar irradiation. This process gives only one MPP in its P-V characteristic curve with respect to given temperature and insolation. Because of the conflict in tracking the Global MPP (GMPP) under multiple local maxima with partial shading condition, the above mentioned conventional algorithms results in PV systems with lower conversion efficiency.

Several solutions have been proposed, to verify the effectiveness of MPPT algorithms even under partial shading condition, with some modifications made on conventional algorithms. A modified Perturb & Observe (P&O) algorithm reported by Abdelsalamet.al. [26] does not need any predefined system dependent constants and it confirms the adaptive tracking and zero steady state oscillations about the MPP. In this method, adaptive perturb is generated with the help of PI control action. In the modified incremental conductance algorithm [4], a simple linear equation that tracks the GMPP dictates the terminal voltage of the panel according to the MPP voltage obtained using incremental and instantaneous conductance of the PV module. This method requires additional circuits at the output of the converter.

Some methodologies [8]-[10], [14] have been presented to improve the efficiency of the solar PV modules even under partial shading condition and are results in significant reduction in overall cost. In the method proposed by Carlos Olalla [8], the converter is designed to process only mismatch fraction of power

Manuscript received 18 December 2017. Received in revised form 17 April 2018 and 20 May 2018. Accepted for publication 5 June 2018.

K. Ramesh is with the Faculty of Electrical Engineering, Department of Electrical and Electronics Engineering, Kuppam Engineering College, Kuppam, Andhra Pradesh, India. phone: +91-9652074806; e-mail: drramkomar@gmail.com).

Giri Ganesh is with School of Electrical and Electronics Engineering, SASTRA University, Thanjavur, Tamilnadu, India.

Sri Lakshmi Vineela Reddy is with Department of Electrical and Electronics Engineering, Madanapalle Institute of Technology and Science, Madanapalle, Andhra Pradesh, India.

Sri Lakshmi Vineela Reddy is with Department of Electrical and Electronics Engineering, Madanapalle Institute of Technology and Science, Madanapalle, Andhra Pradesh, India.

K. Mahalakshmi is with Department of Electronics and Communication Engineering, Kuppam Engineering College, Kuppam, Andhra Pradesh, India

S. Suganya is with Department of Electrical and Electronics Engineering, Paavai Engineering College, Namakkal, Tamilnadu, India

and is capable of effectively tracking the MPP. This method has a limitation is of producing maximum efficiency when the mismatch is lesser than 25% only. For rapidly fluctuating shading condition, Lijun Gao, [16] has proposed a system which consists of PV cells connected in parallel with simple wide bandwidth MPP tracker but it leads to system complexity.

In literature, [25] the fractional open circuit method dealing the effect of nonlinear relationship between maximum peak voltage (V_{mpp}) and open circuit voltage(V_{oc}) of the PV array under change in temperature and irradiance has been reported. But this increased the implementation complexity and experiences additional power loss. The fractional short-circuit current [20] is a result of the linear relation between I_{mpp} and I_{sc}. The power converter used in this method is employed with an additional switch and so that the cost and components involved in the operation are increases.

The partial shading problem [6], [18] in solar PV module results in hot spot and it sometimes leads to permanent damage of the module. In order to predict the hot spot issues and to provide the remedial action, panel temperature is measured with the help of infrared sensors [21], [24] with regular MPP tracking procedures. The differential power processing architecture [12] in the literature helps the solar PV module to overcome the unmatched MPPs due to partial shading and other conditions. Even above said methods are resulted in good conversion efficiency, these leads to critical analysis in finding GMPP.

In solar energy conversion process using DC-DC converters, sometimes the effects of parasitic elements [25] as well as energy conversion efficiency may be suppressed during the conversion process. To overcome these issues, the additional parasitic elements were added along with the DC-DC converter. It improves the PV generation by increasing the output voltage and is achieved by simple MPPT controller with two sensors in feedback.

A fuzzy logic based MPPT [19], [22] methods available in the literature are well suited for varying climatical conditions even system mathematical model is not accurate. It can handle imprecise inputs non-linearity operations but it needs best efforts in constructing the fuzzification, rule base table, look up and defuzzification processes. A Neural Network [11], [15] will be trained as unique for the PV array so that it can be utilized for PV arrays having different characteristics. Particle Swarm Optimization technique [13] which uses the velocity equation for the exploration process for accurate GMPP but it highly depends on few parameters in the governing equation.

TABLE I
Variation of Voltage And Current of the PV Module During the Variation of Solar Irradiation

Solar irradiation	Variation of voltage (dV)	Variation of current (dI)
Increase	Increase	
Decrease	Decrease	

All the methods which are mentioned above have difficulties in GMPP tracking and Have complex additional circuits. In this paper, a simple method for tracking GMPP even under the presence of partial shading conditions in the system is proposed. This is done by the sequential sampling of duty cycle with a time scale of 0.1 followed by general Incremental Conductance algorithm applied to control a ZETA converter. This system is presented in Fig. 1 and Fig. 2.

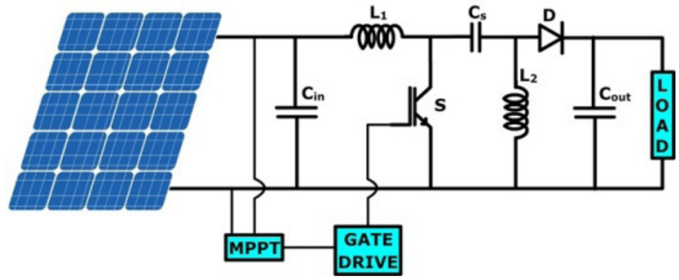

Fig. 1. Proposed PV System with MPPT Controller.

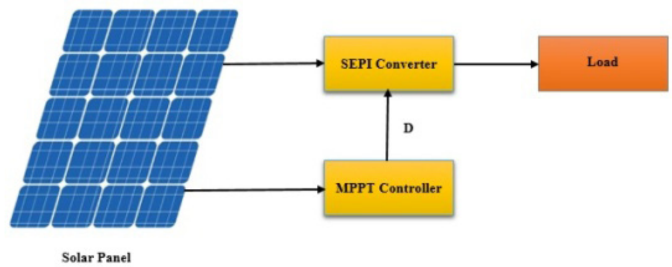

Fig. 2. General block diagram of an MPPT system.

MPPT algorithms achieve maximum power extraction from the panel by adjusting the impedance connected to the panel terminals. The DC-DC converter, which forms the connection between the panel and the load, varies its input impedance as duty cycle varies. In this paper, to track the maximum power from the panel, the duty cycle of the ZETA converter is adjusted. A PV cell is the fundamental building block of a PV panel; a PV panel is a combination of several PV cells in series and parallel connections. The electrical equivalent of solar PV cell is modeled as current source with an anti-parallel diode, a shunt resistance and a series resistance. The V-I characteristics of the solar panel are shown in Fig. 4. The maximum power point is the point where the VI product is maximum for the given V-I curve. In this method, the proposed MPPT algorithm adjusts the duty cycle of the ZETA converter to excerpt the maximum power from the PV panel.

II. Single Ended Primary Inductor Converter (SEPIC / ZETA Converter)

The ZETA converter is like a buck-boost converter, but it has non-inverted output voltage. It employs a series capacitor to pair the energy from the input to the output. The conventional ZETA converter is presented in Fig. 3. It is operated under fixed frequency and exhibits high transient performance.

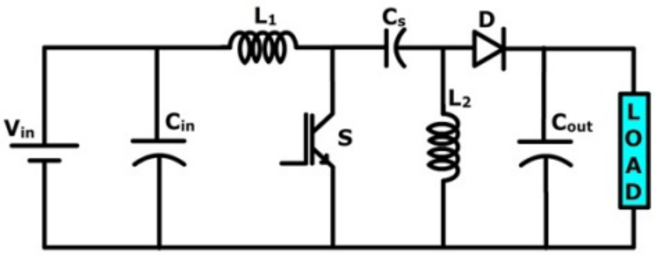

Fig. 3. Circuit diagram of SEPI converter.

A. *Operation*

The ZETA converter is intended to operate in continuous conduction mode. The converter topology consists of inductors L_1 and L_2, capacitors C_S and C_{out} and diode D. An ideal case is assumed for diodes, switches and passive components. Since this topology has only one switch, there are two modes of operation.

Mode 1: Switch S is ON (as shown in Fig. 4)

Inductor L_1 charges to V_{in} through switch S. The voltage across capacitor C_S discharges through S into inductor L_2. Diode D is OFF and capacitor C_{out} supplies the load current.

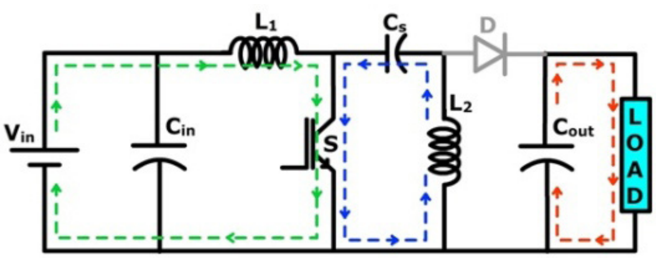

Fig. 4. With S_1 closed current increases through L_1 and C_1 discharges increasing current in L_2.

Mode 2: Switch S is OFF (as shown in Fig. 5)

Inductors L_1 and L_2 reverse polarity. Diode D turns on. Both capacitors C_S and C_{out} are charging in this mode. The input voltage and the voltage across L_1 charges C_S and C_{out} and supplies load current. The voltage across L_2 charges C_{out} and supplies load current through D.

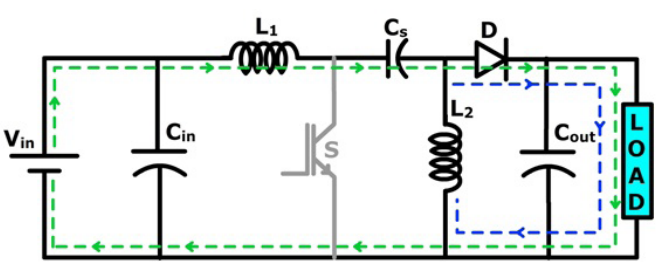

Fig. 5. With S_1 open current through L_1 and current through L_2 produce current through the load.

At Steady-state,

$$V_{in} = V_{L_1} + V_{C_S} + V_{L_2} \tag{1}$$

Because V_{in} and the average voltage of V_{C_S} are equal and $V_{L_1} = -V_{L_2}$

The average currents can be summed as follows:

$$I_D = I_{L_1} + I_{L_2} \tag{2}$$

The Zeta Converter is designed according to Equations (3)-(7) given below,

The Converter output voltage is obtained as,

$$V_{dc} = D.\frac{V_{in}}{(1-D)} \tag{3}$$

Boost inductor L_1 value is,

$$L_1 = \frac{D.\ V_{in}}{f_s\ .\ (\Delta I_{L_1})} \tag{4}$$

Capacitor C_S value is determined by,

$$C_S = \frac{D}{R\ .\ f_s\ .\ \frac{\Delta V_{CS}}{V_0}} \tag{5}$$

Inductor L_2 value is,

$$L_2 = \frac{(1-D)V_{dc}}{f_s\ (\Delta I_{L2})} \tag{6}$$

Output filter capacitor C_{out} value is,

$$C_{out} = \frac{I_{av}}{2\ \omega\ \Delta V_{dc}} \tag{7}$$

III. Characteristics of PV Module Under Partial Shading Condition

PV modules can be connected in different sequences16 such as series, parallel or combination of both depends on the designer's need. Partial shading is an unavoidable in some plant condition and is location dependent. In construction, the PV module consists of strings in which number modules are connected in series. If any of these modules are subjected to partial shading condition, then reverse bias cell operation will be happened and it results in hot spot conditions. If it exceeds beyond some limit condition, then it leads to potential breakdown18 of the shaded cell as shown in Fig. 6(b). This problem can be avoided by connecting bypass diode along with module and this take over the string current in case of partial shading conditions as shown in Fig. 6(a). Solar electrical panel's power is dropped out around by 50% because of partial shading conditions. In order to avoid this, some changes are made in the proposed algorithm to track the accurate GMPP, i.e. in a given time interval, the duty cycle moves across the locus traced by the waveform without any climbing in order to take the samples of the entire waveform, to find the GMPP. While predicting the GMPP, the duty cycle is considered over the waveform to obtain the samples of entire waveform by avoiding the climbing.

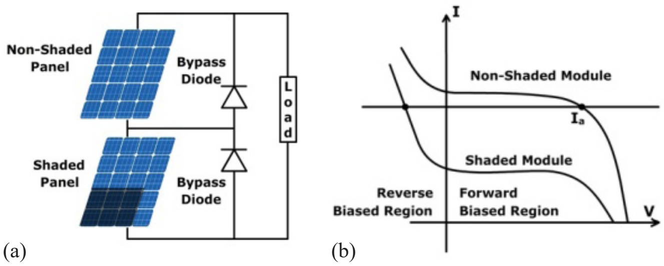

Fig. 6. (a) PV array under partial shading conditions (b) I-V curves of PV module.

IV. The Extended Incremental Conductance Algorithm

In the literature cited, the P&O Algorithm and the Modified Incremental Conductance Algorithm utilize the hill-climbing concept, which tracks the operating point of the PV array. The P&O algorithm is a simple method in which, while considering perturbation in the same alignment, the power value has been increased. In case of decrement in power value, forthcoming perturbation will be considered in opposite direction. But this algorithm fails to track the accurate GMPP. The Modified Incremental Conductance is an intelligent algorithm. The shifting of Duty cycle 'D' in the Modified Incremental Conductance allows the system even works on partial shading conditions. But it is slow because it has to climb all the hills at once and hence lacks accuracy. Here, the proposed algorithm is needed not to climb all the hills; instead the sequential sampling of duty cycle has been applied to reduce the tracking time. Sampling will be taken at specified interval of the duty cycle such as at 10%, 20% …100%. This helps to understand the waveform within 10 samples. By this data, it can get the maximum power near the Global Maximum Power Point (GMPP) and for accuracy; an Incremental Conductance is applied from that point. The quick and accurate locking of GMPP is shown in Fig. 7.

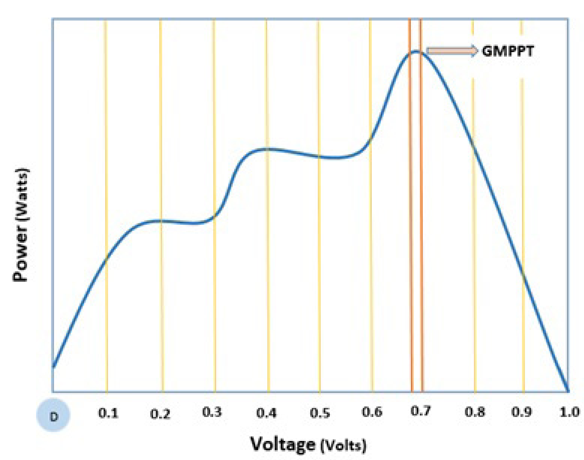

Fig. 7. Power curve by taking 10 rough samples.

A. *Algorithm*

The algorithm has two sections 1.Sequential sampling of the duty cycle for best D and 2.Incremental Conductance. In the flow chart shown in Fig. 8, the power values (P_{mpp1}, P_{mpp2}), the temporary duty cycle value (Temp_D), voltage and current are set to zero, the extension variable (Extent) is set to 1.

The two variables required in this algorithm are Temp D and extension variable.

1. The Temp D is a type of variable which is supposed to hold the temporary duty cycle, until it is finalized where the power is maximized by the sequential sampling of the duty cycle.
2. The extension variable is a type of Boolean variable consists of either 0 or 1 and helps to execute the extension, i.e. if extent>0 it is true then it starts executing the Incremental Conductance algorithm.

The Duty cycle increases sequentially with a time delay of 0.1, then the power is read and stored in a temporary variable Pmpp1. This is compared with previous power P_{mpp2}. If Pmpp1 is greater than the P_{mpp2}, then the value of P_{mpp1} is transferred to P_{mpp2} else the increment at Temp D happens again. After increment of Temp D, again, it read the power and stored it in a P_{mpp1} and the processes as same again, i.e. Pmpp1 is compared with P_{mpp2} for the best power. This process continues so on until the P_{mpp2} holds the maximum power. When the P_{mpp2} holds the maximum power, then the Temp D variable holds the temporary duty cycle which delivers maximum power. This D will be the starting point of the Incremental conductance at the hill of Global maximum power point (GMPP) for tracking accurate GMPP. The algorithm is detailed below.

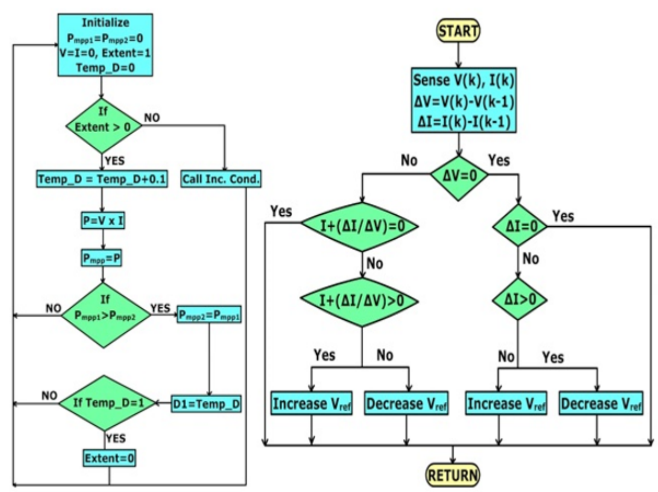

Fig. 8. Flow chart of the proposed algorithm.

Algorithm: An Enhanced Incremental Conductance Algorithm

Label 1: Initialize P_{mpp1}= P_{mpp2} =0, V = I = 0, Extent = 1,
Temp_D = 0
if Extent > 0
Temp_D = Temp_D + 0.1;
P= V *I;
P_{mmp1} = P;
If P_{mpp1}> P_{mmp2}
P_{mpp2} = P_{mpp1};
D_1 = Temp_D;
If Temp_D1 = 1
Extend = 0

else
go to Label 1
else
go to Label 1
else
Call the Incremental Conductance algorithm*
go to Label 1

* - Conventional Incremental Conductance Algorithm 23

V. Duty Cycle Computation of DC-DC Converter

Varying the duty cycle will help the PV system to maintain the MPP which in turn varies the output voltage. The variation in duty cycle changes the input impedance of the converter which directly controls the amount of power drawn from the panel. This power drawn is maintained around MPP. In the proposed system, the duty cycle is controlled in two stages. Prediction of near maximum power point with the help of sequential sampling will be happened first followed by applying the incremental conductance algorithm to track the GMPP as a sequence process.

In the first part of the proposed technique, a sequential sampling of power by incrementing the duty cycle with the specific time delay is considered. In simulation side, the sampling process is considered with sampling interval with 0.1 -time delay. In sequence, the duty cycle varied from 0.1, 0.2, 0.3, … 0.9 and 1. Within this variation of the duty cycle, the voltage reaches from zero to V_{max}. This executes the entire power wave form. The every sample that has taken at every duty cycle increment will help to determine the nearest point of MPP. By comparing the power with previous power when it is sampled will give maximum power in between 0 and the maximum duty cycle. The selection of duty cycle depends on the position where the maximum power is possible. To implement the next technique, the duty cycle at maximum MPP which is nearby is selected from the first technique. In next technique, the Incremental Conductance is going to be applied. In this, If dv/di< 0, then the operating point is after the MPP. If dv/di> 0, then the operating point is before the MPP. If dv/di = 0, then the GMPP is available.

$$\text{Duty Cycle (D)} = \frac{T}{P} \times 100\% \tag{8}$$

Where,

T= ON time of the switch

P= Total period of the signal

The voltage gain of the SEPIC is given by,

$$V_0 = \frac{D}{(1-D)} \times V_{dc} \tag{9}$$

Where,
D = Converter duty cycle ratio
V_o= Output voltage of the converter
V_{dc}= PV panel output voltage

VI. Simulation Results

The proposed algorithm is simulated under the ambient temperature of 25℃ with four different solar irradiation levels as input for partial shading conditions. The proposed system consists of a Model of PV array, Single Ended Primary Inductor Converter (SEPIC) and the MPPT controller are integrated in required sequence in MATLAB/Simulink model. PV module specifications considered in the simulation work is detailed in Table II. The solar panel supplies the load through an SEPI Converter whose values of the components as C_{in} and C_{out} = 3900 µF, L_1 and L_2 =125 µH, Cs= 1000 µF and the load resistance is of 10 -ohm value. For the semiconductor switch operation, the switching frequency is considered as 20 kHz. The sequential sampling of the duty cycle is carried out with a time delay of 0.1, 0.2,….., 0.9 and 1 in the simulation work. Fig. 9 (a) shows the power voltage characteristic curve and Fig. 9 (b) shows the simulation results for PV array under different solar irradiation values such as 1.0 kW/m^2, 0.6 kW/m^2, 0.4 kW/m^2and 0.3 kW/m^2.

TABLE II
Parameters of PV modules at Ambient Temperature of 25°C and Insolation=1000 w/m²

Maximum Power (Pmax)	≈ 64 W
Voltage at MPP (Vmpp)	31.8 V
Current at MPP (Impp)	2.0 A
Open Circuit Voltage (Voc)	39.75 V
Short Circuit current (Isc)	3.69 A

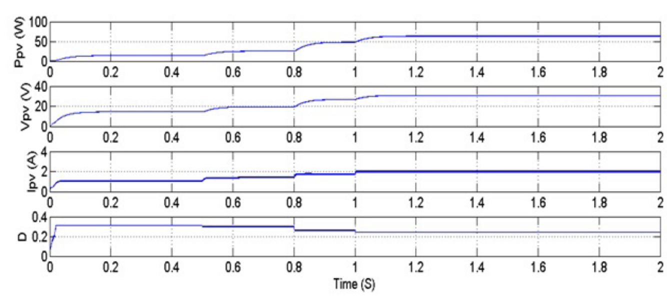

(a)

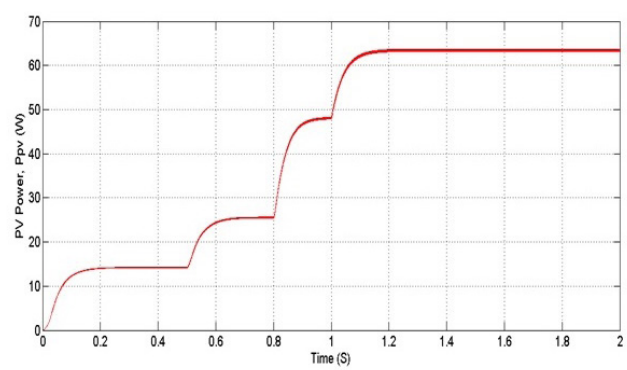

(b)

Fig. 9. (a) and (b) Simulation results for the PV system under partial shading conditions where the solar irridation values are 1.0 kW/m^2, 0.6 kW/m^2, 0.4 kW/m^2 and 0.3 kW/m^2.

The SEPI Converter usually varies the output voltage to vary the power and to retain the operating point at Maximum Power Point as known as GMPPT. This converter is placed between the solar panel and the load and it is controlled by the MPPT controller, which is replicated in the coding of Extended Incremental Conductance algorithm. Here the duty cycle is sampled by taking roughly 10 samples and find the best D. This D is considered as concluding duty cycle value. The P_2 is the GMPP where is located nearly at value $0.8{*}V_{oc}$. The performance of the proposed method is confirmed by likening the results with Perturb and Observe and Modified Incremental Conductance algorithm to ensure its effectiveness and is shown in Fig. 10.

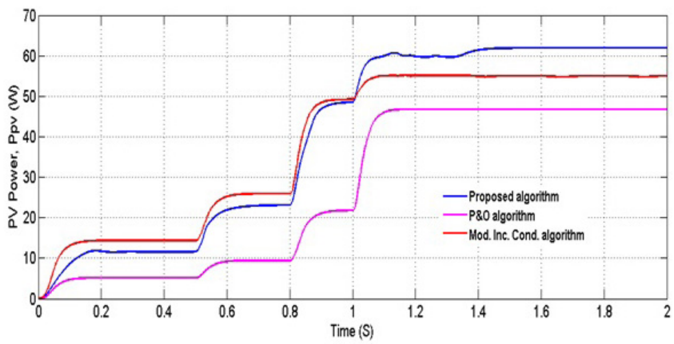

Fig. 10. Simulation results of a comparison of proposed algorithm with the modified Incremental Conductance algorithm and P&O algorithm.

The conventional algorithms show comparatively fewer results in the case of power when compared to proposed algorithm. The P&O algorithm fails to track the accurate GMPP under partial shading conditions. Even the modified Incremental Conductance algorithm is capable of tracking the maximum power point in presence of partial shading conditions, it may produces a delay which creates an inefficiency because of its large execution cycle. The voltage level in P&O, modified Incremental Conductance and proposed algorithms are detailed in Figs. (11)-(13).

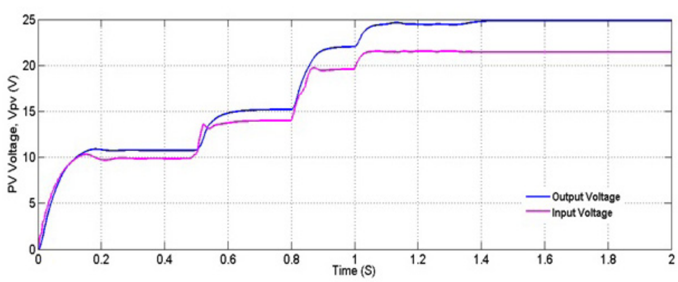

Fig. 11. Input and output voltage waveforms of P&O algorithm with SEPI Converter.

It is observed that the power efficiency has been improved by 2.63% and 28.77% as compared to the modified incremental conductance algorithm and P&O algorithm respectively. The comparison of proposed algorithm with modified incremental conductance and P&O algorithms is detailed in Table III. The proposed algorithm includes sequential sampling process in addition with the modified incremental conductance algorithm

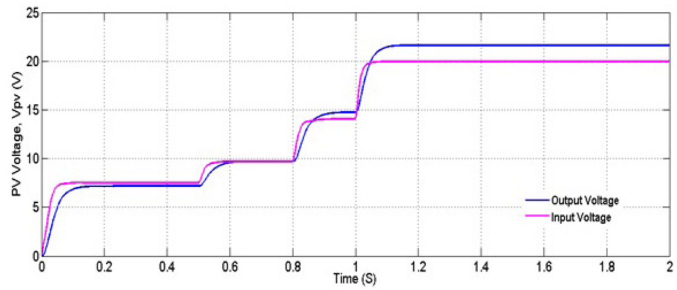

Fig. 12. Input and Output voltage waveforms of Modified Incremental Conductance algorithm with SEPI Converter.

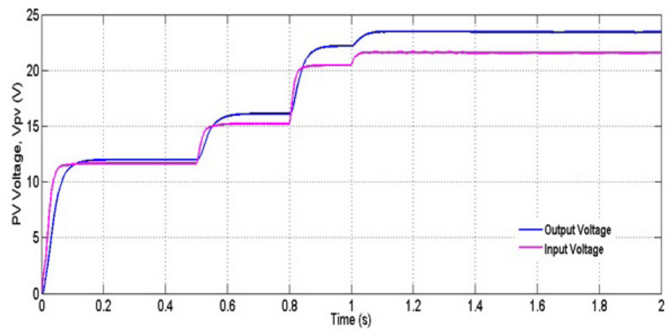

Fig. 13. Input and Output Voltage waveforms of proposed algorithm with SEPI Converter.

and hence the complexity is somewhat more but the tracking the tracking time of GMPP is reduced considerable amount and it results in faster response in tracking process. Also, it acts very fast towards the input changes and gives better performance.

TABLE III
COMPARISON OF PROPOSED ALGORITHM, MODIFIED INCREMENTAL CONDUCTANCE ALGORITHM AND PERTURB & OBSERVE (P&O) ALGORITHM

Evaluated parameters	**Proposed Algorithm**	**Modified Incremental Conductance Algorithm**	**P&O Algorithm**
PV Power	High (63.5W)	Comparatively less (58.5W)	Low (47.5W)
Tracking speed	Effective than Modified Incremental Conductance (based on no.of iterations)	Fast	Slow
Steady state oscillation	No	No	Yes
Ability to track accurate GMPP	Yes	Yes	No
Algorithm complexity	Complex	Complex	Simple

VII. CONCLUSION

In this paper, a new approach for GMPP tracking of a PV system has been proposed based on the sequential sampling of duty cycle and integrated with SEPI Converter. The proposed method retains the Incremental Conductance algorithm as the second stage process after the sampling process. To prove the validity of the enhanced Incremental Conductance algorithm proposed in this paper, the results obtained with the help of MATLAB/Simulink model. Obtained results concludes that the proposed system can replace the conventional algorithm at all partial shading conditions irrespective of the shape of the power waveform and gives a better efficiency. From the results As compared to the Incremental Conductance and P&O algorithms, the power can be extracted from the PV panel by applying the proposed method is improved considerably. Even the complexity of the proposed model is somewhat more; it gives better accuracy in tracking the MPP and gives better power extraction from the PV panel. The proposed method is reliable in sense of reduced complexity in sampling process, easy to develop, apply and can get the accurate GMPP even under partial shading conditions. The proposed algorithm detailed in this paper can be extended to any converter topology with good energy conversion ratio and efficiency for the better power conversion process.

References

[1] Solangi KH, Islam MR, Saidur R. "A review on global solar energy policy: Renewable and Sustainable Energy Reviews." 2011; 15(4): 2149-2163.

[2] Xiao W, Dunford WG. "A modified adaptive hill climbing MPPT method for photovoltaic power systems." *Proceedings of 35th IEEE Power Electronics Specialists Conference;* Germany; 2004. P. 1957– 63.

[3] Femia N, Petrone G, Spagnuolo G, Vitelli M. "Optimization of perturb and observe maximum power point tracking method:" *IEEE Transactions on Power Electronics.* 2005; 20(4): 963-973.

[4] Tey KS, Mekhilef S. "Modified incremental conductance MPPT algorithm to mitigate inaccurate responses under fast-changing solar irradiation level:" solar energy. 2014; 101: 333-342.

[5] Chiang SJ, Hsin-Jang Shieh, Ming-Chieh Chen. "Modelling and Control of PV Charger System with SEPIC Converter:" *IEEE Transactions on Industrial Electronics*. 2009;56 (11): 4344-53.

[6] Patel H, AgarwalV. "Maximum power point tracking scheme for PV systems operating under partially shaded conditions:" *IEEE Transactions on Industrial Electronics*. 2008; 55(4): 1689–98.

[7] Mahmoud YA, Weidong X, Zeineldin HH. "A parameterization approach for enhancing PV model accuracy:" *IEEE Transactions on Industrial Electronics.* 2013,60 (12):5708–16.

[8] Olalla C, Clement D, Rodriguez M, Maksimovic D. "Architectures and control of submodule integrated DC–DC converters for photovoltaic applications:" *IEEE Transactions on Power Electronics.* 2013; 28(6): 2980–97.

[9] Pilawa-Podgurski RCN, Perreault DJ. "Submodule integrated distributed maximum power point tracking for solar photovoltaic applications." *IEEE Energy Conversion Congress and Exposition*. 2012. P 4776-83.

[10] Lopez-Lapena O, Penella MT, Gasulla M. "A closed-loop maximum power point tracker for sub watt photovoltaic panels:" *IEEE Transactions on Industrial Electronics.* 2012; 59(3):1588–96.

[11] Whei-Min L, Chih-Ming H, Chiung-Hsing C. "Neural-network based MPPT control of a stand-alone hybrid power generation system:" *IEEE Transactions on Power Electronics.* 2011; 26 (12): 3571–81.

[12] Shenoy RPS, Kim KA, Johnson BB, Krein PT. "Differential power processing for increased energy production and reliability of photovoltaic systems:" *IEEE Transactions on Power Electronics*. 2013; 28(6): 2968–79.

[13] Yi-Hwa Liu, Shyh-Ching Haung, Jia-Wei Huang, Wen-Cheng Liang. "A Particle Swarm Optimization-Based Maximum Power Point Tracking Algorithm for PV Systems Operating Under Partially Shaded Conditions:" *IEEE Transactions on Energy Conversion*. 2012; 27 (4):1027-1035.

[14] Alonso R, Roman E, Sanz A, Santos VEM, Ibanez P. "Analysis of inverter-voltage influence on distributed MPPT architecture performance:" *IEEE Transactions on Industrial Electronics*. 2012; 59(10): 3900–07.

[15] Ishaque K, Salam Z. "A review of maximum power point tracking techniques of PV system for uniform insolation and partial shading condition:" Renewable and Sustainable Energy Reviews. 2013; 19:475–88.

[16] Lijun TG, Dougal RA, Shengyi L, Iotova AP. "Parallel-connected solar PV system to address partial and rapidly fluctuating shadow conditions:" *IEEE Transactions on Industrial Electronics.* 2009; 56 (5): 1548–56.

[17] Wang F, Wu X, Zhuo F. "Analysis of unified output MPPT control in subpanel PV converter system:" *IEEE Transactions on Power Electronics*. 2014; 29(1), 159-169.

[18] Seyedmahmoudian M, Mekhilef S, Rahmani R, Yosef R, Renani E. "Analytical modeling of partially shaded photovoltaic systems:" Energies. 2013; 6(1).128–144.

[19] Martin AD, Vazquez JR. "MPPT algorithms comparison in PV systems: P&O, PI, Neuro-fuzzy and back stepping controls." *Proceedings of IEEE International Conference on Industrial Technology;* Seville, Spain; 2015.P.2841-47.

[20] Safari A, Mekhilef S. "Simulation and hardware implementation of incremental conductance MPPT with direct control method using cuk converter:" *IEEE Transactions on Industrial Electronics.* 2011; 58(4).1154–61.

[21] ZouZ, Hu Y, Zhao X. Study of the gradual change phenomenon in the infrared image when monitoring Photovoltaic array: Journal of Applied Physics.2014; 115(4).

[22] Gurraoui R. Benhamed M, Sbita L. "Comparison of MPPT algorithms for DC-DC boost converters based PV systems using robust control technique and artificial intelligence algorithm." Proceedings of 12th International Multi-Conference on Systems, Signals & Device; Tunisia; 2015. P 1-6.

[23] Soon TK, Mekhilef S, Safari A. "Simple and low cost incremental conductance maximum power point tracking using buck-boost converter." J Renew. Sustain. Energy, 5, 023106-1–023106-12, Mar. 2013.

[24] Vergura S, Marino F. "A diagnostic workflow and software platform for PV Modules." Proceedings of International Conference on Renewable Energies Power Quality; Cordoba, Spain; 2014. P 661-4.

[25] Sanjeevikumar P, Grandi G. "A simple MPPT algorithm for novel PV power generation system by high output voltage DC-DC boost converter." *Proceedings of 24th IEEE Symposium on Industrial Electronics*; 2015. P.214-220.

[26] Abdelsalam AK, Massoud AM, Ahmed S, Enjeti PN. "High-performance adaptive perturb and observe MPPT technique for photovoltaic-based micro grids:" *IEEE Transactions on Power Electronics.* 2011; 26(4). 1010–1021.

[27] Kakosimos PE, Kladas AG, Manias SN. "Fast photovoltaic system voltage- or current-oriented MPPT employing a predictive digital current-controlled converter:" *IEEE Transactions on Industrial Electronics*.2013; 60(12). 5673–5685.

Drift Free Variable Step Size Perturb and Observe MPPT Algorithm for Photovoltaic Systems Under Rapidly Increasing Insolation

Deepthi Pilakkat and S. Kanthalakshmi

Abstract—**The characteristic of a Photovoltaic (PV) panel is most affected by the incident solar insolation temperature, shading, and array configuration. Maximum power point tracking (MPPT) algorithms have an important role in harvesting maximum power from the solar PV arrays. Among the various MPPT methods Perturb and Observe (P&O) algorithm is the simple and efficient one. However, there will be a drift problem in case of increase in insolation. This drift will be more under rapid increase in insolation. To improve the speed of tracking the Maximum Power Point (MPP), a variable step size P&O (VSSPO) is developed. The drift problem will be more in the case of VSSPO as it will have a larger step size for an increase in insolation. In this paper, the maximum output power extraction from Solar PV under rapidly increasing insolation conditions by a drift free P&O (DFP&O) as well as drift free VSSPO (DFVSSPO) method is presented.**

Index Terms—**Drift Free Analysis, Drift free Variable step size P&O, Maximum Power Point Tracking, Perturb and Observe algorithm, Solar PV Systems.**

Original Research Paper
DOI: 10.7251/ELS1822019P

1. Introduction

Because the global warming is increasing and conventional fossil-fuel energy sources are reducing, renewable energy sources like solar, wind, geothermal etc. are attracting more consideration as alternate energy sources. Among the renewable energy sources, the solar photovoltaic (PV) energy has been widely utilized in many applications due to its advantages such as direct electric power form, easy maintenance, no noise, etc. With a surge in the use of non-conventional energy sources, PV installations are being increasingly employed in several applications. Paper [1] discussed how the solar energy utilization can improve the quality and quantity of products while reducing the greenhouse gas emissions. The output characteristics of PV panel will vary with the temperature and solar insolation and the foremost confront in using a PV supply is to get to work at its nonlinear output characteristics [2].

Manuscript received 20 November 2017. Received in revised form 5 March 2018 and 17 May 2018. Accepted for publication 5 June 2018.

D. Pilakkat and S. Kanthalakshmi are with Department of Electrical and Electronics engineering, PSG college of Technology, 641004, India (e-mail: deepthipilakkat@gmail.com, phone: +91-96-3382-0180).

There are a lot of MPPT algorithms available in literatures such as Perturbation and Observation (P&O), Incremental Conductance (INC), fuzzy logic, Particle Swarm Optimization (PSO), Artificial Bee Colony etc [3]-[7]. The P&O method is the simplest method which can be implemented in real time. Even though P&O method is the simplest among all the MPPTs, it has one major disadvantage of oscillations around MPP, and hence wastage of power. By minimizing the fixed perturbation step size, these oscillations can be reduced. The problem with the small step size is, it will take more time to reach MPP [8]. If the tracking time of MPPT can be successfully minimized, more energy can be gathered from PV at MPP [9]. Numerous improvements for the P&O algorithm have been proposed one by one to diminish the number of oscillations around MPP in steady state, but the response is time-consuming under the rapidly changing atmospheric conditions. This will reduce the efficiency of algorithm and hence the PV systems. A modified variable step size P&O MPPT algorithm is proposed in [10], where the step size is automatically tuned according to the operating point. Variable step size P&O (VSSPO) has better steady-state and dynamic performance than the conventional P&O, and will obtain better efficiency of PV power generation system [11]. Another drawback of P&O method is the presence of drift in case of an increase in insolation (G), and this drift effect is severe in case of a rapid increase in insolation [12]. More over a comparative study of different MPPT algorithms are presented in [13] and [14].

Paper [15] presented a step-by-step process for the simulation of PV cells/modules/arrays with Tag tools in MATLAB/SIMULINK. A complete modeling practice for the circuit model with statistical dimensions is offered using power system block set of MATLAB/SIMULINK and the simulation results are validated with experimental set up in [16].

As the demand for PV electricity generation is increasing day by day, research is going on how to improve the efficiency of the PV systems and thereby reducing the overall cost. In this paper, a drift free variable step size P&O algorithm along with a boost converter is designed and simulated to extract maximum power from the PV panel under the rapidly increasing insolation conditions.

The design of PV system using mathematical model with simulation in MATLAB/SIMULINK environment is presented in Section 2. The P&O MPPT algorithm is used as closed loop control and is integrated with DC/DC boost converter. The algorithm has been analyzed for different irradiation levels. The boost converter adjusts its impedance value by changing duty ratio in order to match the load side impedance with panel's impedance. Section III describes about design of the boost converter used for this study and its specifications in detail. In Sections IV and V, the drift analysis and drift free analysis respectively with P&O and VSSPO MPPT algorithms are explained. Section VI delivers simulation results and Section VII presents the conclusion.

II. Modeling of PV Panel

A. Equivalent Circuit and Mathematical equations of Solar Panel

Fig. 1 depicts the equivalent electrical circuit of an ideal solar cell. The PV module can be modeled mathematically as given in equations below. These equations describes about the V-I characteristics of the PV cell and module.

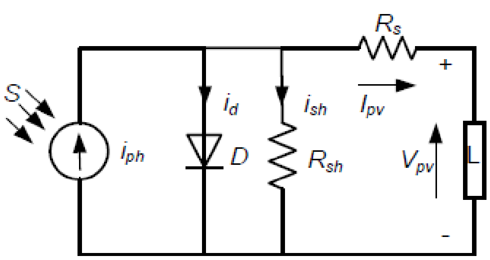

Fig. 1. Equivalent circuit of a solar cell.

The basic equation which describes the PV module output current I_{PV} is given by (1). Sections

$$I_{PV} = N_P.I_{ph} - N_P.I_0 \left[\exp\left\{\frac{q(V_{PV}+I_{PV}R_s)}{N_S.A.k.T_{op}}\right\} - 1\right] \quad (1)$$

The module photo current I_{ph}, depends on both temperature and irradiance as shown in equation (2).

$$I_{ph} = [I_{sc} + K_i(T_{op} - T_{ref})]\frac{G}{1000} \quad (2)$$

The module saturation current, I_o varies with the cell temperature, which is given by

$$I_o = I_{rs}\left[\frac{T_{op}}{T_{ref}}\right]^3 \exp\left\{\frac{q.E_g}{k.A}\left(\frac{1}{T_{ref}} - \frac{1}{T_{op}}\right)\right\} \quad (3)$$

Module reverse saturation current I_{rs} is defined by

$$I_{rs} = \frac{I_{SC}}{\left[\exp\left(\frac{q.V_{oc}}{N_S.A.k.T_{op}}\right) - 1\right]} \quad (4)$$

The symbols and its values used in equations are described in Table I.

TABLE I
Symbols And Descriptions In PV Module

Symbol	Description	Value	Unit
N_P	Number of parallel connected cells		
N_S	Number of series connected cells		
q	Electron charge	$1.6*10^{-19}$	C
V_{PV}	Output voltage of PV module		V
R_S	Series resistance of PV module		Ω
A	Ideality factor	1.5	
K	Boltzman constant	$1.3805*10^{-23}$	J/K
T_{op}	Module operating temperature		K
T_{ref}	Reference temperature		k
K_i	Short circuit current temperature coefficient		A/K
G	Irradiance		W/m^2
E_g	Band gap energy	1.1	eV
I_{SC}	Short Circuit current of PV module		A
V_{OC}	Open circuit voltage of PV module		V

B. Reference PV Module

MAS SPV-P-100 solar module is used as reference module for simulation. The data sheet details are stated in Table II. The electrical specifications are under Standard Test Conditions (STC), with an irradiation of $1000W/m^2$ at temperature 25^0C and air mass 1.5.

TABLE II
Specifications of MAS-SPV-P100 Module

Description	Specification
Maximum Power (P_{max})	100W
Open circuit voltage (V_{OC})	20.59V
Short circuit current (I_{SC})	5.92A
Maximum Power Point voltage (V_{mpp})	18.9V
Maximum Power Point Current (I_{mpp})	5.44A
Module Efficiency	16.8%
Short Circuit Current Temperature Coefficient	0.06%/K

III. Boost Converter

The DC/DC boost converter is used as an interface between the PV array and the load to provide load impedance matching with the PV source.

To track the maximum operating point for certain irradiance and weather conditions a DC-DC converter is inserted between PV module and load. In order to drive the solar panel continually at the maximum power point (MPP), the duty cycle of the switch of DC-DC converter is always tuned with the help of MPPT algorithms. Fig. 2 shows the circuit diagram of a DC-DC boost converter.

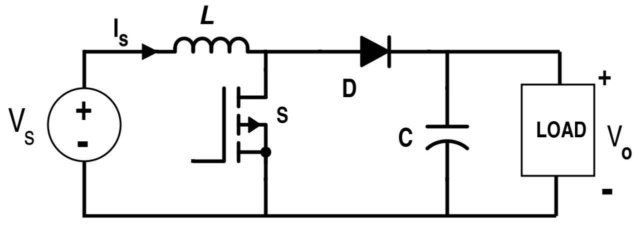

Fig. 2. Circuit diagram of a boost converter.

A. Design of Boost Converter

The design of the boost converter is done with the necessary parameters of the power stage, as follows. The values of the components for boost converter used in the present work are given in Table III.

TABLE III
SPECIFICATIONS OF BOOST CONVERTER

Components	**Specification**
Input Voltage (V_{in})	19V
Output Voltage (V_o)	150V
Output Current (I_o)	1A
Output capacitance (C)	90μF
Load Resistance (R_L)	150Ω
Nominal duty ratio (D)	0.873
Inductance (L)	530μH

a. Design of Duty Ratio:

The duty ratio is calculated by the equation (5).

$$D = 1 - \frac{V_s}{V_o} = 1 - \frac{19}{150} = 0.873 \tag{5}$$

b. Design of Inductor:

The inductor is designed based on the following equation.

$$L = \frac{V_s * (V_o - V_s)}{\Delta I_L * f * V_o} \tag{6}$$

Where, ΔI_L is inductor ripple current which is 20% to 40% of the output current.

$$\Delta I_L = (0.2 \text{ to } 0.4) * I_o * \frac{V_o}{V_s} \tag{7}$$

$$\Delta I_L = 0.2 * 1 * \frac{150}{19} = 1.57A$$

Therefore, $L = \frac{19*(150-19)}{1.57*20K*150} = 528\mu F$

c. Design of Capacitor:

The capacitor value can be calculated using equation (8). The duty ratio is taken as 0.9

$$C = \frac{I_o * D}{f * \Delta V_o} \tag{8}$$

$$= \frac{1 * 0.9}{20K * 0.5} = 90\mu F$$

IV. MPPT AND DRIFT ANALYSIS

A DC/DC boost converter is used as an interface between the PV array and the load to provide load impedance matching with the PV source. To track the maximum operating point for certain irradiance and weather conditions, a DC/DC converter with MPPT is inserted between PV module and load. The duty cycle of the switch of DC/DC converter is always adjusted in such a way as to operate the PV panel at its MPP.

While considering the MPPT methods under a given temperature and irradiance, the main objective is to automatically find the current IMPP or voltage VMPP at which a PV array delivers maximum power [17]. Drift problem is due to the lack of knowledge in knowing whether the increase in power (ΔP>0) is due to perturbation or due to increase in insolation [12]. If the insolation is increased, the power also will increase (ΔP>0). If there is a rapid increase in insolation the drift problem will be more. Drift can occur from any of the three steady state points as shown in Fig. 3 (a) and (b) depending on the instant of change in insolation in between the perturbation time interval (Ta). Suppose there is an increase in insolation while operating at point 1 as shown in Fig. 3 (a), the operating point will be then moved to a new point 4 in corresponding insolation curve for the period of the same kTa perturbation interval.

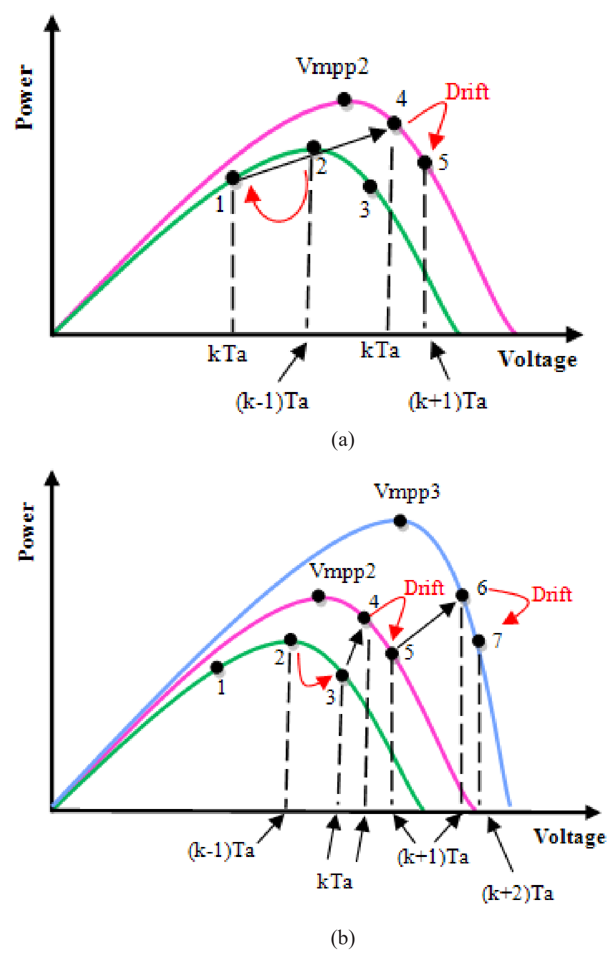

Fig. 3. (a) Drift analysis for one time increase in insolation and (b) rapid increase in insolation.

Now at point 4 as $\Delta P = P_4(kTa) - P_2((k-1)Ta) > 0$ and $\Delta V = V_4(kTa) - V_2((k-1)Ta) > 0$ the algorithm decreases the duty cycle and thereby moving to point 5 away from the MPP in the new curve which is called drift. Likewise for an increase in insolation at point 2 and point 3, the drift problem occurs due to uncertainty of this conventional P&O MPPT technique.

A. Conventional Perturb and observe (P&O) MPPT

The P&O algorithms operate by periodically perturbing (i.e. incrementing or decrementing) the array terminal voltage and comparing the PV output power with that of the previous perturbation cycle [18]. Then the PV voltage and current are measured and the corresponding power is calculated. Considering a small perturbation of voltage (ΔV) or duty cycle (ΔD) of the DC/DC converter in one direction, corresponding power is calculated and compared with the previous value. If change in power, ΔP is positive then the perturbation is in the correct direction; otherwise it should be reversed.

The flowchart shown in Fig. 4 describes the P&O algorithm in detail. The main drawback of P&O algorithm is that it fails to track true power peak in a PV system under partial shading conditions (PSC) and hence settles to local power peak. This results in reduced energy extraction and hence the efficiency of system gets decreased.

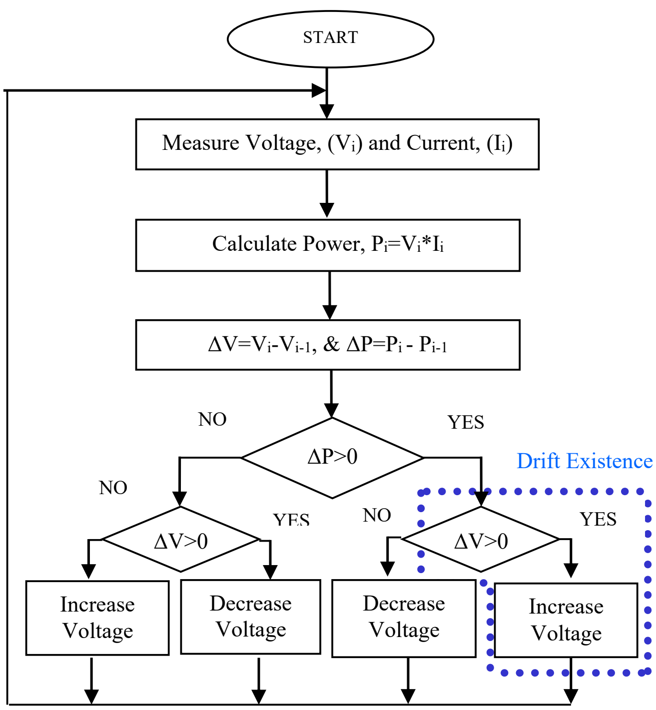

Fig. 4. Flow chart of conventional P&O algorithm.

Another disadvantage of P&O method is its oscillation around MPP. This oscillation can be minimized by reducing the perturbation step size. However, small step size slows down the MPP. To mitigate this problem, a variable step size P&O method can be used, in which step size gets smaller towards MPP.

B. Variable Step size P&O (VSSPO) MPPT

The conventional P&O MPPT method uses fixed step size in order to track the MPP. The VSSPO is a variation of the conventional P&O method. In this algorithm, the step size is automatically tuned to achieve fast and accurate tracking. The dynamic performance is improved by using a large perturbation value, whereas steady state performance can be improved by smaller values [19]. The duty ratio with adaptive step size is given as follows.

$$\Delta D = D(k) - D(k-1) = \pm M * \left|\frac{\Delta P}{\Delta V}\right| \tag{9}$$

Where M is the scaling factor, which is to be tuned at the time of design. For an increase or decrease in insolation, the adaptive technique generates large value of ΔD depending on the value of $\frac{dP}{dV}$. Thus, the effect of drift will be more on VSSPO for an increase in insolation due to the large value of generated ΔD [12]. The VSSPO algorithm with the drift existence loop is shown in Fig. 5.

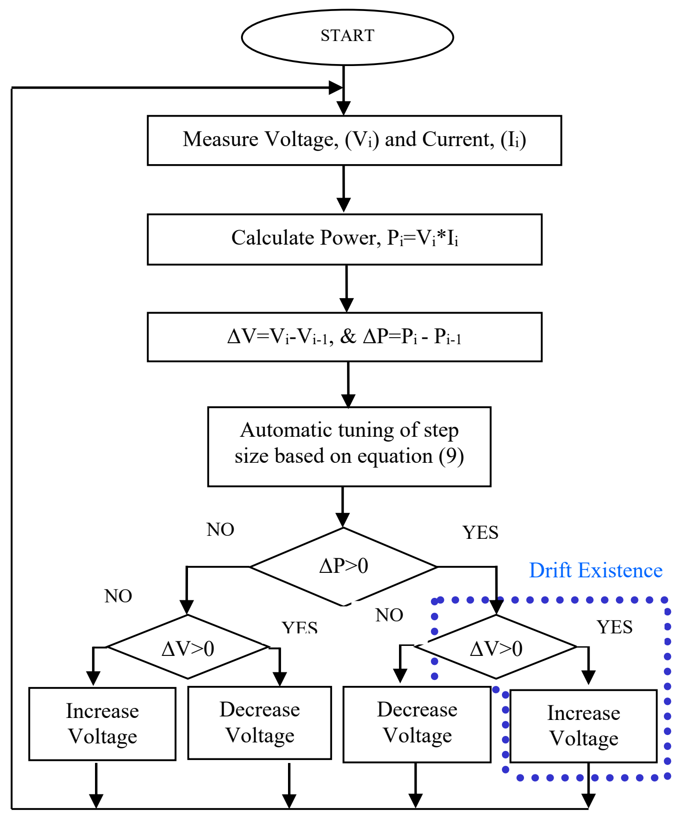

Fig. 5. Flow chart of VSSPO algorithm.

V. Drift Free Analysis

As mentioned before, the conventional P&O has a drift in case of rapid increase in insolation and this is due to lack of knowledge about increase in insolation. This drift can be eliminated by analysing another parameter ΔI (change in current) rather than considering ΔV and ΔP as in conventional P&O. By analysing the PV characteristics, one can see that the increase in power is due to increase in perturbation or due to increase in insolation. The insolation change can be detected by determining ΔI.

From the I-V characteristics shown in Figure 6 one can observe that both ΔV and ΔI will never have the same sign for a single insolation. It is also observed from the same figure both ΔV and ΔI will be positive only for an increase in insolation. Thus it can conclude that, by analyzing ΔI and controlling ΔD the problem of drift can be avoided. A modified drift free P&O algorithm including ΔI is proposed in the next section.

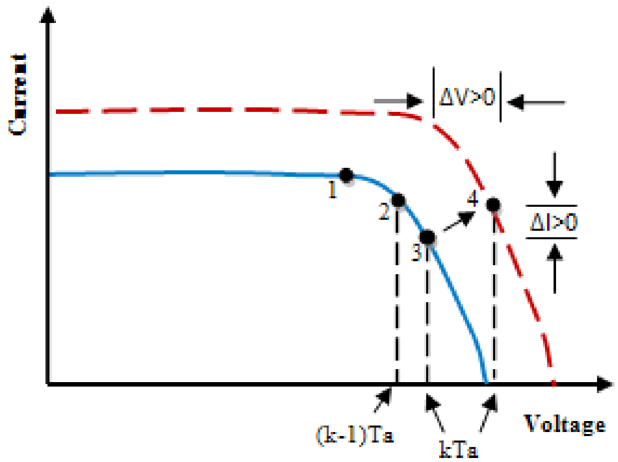

Fig. 6. I-V characteristics for analyzing the change in current with increase in insolation.

A. Drift Free Perturb and observe (DFP&O) MPPT

The basic principle of conventional P&O is controlling duty cycle based on considering ΔV and ΔP. In order to avoid drift free problems during large change in insolation, researchers have already developed some drift free algorithms such as optimized dP-P&O [20] and optimized P&O [3]. According to [20], in order to avoid drift, there is some criteria for setting threshold values. The dP-P&O method uses an additional sampling instant in every iteration, which increases the complexity of the system. The other method optimized P&O uses a higher value of perturbation step size ΔD, for avoiding drift. In such cases drift can be avoided under rapid insolation changes, but the large perturbation step size will result in power loss due to the oscillations around MPP.

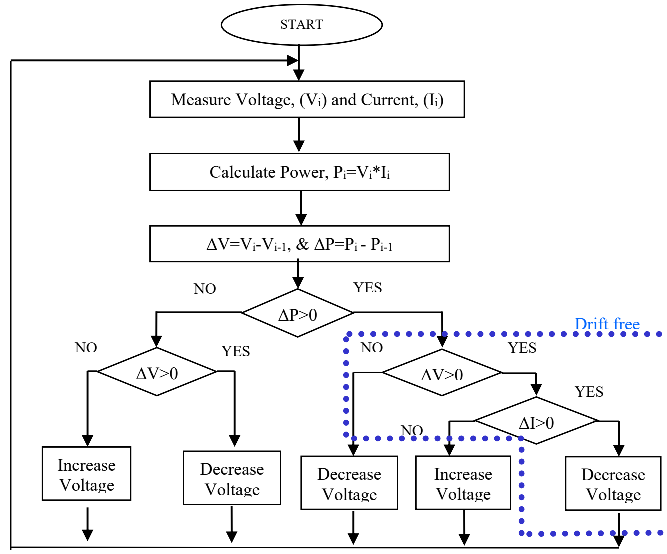

Fig. 8. Flow chart of DFP&O MPPT algorithm.

The remarkable advantage of the proposed DFP&O is, there is no such restraint on ΔD or sampling time as on the above mentioned methods. Here, in DFP&O, one more parameter, ΔI is analyzed in order to avoid the drift problem. Fig. 7(a) and (b) shows the P-V characteristics with drift free P&O MPPT. From these figures it is clear that the drift is avoided as the MPPT understands the change in power is due to increase in insolation and not due to change in perturbation.

When operating at point 3, suppose an increase in insolation occurs and the operating point is shifted to point 4. As the DFP&O understands both ΔV and ΔI are positive, the duty cycle increases and hence voltage decreases. Thus the new operating point is shifted to point 5 as shown in Fig. 7(a). Drift free analysis in case of rapid increase in insolation is shown in Fig. 7(b). The flowchart of DFP&O MPPT is shown in Fig. 8. The drift avoidance loop can be seen in flowchart separately.

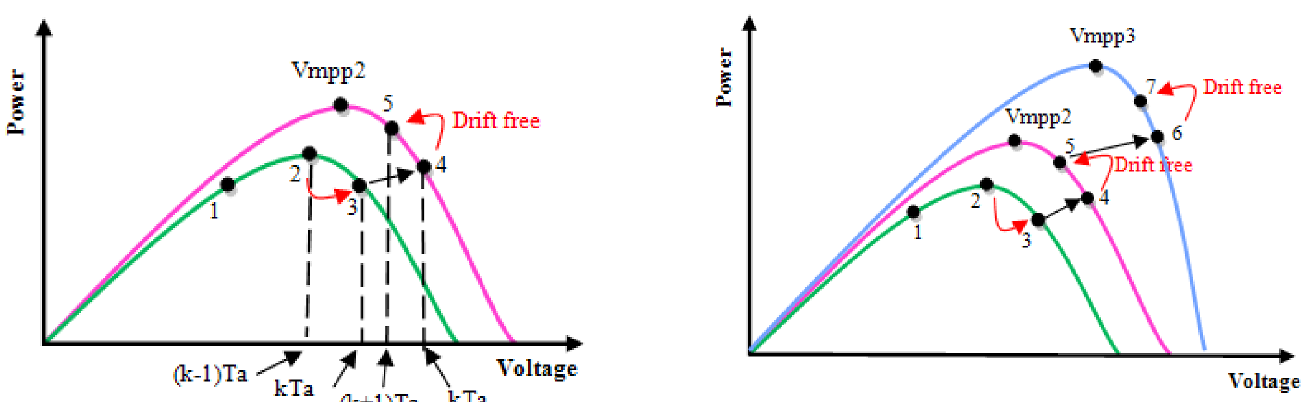

(a) (b)

Fig. 7. Drift free analysis with DFP&O MPPT. (a) One time increase in insolation and (b) rapid increase in insolation.

B. Drift Free Variable Step Size P&O (DFVSSPO) MPPT

In addition to the automatic tuning of step size, the DFVSSPO MPPT uses drift analysis along with VSSPO. As mentioned before, the effect of drift will be more on VSSPO for an increase in insolation due to the large value of generated ΔD. This drift problem can be eliminated with the help of DFVSSPO MPPT. The Fig. 9 depicts the flowchart of DFVSSPO algorithm.

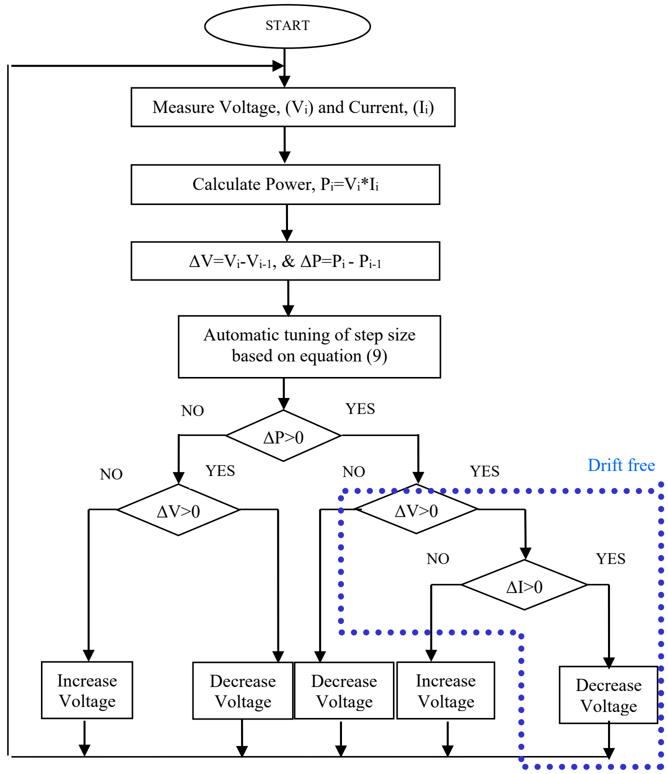

Fig. 9. Flow chart of DFVSSPO MPPT algorithm.

VI. Simulation And Results

This section describes about the simulation of PV module integrated with boost converter along with MPPT algorithms in MATLAB/SIMULINK environment. The MAS-SPV-P-100W PV panel is used for reference.

Fig. 10 represents the MATLAB/ SIMULINK model of the proposed system. Fig. 11 (a) and (b) depicts the P-V (power-voltage) and I-V (current-voltage) characteristics of MAS-SPV-P100 solar panel for varying irradiation and constant temperature of 25^{0}C respectively. As it is a 100W PV panel, at STC, the maximum available power is 100W as shown in Fig. 11 (a). Also it is clear that the output power gets reduced as the irradiance decreases. The output power is reduced to 800W and then to 500W for an irradiation decrease of 800W/m^2 and 500W/m^2 respectively.

Similarly from Fig. 11(b) it is clear that as the irradiation decreases the short circuit current also decreased. From both P-V and I-V characteristics it is seen that there is a slight decrease in open circuit voltage of PV panel as the irradiation gets reduced.

A. Drift analysis with conventional P&O and DFP&O MPPT

The proposed MPPT algorithm has been tested for a step change in insolation level from 500W/m^2 to 800W/m^2 at 1.5s and from 800W/m^2 to 1000W/m^2 at 3s. The perturbation step size is chosen as 0.002. The duty cycle, voltage, and power waveforms with the help of P&O and DFP&O are shown in Fig. 12. Both the MPPT methods are tracking the equivalent MPP efficiently, but the drift in P&O is eliminated in DFP&O method. From Fig. 12 (d) it is clear that the conventional P&O method has a power loss of around 1W when compared to that of a DFP&O.

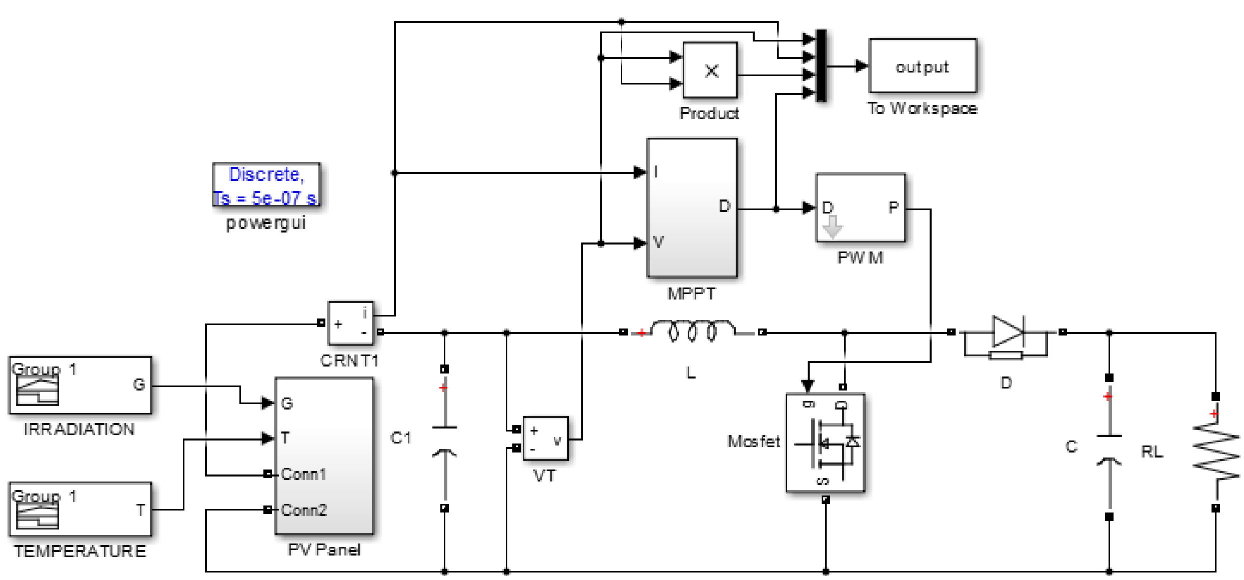

Fig. 10. MATLAB/SIMULINK model of the PV system.

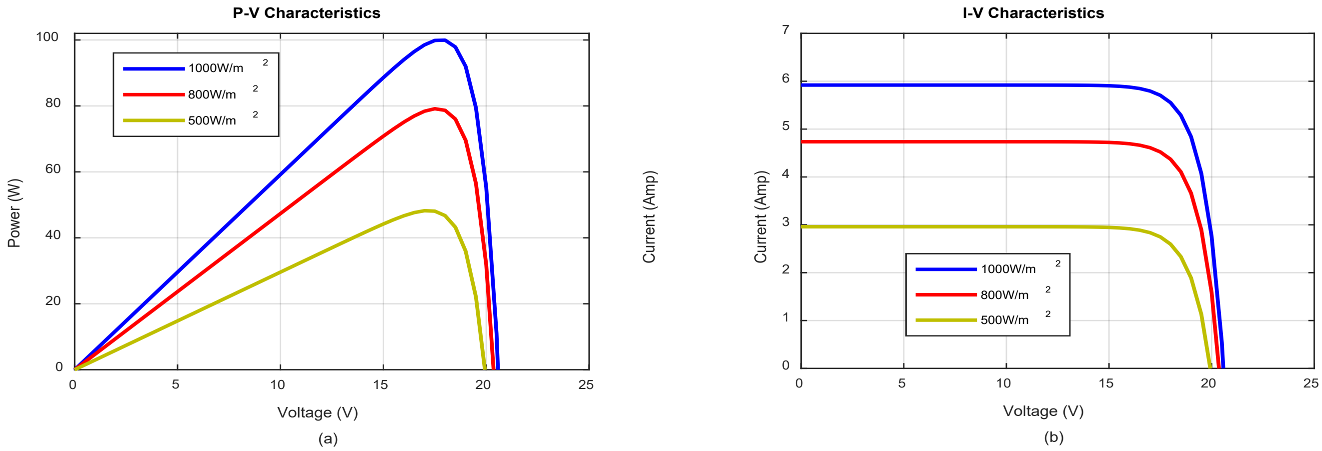

Fig. 11. (a) P-V characteristics and (b) I-V characteristics of MAS-SPV-P100 solar panel for varying irradiation and constant temperature of 25^{0}C.

B. Drift analysis with VSSPO and DFVSSPO MPPT

Fig. 13 shows the duty cycle, voltage and power output of PV panel using VSSPO and DFVSSPO. When the insolataion changed from 500W/m^2 to 800W/m^2 at 1.5s, the VSSPO method tracks the output power of 78W at 1.67s. At the same time DFVSSPO was able to track 78.5W within 1.52s. From Fig. 13(d) it is clear that the VSSPO method suffers a lot from drift problem, whereas the DFVSSPO is free from drift. Almost 13W power loss is obtained in VSSPO at the time of insolation increase at 1.5s as shown in Fig. 13(d). This power loss will result in reduction in efficiency. With the help of DFVSSPO this drift is eliminated.

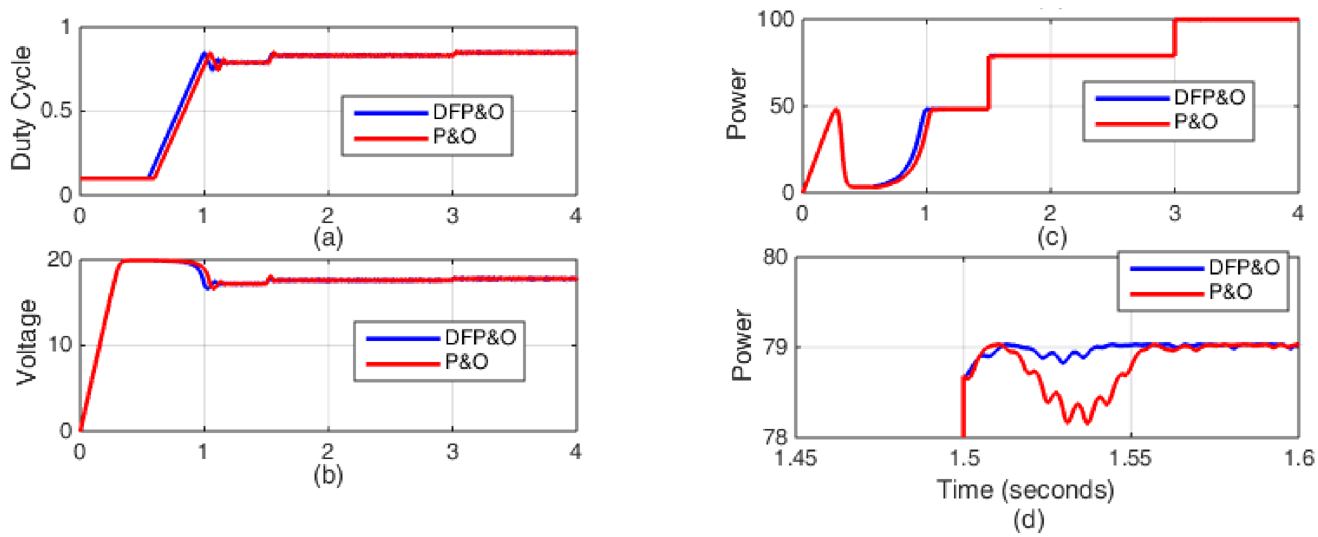

Fig. 12. With conventional P&O and proposed DFP&O for rapid increase in insolation (a) duty cycle, (b) voltage, (c) power and (d) zoomed portion of power at 1.5s.

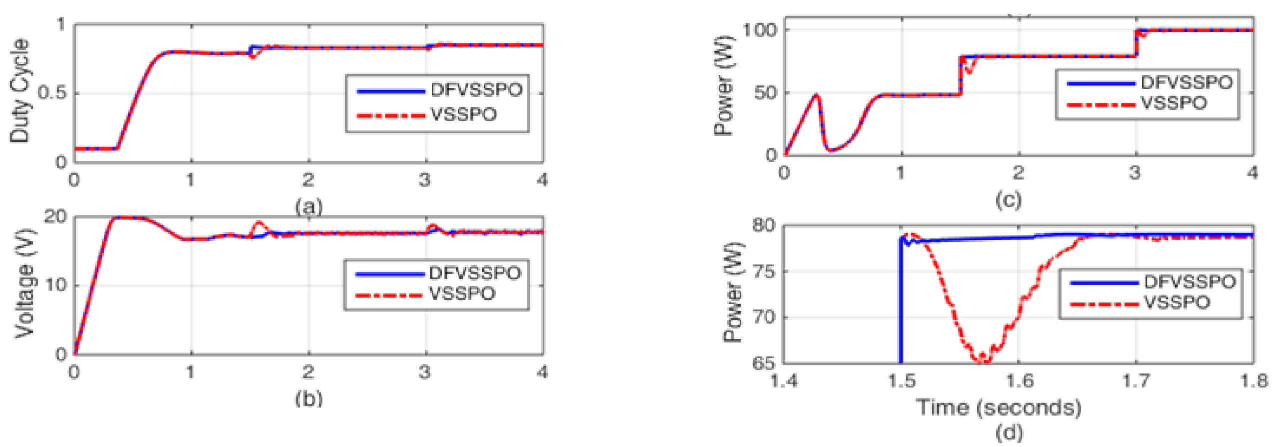

Fig. 13. With VSSPO and proposed DFVSSPO for rapid increase in insolation (a) Duty cycle, (b) Voltage and (c) Power (d) zoomed portion of power at 1.5s.

VII. Conclusion

This paper initially explains the modeling and simulation of a PV panel along with the design of a DC-DC boost converter. The reason for drift phenomena and modifications to avoid drift problem is also explained with the help of conventional P&O and variable step size P&O algorithms. The comparison of conventional P&O with drift free P&O has done and corresponding waveforms are obtained. Similarly, variable step size P&O and modification to VSSPO in order to avoid drift is also proposed and simulated. The basic idea of avoiding drift problem is to include an additional loop and analyze change in current in the conventional P&O algorithm.

The simulation has been done by incorporating a DC/DC boost converter with MPPT control. The simulated results show that the drift free MPPT algorithm reduces the power loss as well as the tracking time when compared to the conventional P&O and VSSPO. This improves the efficiency of the system by gaining a significant amount of power over the complete life cycle of the PV panel. When considering the overall life span of a PV system, drift free operation has an important role in reducing power loss.

The future enhancement of this project can be incorporated along with the merging of IoT (Internet of Things) with the solar system. The voltage and current ratings of the solar plant can be accessed by the owner across the globe.

References

[1] Mekhilef, S.; Saidur, R.; Safari, A. "A review on solar energy use in industries." *Renew. Sustain. Energy* Rev. 2011, 15, 1777–1790, doi:10.1016/j.rser.2010.12.018.

[2] Patel, H.; Agarwal, V. "MATLAB-based modeling to study the effects of partial shading on PV array characteristics." *IEEE Trans*. *Energy Convers*. 2008, 23, 302–310, doi:10.1109/TEC.2007.914308.

[3] Femia, N.; Petrone, G.; Spagnuolo, G.; Vitelli, M. "Optimization of perturb and observe maximum power point tracking method." *IEEE Trans. Power Electron.* 2005, 20, 963–973, doi:10.1109/TPEL.2005.850975.

[4] Mei, Q.; Shan, M.; Liu, L.; Guerrero, J. M. "A novel improved variable step-size incremental-resistance MPPT method for PV systems." *IEEE Trans. Ind. Electron.* 2011, 58, 2427–2434, doi:10.1109/TIE.2010.2064275.

[5] Lalouni, S.; Rekioua, D. "Modeling and Simulation of a Photovoltaic System Using Fuzzy Logic Controller." 2009 Second Int. Conf. Dev. eSystems Eng. 2009, 23–28, doi:10.1109/DeSE.2009.17.

[6] Ishaque, K.; Salam, Z.; Amjad, M.; Mekhilef, S. "An improved particle swarm optimization (PSO)-based MPPT for PV with reduced steady-state oscillation." *IEEE Trans. Power Electron.* 2012, 27, 3627–3638, doi:10.1109/TPEL.2012.2185713.

[7] Sundareswaran, K.; Sankar, P.; Nayak, P. S. R.; Simon, S. P.; Palani, S. "Enhanced Energy Output From a PV System Under Partial Shaded Conditions Through Artificial Bee Colony." *Ieee Trans. Sustain. Energy* 2015, 6, 198–209, doi:10.1109/TSTE.2014.2363521.

[8] Kollimalla, S. K.; Member, S.; Mishra, M. K.; Member, S. "Variable Perturbation Size Adaptive P & O MPPT Algorithm for Sudden Changes in Irradiance." *IEEE Trans. Sustain. Energy* 2014, 5, 718–728, doi:10.1109/TEC.2014.2320930.

[9] Teng, J.-H.; Huang, W.-H.; Hsu, T.-A.; Wang, C.-Y. "Novel and Fast Maximum Power Point Tracking for Photovoltaic Generation." *IEEE Trans. Ind. Electron.* 2016, 0046, 1–1, doi:10.1109/TIE.2016.2551678.

[10] Al-Diab, A.; Sourkounis, C. "Variable step size P&O MPPT algorithm for PV systems." *Proc. Int. Conf. Optim. Electr. Electron.* Equipment, OPTIM 2010, 1097–1102, doi:10.1109/OPTIM.2010.5510441.

[11] Qin, L.; Lu, X. "Matlab/Simulink-Based Research on Maximum Power Point Tracking of Photovoltaic Generation." *Phys. Procedia* 2012, 24, 10–18, doi:10.1016/j.phpro.2012.02.003.

[12] Killi, M.; Samanta, S. "Modified perturb and observe MPPT algorithm for drift avoidance in photovoltaic systems." *IEEE Trans. Ind. Electron.* 2015, 62, 5549–5559, doi:10.1109/TIE.2015.2407854.

[13] Subudhi, B.; Pradhan, R. "A Comparative Study on Maximum Power Point Tracking Techniques for Photovoltaic Power Systems." *Sustain. Energy, IEEE Trans.* 2013, 4, 89–98, doi:10.1109/TSTE.2012.2202294.

[14] Esram, T.; Chapman, P. L. "Comparison of Photovoltaic Array Maximum Power Point Tracking Techniques." *IEEE Trans. Energy Convers.* 2007, 22, 439–449, doi:10.1109/TEC.2006.874230.

[15] Nguyen, X. H.; Nguyen, M. P. "Mathematical modeling of photovoltaic cell/module/arrays with tags in Matlab/Simulink." *Environ. Syst. Res.* 2015, 4, 24, doi:10.1186/s40068-015-0047-9.

[16] Pandiarajan, N.; Ramaprabha, R.; Muthu, R. "Application of circuit model for photovoltaic energy conversion system." *Int. J. Photoenergy* 2012, 2012, doi:10.1155/2012/410401.

[17] Nedumgatt, J. J.; Jayakrishnan, K. B.; Umashankar, S.; Vijayakumar, D.; Kothari, D. P. "Perturb and observe MPPT algorithm for solar PV systems-modeling and simulation." *Proc. - 2011 Annu. IEEE India Conf. Eng. Sustain. Solut.* INDICON-2011 2011, 19, doi:10.1109/INDCON.2011.6139513.

[18] Faranda, R.; Leva, S.; Maugeri, V. "MPPT techniques for PV systems: Energetic and cost comparison." *IEEE Power Energy Soc. 2008 Gen. Meet. Convers. Deliv. Electr. Energy* 21st Century, PES 2008, 1–6, doi:10.1109/PES.2008.4596156.

[19] Piegari, L.; Rizzo, R. "Adaptive perturb and observe algorithm for photovoltaic maximum power point tracking." *IET Renew. Power Gener.* 2010, 4, 317, doi:10.1049/iet-rpg.2009.0006.

[20] Sera, D.; Teodorescu, R.; Hantschel, J.; Knoll, M. "Optimized Maximum Power Point Tracker for fast changing environmental conditions." *IEEE Int. Symp. Ind. Electron.* 2008, 2401–2407, doi:10.1109/ISIE.2008.4677275.

An Intelligent Hybrid Protocol for Effective Load Balancing and Energy Efficient Routing for MANETs

C. Kalaiselvi and S. Palaniammal

***Abstract* — MANET (Mobile ad hoc network) is an autonomous decentralised network. And it is a collection of wireless mobile nodes that dynamically form a temporary network without the reliance of any infrastructure or central administration. Routing is a challenging task in manet. When the size and complexity increases the important challenge in manet is to avoid congestion with effective load balancing and improve energy, QoS parameters inside the network. In this work we propose a new hybrid protocol by combining ACO and Predator prey (LV) model which known as ACRRCC (Ant colony based rate regulating congestion control) method, which works efficiently in two phases. The efficient and optimal routing strategy is done by phase I using ant colony optimization. In phase II the congestion is majorly controlled by employing a mathematical model named predator-prey model which regulates the rate of the traffic flow in the network path. Performance of our proposed hybrid model ACRRCC yields good results under simulation study when compared with simple ACO.**

***Index Terms*—ACO, Cogestion, Manets, Routing.**

Original Research Paper
DOI: 10.7251/ELS1822027K

I. Introduction

Mobile adhoc network is a decentralized and infrastructure-less network where all nodes interact with one another by hop-by-hop manner through intermediate nodes within the transmission range under a wireless medium. Since, the topology in Manet is ever changing, efficient routing and congestion control is a challenging task, and which seriously affects the required QoS in the network. To ensure the required Qos in manets enormous routing algorithms is proposed by many authors which can be categorized as proactive, reactive and hybrid protocols. In the proactive method, always a route will be maintained in the network whether it is needed or not, but in reactive or on demand method a route is explored when there a need of route to send data, whereas in hybrid routing method combines both methods which will give the complete information about the routing table and overcome disadvantages. The reactive method is very much useful where the route is used in uneven intervals.

ACO (Ant Colony Optimization) is a metahuristic approach which works efficiently for finding the optimal path. Many authors have discussed the ACO based routing protocols for MANETS [1]-[2] which are more reliable in nature. In ACO algorithm several ants starts to traverse from its nest in a random manner in the network to find the food source. While traversing the ants lay a chemical substance called pheromone. This pheromone value is used to find the optimal path. If the pheromone value is more in a path, the probability of use of that path increases. In such a way ACO exhibits various interesting properties for MANETS and works in a distributed manner.

Congestion control is the major problem in mobile ad hoc networks which is related to controlling the traffic entering into a telecommunication network. Since manets works in a smaller transmission range, if there is link failure or a queue overflow then congestion may arise. Due to this congestion there will a packet loss, increased overhead, delay in sending packets, low bandwidth, which all in a core seriously effects the required QoS in the network. Severe throughput degradation and massive fairness problems are some of the identified congestion related problems. These problems are incurred from MAC, routing and transport layers. To avoid congestive collapse or link capabilities of the intermediate nodes and networks and to reduce the rate of sending packets congestion control is used extensively. End system flow control, network congestion control, network based congestion avoidance, and resource allocation includes the basic techniques for congestion control.

The rest of this paper is structured as follows. Section II deals the review of the works related to routing problems in manets. In Section III, the proposed method is explained and, in Section IV, the mathematical model is presented. In Section V, the evaluation if the proposed model is done under simulation setup. Finally, the conclusion of the work is presented in Section VI.

II. Related Works

Several researchers have contributed their extreme efforts to improve the multi-constrained QoS in wireless ad-hoc networks. The Qos in manets totally rely on three major key functionalities such as, optimal routing, scheduling of packets and congestion control in the network. The overall network throughput can be increased by the above mentioned aspects. The end-to-end delay and the cost can be reduced by proper routing process. Appropriate scheduling algorithm helps in

Manuscript received 18 December 2017. Received in revised form 11 April 2018 and 20 May 2018. Accepted for publication 5 June 2018.

C. Kalaiselvi is with the Department of Mathematics, Sri Krishna College of Technology, Tamil Nadu, India, 641042 (phone:+91-9944518606; e-mail: c.kalaiselvi@skct.edu.in).

S.Palaniammal is with the Department of Mathematics, Sri Krishna College of Technology, Tamil Nadu, India, 641042 (e-mail: s.palaniammal@skct.edu.in).

effective bandwidth allocation. Congestion control measures are used to overcome the congestion in the network. Many related works for the above mentioned constraints are briefly discussed in the following.

Enormous works have been established by the authors for the efficient routing process in networks based on various constraints such as reliable route selection, power aware routing, maximum battery life routing, routing with minimum contention time, load balancing ,maximum network life time, pre-emptive multipath routing etc., In the research work [3] the authors made a survey on existing routing protocols.

In the research work [4] the authors compared three protocols AODV (Ad-Hoc On Demand Distance vector), DSR (Dynamic source routing) and DSDV (Destination-Sequenced Distance-Vector Routing) protocol by considering the performance measures such as energy consumption, average delay, average throughput, average end-to-end delay, and packet delivery ratio beneath wavering node movements. In the DSR protocol the average throughput of the network is increased by increasing the number of nodes with a node speed 15m/sec. The protocol AODV becomes more static and outlines a stable path from source to destination for the same no of nodes and speed. Whereas the performance of DSDV is not so better when compared the above two protocols. In DSDV when the node count is increased the result is dropped because of the link failure in the network. The authors in [5] have compared and concluded that the protocols DSR and AODV consumes more when compared with DSDV which is a table driven one. And also in the same work they have exposed that DSR works good compared to AODV.

In the paper [6] the authors have explored a Neighbour Coverage based Probabilistic rebroadcast protocol (NCPR). This model is a combination of probabilistic method with neighbour knowledge method. In this protocol a novel rebroadcast delay system is designed to determine the rebroadcast order by which they obtain a more accurate additional coverage ratio. The additional coverage ratio is the ratio of the number of nodes that should be covered by a single broadcast to the total number of neighbours. The network connectivity is tracked frequently by a metric called connectivity factor. The connectivity factor reveals the information about the network connectivity and the number of neighbour nodes of a particular node and also it decides the number of neighbours should receive the Route Request (RREQ) packet. Then the additional coverage ratio and the connectivity factor are merged to find the rebroadcast probability which is used to reduce the number of rebroadcasts of the RREQ packets and helps in improving the routing performance. Additionally NCPR works well for the broadcast storm problem and helps in decreasing the routing overhead.

Vast number of evolutionary and optimizing algorithms have been analysed by many researchers which includes genetic algorithm (GA) [7], Particle Swarm optimization [8], Bee colony optimization [9], Bird flight technique [10] and etc. ACO and GA are some of the prominent algorithms used for efficient routing and to attain expected QOS in manets. The routing requirements of manets coincide with ACO technique because of its foraging and self-configured nature. In the research work [11] the authors examined a new hybrid routing algorithm for ad-hoc networks named Ant-Hoc-Net which works for link failure problem by both reactive and proactive methods. In paper [12] a new protocol named Ant-based On-demand Energy Routing (AOER) is analysed where three different factors like, energy resolved in each node, the cost accounts for the path and number of hops used in the network are considered.

The authors Genhang Ding et al., [13] have acquainted with an algorithm called Improved Ant-Colony Algorithm (IACA) in which the QoS routing problems are fingered by multiple strategies, by revamping the pheromone update rule. In the route selection process the piecewise function Q(t) is substituted for the probability constant and in this work two sets of metrics are considered. One set consists of cost, delay, delay- jitter with packet loss and another set includes bandwidth instead of packet loss. The algorithm allows a large search space and also it utilizes the existing current information for searching the ranges to get the best fitness ant, which leads to an optimal solution.

In the work [14] the authors proposed a Multi-objective ACO (MOACO) algorithm. In this work they have innovated a new encoding and decoding scheme. The encoding method converts the solution space to the search space. The author suggested a bit-string encoding method which deals with the binary numbers 0 and 1. Depending on these binary values the cluster heads are chosen in which 1 means the node is chosen as a cluster head and 0 means the node is not and the pheromone values are associated with the nodes in the network. This pheromone value indicates the probability of a node to be chosen as a cluster head. Whereas the decoding scheme is a reverse process of encoding scheme which changes the search space back to the solution space. In this scheme the nodes which are tagged as a binary number 0 is chosen as a cluster heads as well as the cluster members. The main drawback of decoding method is, in a particular transmission range we have one cluster head and the remaining cluster members miss the opportunity to be chosen as cluster head which may also leads to a good solution.

In the paper [15] the authors have investigated an ant-based multi-objective QoS routing protocol (AMQR) which satisfies the various QoS requirements in manets for time varying topology. This algorithm mainly deals with two phases such as route discovery and route conservation. Each node in this algorithm maintains three different tables namely neighbour table, path preference table and routing table. The job of neighbour table is it highlights the virtue of the outgoing links in various paths to destination using the pheromone substance and it indicates the available bandwidth of the outgoing link from that neighbour. In the path preference table has a probability value for every node associated with the list of neighbour nodes which is used to choose the best next hop in the desired path. The higher path preference value of a neighbour node is used in the routing table to reach the desired destination.

In the research paper [16] the authors have used the Lotka Volterra (LV) [17]-[18] competition model to design a scalable and self-adaptable congestion control approach for autonomous decentralized networks. By employing this LV based rate regulating congestion control method and by using effective parameter values the system achieves high packet delivery ratio and less end-to-end delay. The same authors in the research work [19] used the stable equilibrium condition [20]-[21] of the general LV model and proved that there is a positive and stable equilibrium point when the interspecific competition is weaker than the intra-specific competition.

III. Proposed System

The proposed algorithm ACRRCC, is an efficient routing algorithm for manets which works in two phases such as route exploration process and route maintenance process to obtain the desired QoS. In the proposed algorithm ant colony optimization technique is used to find the optimal path from source to destination. In the theory of ACO the foraging behaviour of the ants is studied [1]. The structure of ACO is very much similar to manets i.e., in ACO the artificial ants wander randomly to find their food whereas in manets the nodes will move in a random nature and they search for their neighbour nodes to transmit data packets to the destination nodes. In the route finding process the ants lay a chemical substance called pheromone. More pheromone on the path increases probability of path being followed. The pheromone trail starts to evaporate in an unused path and the pheromone are reinforced in the mostly used path. In such a way ACO algorithm is used for optimization problems. In our problem pheromone of each edge is found and then the global pheromone value is calculated and it is used to find the optimal path. In transmission of data from SN (source node) to DN (destination node) congestion is a major problem which arises when demand exceeds the available buffer of the neighbour nodes. If a SN initiate a traffic flow to its NN (neighbour node), and in case this NN receives data packets from some other SN then, there will be a congestion if the incoming bytes of data is more than the available buffer of the NN. To overcome the congestion and effective load balancing, the rate at which a SN can initiate a traffic flow is regulated using a Predator prey (Lokta Volterra competition model) biological model. In this biological model a natural ecosystem is studied, which comprises of species of same kind and different kind which are called intra-specific and inter-specific species respectively. This model exhibits the behaviour of manets i.e., in ecosystem the species compete with one another for the available resources, where as in manets the data flows compete with themselves for available buffer of the NN.

IV. Mathematical Model

MANET is considered to be analogous to an ecosystem. An ecosystem comprises of multiple species that live together and interact with each other as well as the non-living parts of their surroundings (i.e. resources) to meet their needs for survival and coexist. Similarly, a Mobile ad hoc network involves a number of cooperative nodes. Each node has a buffer in order to store packets, a communication channel of a certain (dynamic) capacity, and is able to initiate a traffic flow. Traffic flows can be seen as species that compete with each other for available network resources (buffer space communication channel capacity) while traversing a set of intermediate nodes forming a multi-hop path leading to the sink. The population size of each species corresponds to the rate of each traffic flow. In analogy with ecosystems, the goal is the coexistence of traffic flows.

A. Route Exploration

To explore a path from SN to the DN, the SN first find all its NN and send a route request to all its available neighbour. Now the neighbour nodes send a route request to their NN the process is continued until the route request reaches the DN. The DN gives a route reply to nodes from whom it got a route request and it continues until the rout reply reaches the SN. By using this method a general structure of all possible paths are found. Once after getting the information about the available paths the SN search for the neighbour nodes based on the pheromone value. From the available neighbours the SN will choose a NN with highest pheromone value and sends the data. If a SN have more than one NN with the same highest pheromone value each of it selected one by one and SN starts to send the data till the destination and every route is stored in the routing table. The pheromone value of each link is calculated by considering the bandwidth , energy and the distance between the nodes i and j which is given by the following equation

$$Pheromone(ij) = \frac{Q*\left(\frac{banwidth\ of\ neighbour\ 'j'}{banwidth\ threshold}\right)}{distance(ij)} * \frac{\left(\frac{energy of\ neighbour\ 'j'}{energy threshold}\right)*}{traffic flow} \quad (1)$$

where Q is the size of the queued packets, *traffic flow* of each node is regulated using the predator prey model which is briefly explained in the next section.

By using the pheromone values, all the available paths in networks are found. From these possible path we have to find the efficient and shortest path from the source to destination which is found using the global pheromone value given by the formula (2). After finding the global pheromone value of each path, the path with highest global pheromone value is selected as the efficient path and it is saved in the routing table and the SN starts to send the data packets.

$$\left.\begin{array}{l} Global\ pheromone\ value \\ of\ a\ path \end{array}\right\} = Sum\ of\ all\ the\ pheromone\ values\ in\ the\ path\ from\ i\ to\ j. \quad (2)$$

B. Rate regulating System using predator prey model

In the predator prey model the whole ecosystem is divided into smaller sub-ecosystems involves all nodes that send traffic to a particular one-hop-away node (neighbour node). The traffic flows initiated by each node play the role of competing species and the buffer (queue) capacity of the parent node is considered as the limiting resource within the sub-ecosystem.

Within a virtual ecosystem, participant nodes may perform different roles. In particular, each node is able to either initiate a traffic flow i.e. is a source node(SN), or serve as a neighbour node (NN) to forward packets of multiple flows passing through it, or perform both roles being a source-neighbour node (SNN).

The general form of a n-species LV [19] system is expressed as below

$$\frac{dx_i}{dt} = x_i\left[r_i - \left(\frac{\psi_i x_i}{B_i}\right) - \frac{r_i}{B_i}\left(\sum_{j=i\ i\neq j}^{n}\phi_{ij}x_j\right)\right] \qquad for \quad i = 1,2,3........,n \tag{3}$$

where $x_i(t)$ is the population size of species i at time t ($x_i(0) > 0$). Parameter Φ_{ij} measures the intensity at which the packets of same traffic flow interact with each other, whereas parameter Ψ_i measures the intensity at which the packets of different traffic flows interact with each other and the parameter 'r' corresponds to the speed (how quickly) each traffic flow's rate increases. Also B_i the carrying capacity of species and also it represents the maximum number of individuals of a species that can be sustained in the ecosystem in the absence of all other species competing for the same resource when $\Psi_i = 1$. Finally, parameter B is the buffer's capacity on each node (the shared resource) otherwise, the maximum population size of species i can reach B_i/Ψ_i . If only one resource exists and all species (having the same carrying capacity B_i) compete for it, then B_i can be seen as the resource's capacity. The LVCC [19] approach is developed on the basis of the n-species LV model, assuming that the n species have the same characteristics: $r_i = r$, $B_i = B$, $\Psi_i = \Psi$ and $\Phi_{ij} = \Phi$ for every i and j. Therefore the above equation becomes

$$\frac{dx_i}{dt} = rx_i\left[1 - \left(\frac{\psi}{B}\right)x_i - \left(\frac{\phi}{B}\right)K_i\right] \quad for \ \ i = 1,2,\ldots,n \tag{4}$$

where $K_i = \sum_{j=i\ i\neq j}^{n} x_j$

$x_i(t)$ is the number of bytes sent by node i corresponds to the rate of each traffic flow at time t. Here, the terms flows and species are interchanged. Model involves four parameters: r, Φ, Ψ and B. In order to solve for a single node i, it is necessary to be aware of the aggregated number of bytes sent from all other nodes which compete for the same resource and it is denoted by K_i

C. Calculation of Traffcic flow rate of SN

Pure source nodes are end-nodes which are attached to the rest of the network through a downstream node e.g. a neighbour node (NN), or a source-neighbour node (SNN) located closer to the sink. Each SN is expected to initiate a traffic flow when triggered by a specific event. By using (2) we can identify traffic rate. In manet architectures, the assumption of K_i-awareness is quite unrealistic. However, each SN can indirectly obtain this information through a small periodic backpressure signal sent from its downstream SNN/NN (parent node) containing the total number of bytes sent from all parent's children, denoted by BS. Each node can evaluate its neighbour's contribution C_i by subtracting its own contribution x_i from the total contribution BS and the transmission rate x_i for SN/SNN is given below which is obtained by integrating (2)

$$x_i(t) = \frac{wx_i(0)}{\psi x_i(0) + [w - \psi x_i(0)]e^{-\left(\frac{wrt}{B}\right)}}$$

$$\text{where} \qquad w = B - \phi K_i \tag{5}$$

The authors [19] have studied an ecosystem based network of flows compete for the available resources in which the rate of flow is regulated using the formula given in (3) and they proved that the system is in an stable equilibrium position when Ψ> Φ and Ψ,Φ>0. Using this equilibrium condition the values generated by SN's that converges to a coexistence solution is given by (4) refer [19] for detailed proof.

$$x_i^* = \frac{B}{\phi[n-1]+\psi} \qquad i = 1,2,.....,n \tag{6}$$

To avoid buffer overflows, it should be ensured that when a system of n active nodes converges to the coexistence solution the bytes send by each node is less than or equal to B/n i.e.,

$$x_i^* \leq \frac{B}{n} \tag{7}$$

Hence equation (4) is satisfied when

$$\phi[n-1]+\psi \geq n \quad o \quad \psi - \phi \geq n(1-\phi).$$

If we set Φ ≥ 1 and we need Ψ > Φ (as given by the equilibrium stability condition in [19]), then the above-mentioned inequality is always satisfied. Therefore, to confirm both convergence and no buffer overflows the following two conditions must be satisfied:

$$\Psi > \Phi\,, \quad \Phi > 1$$

The calculated transmission rate of each node $x_i(t)$ converges to the stable coexistence solution, x_i* within time period Tcn. The convergence time, (Tcn) of a traffic flow is calculated by x_i(Tc)= x*, using (4), and it is observed that it is proportional to parameter Φ and inversely proportional to parameter r. This practically implies that there is fast convergence of time when Φ is small or r value is large

Using (4), a series of values corresponds number of bytes sent every period T is evaluated. In (4), when we set the initial value of the transmission rate $x_i(0)$ at time t=0, we can directly obtain the transmission rate $x_i(t)$ for any time t. The transmission rate can be calculated iteratively using the following formula.

$$x_i((k+1)T) = \frac{w(kT)x_i(kT)}{\psi x_i(kT) + [w(kT) - \psi x_i(kT)]e^{-\left(\frac{w(kT)r}{B}\right)*T}} \tag{8}$$

D. Calculation of Traffic flow rate of NN

Pure neighbour nodes are entities which do not initiate any packets, but forward packets belonging to several flows traversing themselves which compete for their resources. The main function of a NN is to combine (or multiplex) all incoming flows into a super flow and relay it to the dedicated downstream node (SNN or NN). Each NN allocates resources for its active upstream nodes based on a slightly modified expression (6) which is given below.

$$x_{NN}((k+1)T) = \frac{w(kT)H(kT)}{\psi x_i(kT) + [w(kT) - \psi x_i(kT)]e^{-\left(\frac{w(kT)r}{B}\right)*T}}$$

$$H(kT) = \frac{1}{m} x_{NN}(kT) \qquad and \qquad w(kT) = B - \phi \tag{9}$$

where 'm' is the total number of active sender nodes which belong to the tree having NN as root. Each NN can calculate the number of its active sender nodes m by scrutinizing the source id field of each packet traversing itself. K*NN(kT) reflects the total number of bytes sent (BS) to the receiver node from all its competing children nodes, subtracting the contribution of a single flow belonging to the superflow, given by

$$K^*_{NN}(kT) = BS - \frac{1}{m} x_{NN}(kT) \tag{10}$$

E. Source node as neighbour nodes (SNNs)

A source-neighbour node acts as both source and neighbour node, having both functions concurrently operated as described above. The development of the LVCC protocol on the basis of the Lotka Voltera population model that governs the coexistence of species competing for limited resources.

V. Simulation Results

The proposed ACRRCC routing protocol is tested under the certain simulation setup which is given in Table I.

TABLE I
Simulation Parameters

Property	Values
set val(chan)	Channel/WirelessChannel
set val(prop)	Propagation/TwoRayGround
set val(netif)	Phy/WirelessPhy
set val(mac)	Mac/802_11
set val(ifq)	Queue/DropTail/PriQueue
set val(ll)	LL
set val(ant)	Antenna/OmniAntenna
set val(ifqlen)	100
set val(nn)	50
set val(rp)	ACRRCC
set val(x)	1000
set val(y)	1000
set val(stop)	200s
set val(chan)	Channel/WirelessChannel

A. Energy

Energy consumption in a network is a very important aspect. The energy consumption of the proposed congestion control routing protocol works very effectively for various speeds of the node when compared to simple ACO routing. In the Fig. 1 the performance of the proposed ACCRRC protocol is compared with simple ACO and it indicates that the energy used by the proposed one is less.

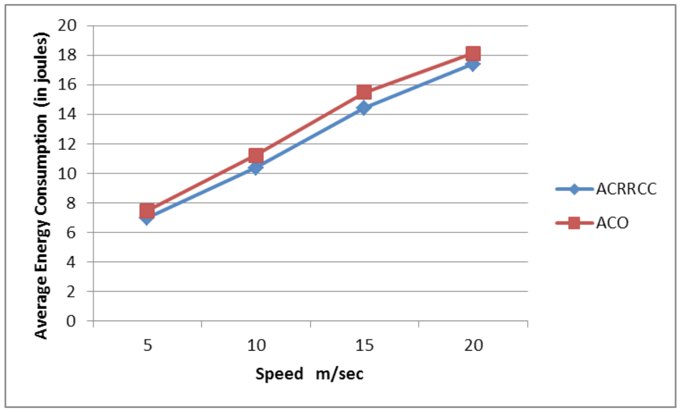

Fig 1. Speed vs Energy.

B. Throughput

Fig. 2 shows that the overall throughput of ACRRCC is high when compared with simple ACO, because in simple ACO the routing part alone is done but in ACRRCC the routing is done along with the effective load balancing due to congestion control mechanism.

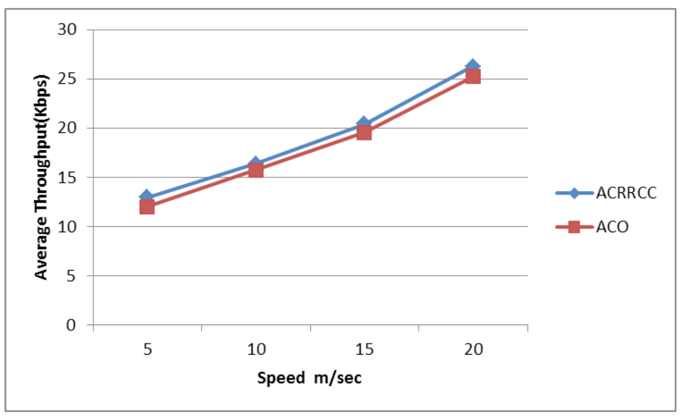

Fig. 2. Speed vs Throughput.

C. Packet delivery Ratio

Packet delivery ratio may decrease in the network due to path disconnections and congestion. The proposed ACRRCC protocol works well in finding an efficient path and controlling the congestion which leads to increase in percentage of packet delivery ratio when compared with simple ACO which is presented in Fig. 3.

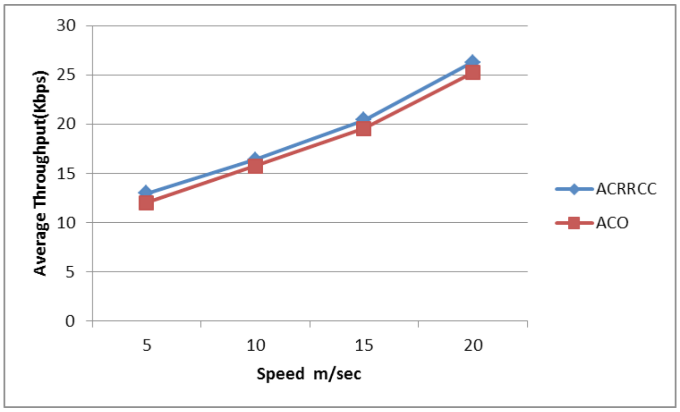

Fig. 3. Speed vs Packet delivery ratio.

D. Routing overhead

The routing overhead of the proposed model is decreased when compared with simple ACO which is shown in Fig. 4.

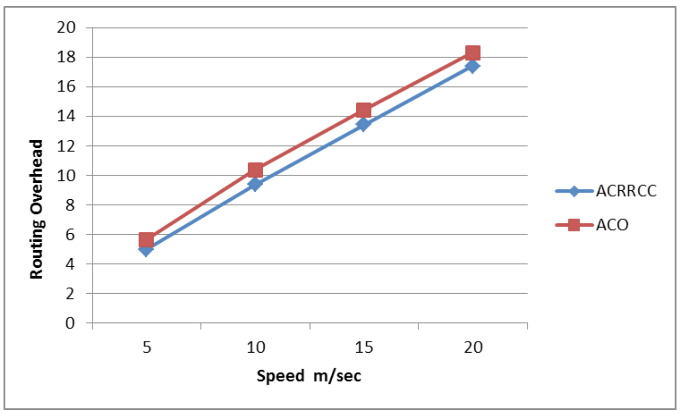

Fig. 4. Speed vs routing overhead.

E. Packet Loss Ratio

In the networks there will be packet loss when there a queue overflow or improper routing information. Both the above mentioned difficulties is taken into account and the packet loss is decreased in the proposed ACRRCC routing protocol is less than the ACO.

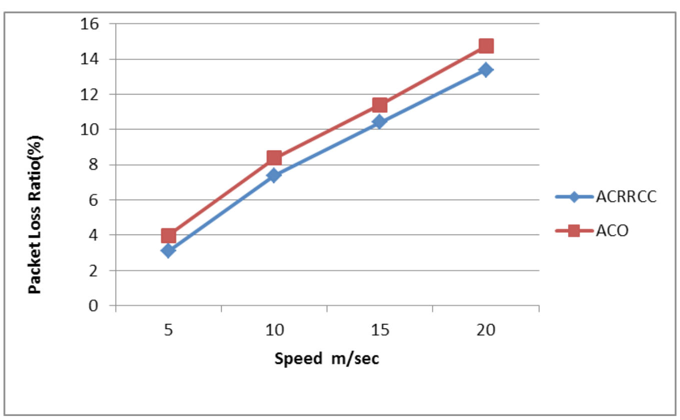

Fig. 5. Speed vs Packet loss ratio.

F. Delay

Fig. 6 shows the end-to-end delay of the ACRRCC model is reduced than the simple ACO because the traffic flow rate is adjusted according to the available buffer of the next hop neighbor.

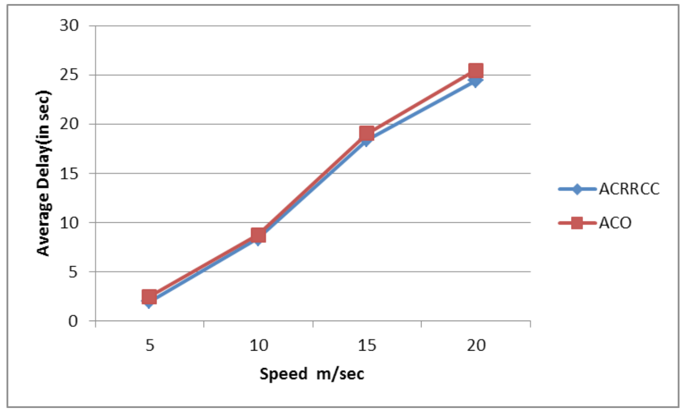

Fig. 6. Speed vs Average Delay.

VI. Conclusion

In this is research work a hybrid protocol for effective load balancing and energy efficient routing using ACRRCC protocol is proposed. Energy efficient routing is done by ACO technique and effective load balancing is handled by employing a bio-inspired mathematical model named LVCC [19] in which the traffic flow rate is regulated according to the receiver node's buffer capacity. In routing process the efficient path is selected using ACO technique by considering the global pheromone values of all the selected paths. By regulating the traffic flow rate of each node there will be no buffer overflow and congestion. Thus our proposed ACRRCC hybrid model works effectively and simultaneously in routing and congestion control. As a result of the proposed work the average end-to-end delay, energy consumption in the network, packet loss ratio, and the routing overhead are decreased, and the network throughput, packet delivery ratio are increased when ACRRCC is compared with simple ACO and which all in a core improves the QoS in the network.

References

[1] Camilo,T, Carreto, C, Silve, J.S & Boivida, F. "An Energy Efficient ant-based routing algorithm for wireless sensor networks" International conference on Ant Colony optimization and Swarm Intelligence, *Springer*, September 2006

[2] Baskaran, R., Victer Paul, P., & Dhavachelvam,P., "Ant Colony Optimization for data catche technique in MANET". Advances in intelligent systems and computing, *Springer*, India, pp 873-878, 2012

[3] Boukerche, B. Turgut, N. Aydin, M. Z. Ahmad, L. Bölöni, and D.Turgut, "Routing protocols in ad hoc networks: A survey," *Elsevier Computer Networks*, vol 55, 3032–3080, 2011

[4] V. Anand, S. Chandra Gupta, "Performance of AODV, DSR and DSDV Protocols under varying node movement", World Congress on Information and Communication Technologies 2012.

[5] A. Kumar, M. Q. Rafiq, K. Bansal, "Performance Evaluation of Energy Consumption in MANET", *International Journal of Computer*

Applications, vol 42, no.2, March 2012.

[6] X. M. Zhang, Member, IEEE, En Bo Wang, Jing Jing Xia, and Dan Keun Sung, "A Neighbor Coverage-Based Probabilistic Rebroadcast for Reducing Routing Overhead in Mobile Ad Hoc Networks" Senior Member, IEEE. *IEEE Transaction On Mobile Computing*, vol. 12, no. 3, March 2013.

[7] Kotecha DK, Popat S, "Multi-objective genetic algorithm based adaptive QoS routing in MANET", *IEEE Congrss on Evolutionary Computation* (CEC); pp-1423-28 , 2007

[8] J. Zhou, H. Tan, Y. Deng, L. C. and D. D. Liu, "Ant Colony based energy control routing protocol for mobile ad-hoc networks under different node mobility models" *EURAJIP Journal on wireless communications and networking 2016*.

[9] Ali H, Shahzad W, Khan F, "Energy-efficient clustering in mobile ad-hoc networks using multi objective particle swarm optimization" *Appl soft comput* vol,12, pp 1913-1928, 2012,

[10] Bitam S, Mellouk A, Zeadally S, "Hybr: a hybrid bio-inspired bee swarm routing protocol for safety applications in vehicular ad-hoc networks(VANETS)", *Journal of system Architecture*, Elsevier.com vol 59 no 10, pp 953-67, 2013

[11] Misra S, Rajesh G, "Bird flight-inspired routing protocol for mobile ad-hoc networks", *ACM Transactions Auton Adapt system*, vol 6 no. 4, pp,1-37, 2011.

[12] Gianni D.C, Frederick and Luca M.G., Ant Hoc Net: ant-based hybrid routing algorithm for mobile ad-hoc networks", *Proceedings of parallel problem solving from nature (PPSN)*, pp 461-470, 2004.

[13] Bing S, Yang L., Zhenbo L and Jaiapinc C., "Ant-Based On-Demand Energy Routing Protocol for Ad-hoc Wireless networks", *Proceedings of IEEE International Conference on WiCom*, pp 1516-1519, 2007

[14] G.Ding, L.Shi, X.Wu and Y.Zhang, "Improved Ant Colony Algorithm with Multi-Strategies for QoS Routing Problems." *IEEE 8th International Conference on Natural Computation*, pp 767-771, 2012.

[15] C. W. Wu, T. C. Chiang, and L. C. Fu, "An Ant Colony Optimization for Multi-objective Clustering in Mobile Ad Hoc Networks" *IEEE Congress on Evolutionary Computation (CEC)*, pp 2963-68 2014.

[16] Deepalakshmi and Radhakrishnan, "An ant based multi objective quality of service rouing for mobile ad hoc networks " *EURASIP Journal on wireless communications and networking 2011*.

[17] Antoniou, P., Pitsillides, A., Towards a Scalable and Self-adaptable Congestion Control Approach for Autonomous Decentralized Networks, Nature-Inspired Smart Information Systems Annual Symposiu (NiSIS07), St Julians, Malta, 26 November-27, 2007.

[18] Lotka, Alfred, "Elements of Physical Biology", Williams and Wilkins, Baltimore, MD, 1925, Volterra, Vito, "Variations and fluctuations of the numbers of individuals in animal species living together", translation in Chapman, R., 1931, Animal Ecology, New York, McGraw Hill, pp. 409 – 448, 1926

[19] Antoniou, P., Pitsillides, A "Congestion Control in Wireless Sensor Networks based on the Lotka Volterra Competition Model", *Biologically Inspired Networking and Sensing*, August 2011

[20] Takeuchi, Yasuhiro; Adachi, Norihiko, "The existence of Globally Stable Equilibria of Ecosystems of the Generalized Volterra Type", *Journal of Mathematical Biology*, Vol.10Springer- Verlag, pp. 401 – 415, 1980,

[21] Roy, A. B.; Solimano, Fortunata, "Global stability and oscillations in classical Lotka-Volterra loops", *Journal of Mathematical Biology*, Vol. 24, pp. 603-617, 1987.

Epilepsy Detecting and Halting Mechanism Using Wireless Sensor Networks

Sayantani Basu, Ananda Kumar S. and Bhuvana Shanmugam

Abstract—**Epilepsy is a condition that affects thousands of people worldwide. In the laboratory setting, it becomes difficult to monitor patients and analyze when the next seizure would recur. Although algorithms have been proposed for deriving when the next seizure is probable, it is difficult to generalize such models for the various types of epilepsy that are occurring every day. A more promising solution is the use of Wireless Sensor Networks (WSNs) that is proposed to simulate small electrodes used in EEG that will be placed on the scalp of the patient as a wearable device along with a portable kit that is capable of monitoring the patient in both ambulatory and resting condition. As much as a detection system is required for epilepsy, a halting mechanism is also needed to prevent such high flow of bio-electrical signals in the brain during seizures. It is estimated that millions of brain cells die during epileptic seizures, which can prove detrimental or even fatal in some cases. In order to overcome this, an IoT-based epilepsy detection and halting system with wireless sensor networks and focal cooling mechanism has been proposed in order to regionally cool the regions of the brain when a seizure is probable or suddenly occurs.**

Index Terms—**epilepsy, seizure detection, seizure halting, wireless sensor networks.**

Original Research Paper
DOI: 10.7251/ELS1822034B

I. Introduction

Wireless sensor networks (WSNs) are a class of wireless networks that use sensors to monitor a specific environment. WSNs have made their way to several interesting applications in healthcare over the last decade [1]. In addition to being of potential use to patients, such systems also find considerable applications for children and elders.

Usually the group of sensors carried or worn by the patient (in the form of wearable sensors) forms the Body Area Network (BAN). The sensors located in the immediate surrounding environment form the Personal Area Network (PAN). Generally, monitoring systems consist of healthcare professionals viewing and interacting with the patient via a Graphical User Interface (GUI) in the form of a mobile application whereas in detecting systems, an algorithm judges the condition of a patient using Artificial Intelligence and Statistical models.

In the healthcare domain, WSN systems commonly comprise the following components: (i) BAN Subsystem, (ii) PAN Subsystem, (iii) Wide Area Networks (WAN), (iv) Gateway to Wide Area Networks (GWAN), and (v) Patients and other users. The BAN subsystem consists of an ad hoc sensor network that is wearable by the patients. Some examples include RFID tags, accelerometers and EEG sensors. Care should be taken so that the sensors do not cause any harm to the patients since they will be required to wear them for prolonged durations. The PAN subsystem consists of the devices in the immediate surrounding environment of the patient. Such a subsystem is also capable of features like location tracking, which may necessitate the use of RFID, Bluetooth, Near Field Communication (NFC) and GPS facilities as well. The Medium Access Control (MAC) layer should be made energy efficient to make the system low-power. All constituents among a subsystem should be interconnected appropriately. The WAN subsystem is needed for remote monitoring scenarios. If the healthcare system is to be implemented globally, satellite networks may also be employed. GWAN is used for the purpose of connecting PAN subsystem and WAN subsystem to the WAN. Finally, as mentioned earlier, the entire system is used by patients or other users like children or elders.

The evolution of IoT (Internet of Things) has resulted in efficiency and better exchange of data using technologies like WSNs and embedded systems. The present work has focused on an IoT-based system involving usage of WSNs for detecting and halting epilepsy. Epilepsy is a condition of the brain defined by at least 2 unprovoked seizures occurring at >24 hrs apart and one unprovoked seizure or probable seizures occurring during the next 10 years [2]. This disease affects thousands of people worldwide and can be fatal in extreme conditions. Epilepsy detection has been an important topic in medical research. The exact cause of epilepsy and how to completely cure it is still an unsolved puzzle. Research has uncovered various types of epilepsy, broadly categorized as generalized epilepsy and partial epilepsy, and specific types including childhood epilepsy, temporal lobe epilepsy and focal epilepsy.

Epilepsy is most commonly detected using the technique of EEG (Electroencephalography). The graphs are then analyzed by doctors or healthcare professionals who determine the type

Manuscript received 18 December 2017. Received in revised form 22 April 2018 and 26 May 2018. Accepted for publication 5 June 2018.

Sayantani Basu is with the School of Computer Science and Engineering, VIT University, Vellore, Tamil Nadu, India (e-mail: sayantani.basu2014@vit.ac.in).

Ananda Kumar S. is with the School of Computer Science and Engineering, VIT University, Vellore, Tamil Nadu, India (e-mail: s.anandakumar@vit.ac.in)

Bhuvana Shanmugam is with the Sri Krishna College of Technology, Coimbatore, India, Vellore, Tamil Nadu, India (e-mail: ss.bhuvana@skct.edu.in).

of epilepsy and the associated course of treatment. In some cases, MRI and CT imaging is also used. However, in most cases, EEG graphs show continuing occurrences of seizures or only slightly decrease using medications. Most medications even cause harmful side effects. In other words, it is difficult for doctors to determine the exact type and origin of seizures from a single EEG report. It is even more challenging to predict the occurrence of the next possible seizure and immediately halting it. Common approaches to reduce epileptic seizures include using one or a combination of medications, surgery, brain stimulation and focal cooling [3].

During an epileptic attack, seizures may happen due to sudden misfiring or incorrect connections in neurons in the brain. This results in sudden increases in electrical voltage in the neural cells. Each epileptic attack damages hundreds of brain cells that can be very harmful for the patients. As a result, it is important to halt or at least reduce the intensity to prevent such damages.

In the present work, a model has been proposed that uses WSNs to monitor and detect epileptic seizures as well as a mechanism using focal cooling to halt the seizures.

The rest of this paper is organized as follows: Section II gives an overview of previous related work. Section III discusses about the proposed method. Section IV highlights the implementation and results. Section V concludes the paper and suggests possible future work.

II. Related Work

Previously, several methods have been proposed for seizure detection. Lay-Ekuakille et al. [4] have developed a system using WSNs to detect epilepsy from joint EEG-ECG-Ergospirometric signals. It consists of a wireless ECG and EEG systems. It uses a K4b^2, which is a device worn by patients for pulmonary monitoring purposes. It can be worn while the patient is in motion and operates on battery power. Generally, the wave ranges for a normal EEG have been observed to be as follows [5]: (i) alpha (8-13 Hz), (ii) beta (13-30 Hz), (iii) delta (0.5-4 Hz) and (iv) theta (4-7 Hz). Along with acquiring the ECG and EEG signals, authors have then measured the Heart Rate Variability (HRV) before and after exercise, while simultaneously observing the corresponding changes in the Average Message Transmission Time (AMTT). Amplitudes over 45 and 100 microvolts imply suspected cases of epilepsy. The authors have noted that a simulator can enhance their results and that the method can be improved if WSNs can be related to the foci.

Otoum et al. [6] have developed Epilepsy Patients Monitoring System (EPMS) using WSNs. More specifically, they have proposed an SMAC (Sensor Medium Access Control) based system in order to reduce the power consumption of the system. They have designed the system using MICAz sensor motes (developed by Crossbow Technology). The EPMS consists of five sensor nodes that acquire the seizure information and pass it on to the coordinator. The coordinator then sends the information to the receiver. They have evaluated the performance of their system using NS2 simulator. Their SMAC protocol has shown lower average delay in packets compared to the ZigBee protocol. Their future work suggests allowing patients more freedom of movement by incorporating GPS and routing protocols.

Sareen et al. in [7] have proposed a mobile framework to predict seizures from EEG data. They acquired the EEG signals using Emotiv EPOC headset containing 14 sensors. They have extracted the desired features using fast Walsh-Hadamard transform (FWHT) and Higher Order Spectral Analysis (HOSA). Then k-means has been used to obtain a classification accuracy of 94.6%. They have tested their model in Amazon EC2 cloud. The data stored in the cloud is also used to connect to other family members and doctors in case of medical emergencies. A drawback of their work is they are only predicting seizures and not proposing any first hand technique of combatting the seizures by the time medical help arrives.

Salem et al. [8] have proposed a Discrete Wavelet Transform (DWT) and Ant Colony Optimization (ACO) based approach with WSNs for detecting seizures. They have acquired the data by placing electrodes on the scalp of the patient and acquiring the data and forwarding it to a transceiver and storing the data on a Local Processing Unit (LPU). They have identified the ictal period (during which a seizure is occurring) as being characterized by a discharge of polymorphic waveforms of varying amplitude and frequency that exhibit continuous spikes. Their model has shown a detection rate (DR) of 100% and a False Alarm Rate (FAR) of 9%. The shortcoming of this model is that the data is being processed after recording, that is, it is not being implemented in a real-time scenario.

Borujeny et al. in [9] have proposed an algorithm using WSNs and k-nearest neighbors (kNN) for detection of epilepsy using accelerometry and have proved that it gives better performance compared to using neural networks. For the purpose of acquiring signals, they have used MICAz wireless motes. Three 2D accelerometer sensors are placed on the left thigh, left arm and right arm of the patient. The system is also capable of monitoring the patient and sending the location of the patient to the family members or hospital staff when a seizure occurs. However, the system is capable of detecting epilepsy only when the acquired signals show at least 50% of seizures.

Kramer et al. [10] have designed a system that works to detect seizures and alert close family members of an epilepsy patient. The motion sensing unit comprising an accelerometer and transmitter were fitted in the form of a bracelet on the patient's wrist. They have developed an algorithm using time and frequency domain analysis to map the motion of the subject with previously gathered ictal data obtained from video EEG. Their system correctly identifies 91% of the captured seizures. They have suggested refining the algorithm to have above 95% accuracy and test it on larger populations.

Jeppesen et al. in [11] have developed a portable device capable of seizure detection that uses Near infrared spectroscopy (NIRS). For recording the signals, they have used two PortaLite wireless NIRS devices. They have then evaluated the changes in levels of oxygenated- (HbO), deoxygenated- (HbR) and total-hemoglobin (HbT). Their method has shown that the levels change by 6-24% during seizures. They have suggested individual tailor-made seizure detection for patients in the future.

Yilmaz and Dehollain [12] have used a wireless approach for data transmission for the purpose of monitoring intracranial epilepsy. They have used inductive coupling which is performed with the same frequency as that of the power transfer. Implantation is necessary in order to sense the signals and full-duplex communication has been established between the implant and the external unit. The authors have suggested using energy-per-bit connections between the uplink and downlink channels for future designers.

Conradsen et al. in [13] have suggested a wireless surface electromyography (sEMG) device that can be used for recording epileptic seizures. Their system was capable of detecting 4 out of 7 seizures with a false detection rate of 0.003/h. However, in some instances the model was unable to record data and the authors have suggested testing sEMG on the biceps instead of the tibia.

El Menshawy et al. [14] have developed an algorithm for automated detection and analysis of epileptic seizures using signal processing techniques. Using MATLAB, they have also used feature extraction to reduce the vector space. They have stated that the limitation is that their approach has no error detection mechanism and absence of domain ontology for EEG.

TABLE I
Survey Table

Reference	Proposed Work	Limitations	Year
Lay-Ekuakille et al. [4]	EEG, ECG and HRV analysis	WSNs not related to the foci	2013
Otoum et al. [6]	EPMS and SMAC for monitoring	Does not allow patients enough freedom of movement	2015
Sareen et al. [7]	Mobile framework using FWHT and HOSA in cloud	Only predicting seizures	2016
Salem et al. [8]	DWT and ACO approach with LPU	It is not implemented in a real-time scenario	2014
Borujeny et al. [9]	kNN based detection model with accelerometer sensors	Detects only >50% of seizures	2013
Kramer et al. [10]	Bracelet for ictal data analysis using accelerometry	Not tested on larger populations	2011
Jeppesen et al. [11]	NIRS and changes in HbO, HbR and HbT levels in blood	Seizure detection is not tailor-made for different patients	2015
Yilmaz and Dehollain [12]	Inductive coupling and full-duplex communication between internal implant and external sensing unit	No presence of energy-per-bit connections between uplink and downlink channels	2014
Conradsen et al. [13]	sEMG placed on tibia for detection of seizures	Unable to record data in some cases; Not tested on biceps of patient	2012
El Menshawy et al. [14]	Automated detection using signal processing and feature extraction	No error detection mechanism; Absence of domain ontology	2015

III. Proposed Method

In the proposed method, the data is first acquired using WSNs. The EEG signals are recorded and processed simultaneously. This proposed system will work with inputs of both non-seizure as well as seizure data.

An independent component analysis is performed on the data in order to extract the channel spectra for quantitative analysis. The unwanted artifacts are then rejected by visualizing the 2-D component maps and individual activity power spectra of each of the components. Once this step is completed, the peak and amplitude (peak-to-peak) are calculated for each of the remaining channels.

The data points are then plotted for both seizure and non-seizure data. The classification boundary is then used for detection of the seizure data. Additionally, focal cooling mechanisms can also be included in this system for halting the seizures whenever they are detected. The proposed methodology is shown in Fig. 1. The entire proposed methodology consists of the following steps:

1. Data Acquisition from Epilepsy patient using WSN electrodes: Data is acquired from the patient through wireless electrodes.
2. Input Seizure/Non-seizure data: The data (seizure/non-seizure) is input into the system.
3. Perform ICA: Independent Component Analysis is performed to evaluate the spectra of the EEG. ICA is also later used to perform artifact rejection.
4. Plot Channel Spectra: The channel spectra are plotted to find the frequencies at which peaks occur in seizure and non-seizure data.
5. Plot Activity Power Spectrum for each component: The activity power spectrum is also a useful parameter for visualizing peak and amplitude of seizures occurring in every individual Independent Component (IC).
6. Rejection of Artifacts: Rejection of artifacts is done to eliminate all unwanted signals which may give erroneous results in the model. This is done manually based on the ICA, channel spectra and activity power spectra.
7. Calculate peak and amplitude from Activity Power Spectrum: After rejection of artifacts, the activity power spectrum is considered only for the useful components.
8. Plot obtained data points: The data points are plotted using the peak and amplitude values obtained.
9. Classification boundary for seizure detection: A classification boundary is set for classifying seizure and non-seizure data.
10. Focal Cooling for Halting: Based on the classification, focal cooling is used to lower the temperature of the electrodes which can help in controlling and possibly halting the seizures.

IV. Implementation and Results

The EEGLab Toolbox [15] in MATLAB has been used for the purpose of this simulation. Data was obtained from the PhysioNet [16] database on CHB-MIT Scalp EEG [17]. This dataset contains both seizure and non-seizure EEG data of ep ilepsy patients.

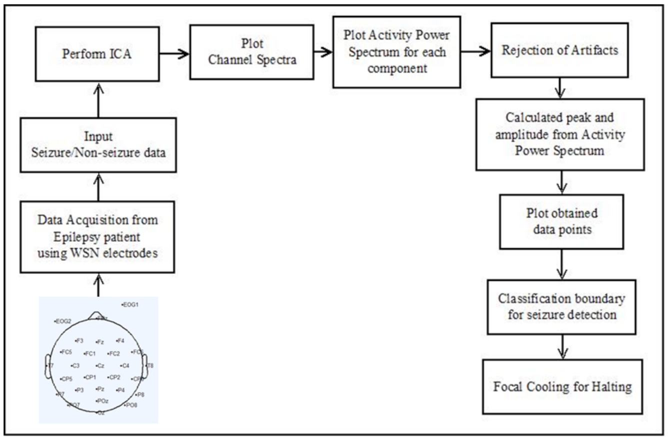

Fig. 1. Proposed Methodology.

A. Data Acquisition

The data considered from subject chb21 was evaluated for both non-seizure data and seizure data. The EEG signals were acquired using 28 electrodes. The locations of all the electrodes on the scalp are shown in Fig. 2.

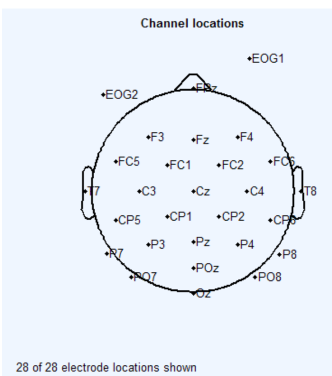

Fig. 2. Locations of 28 channels (WSN electrodes).

The EEG signals that have been acquired using this setup are shown in Fig. 3.

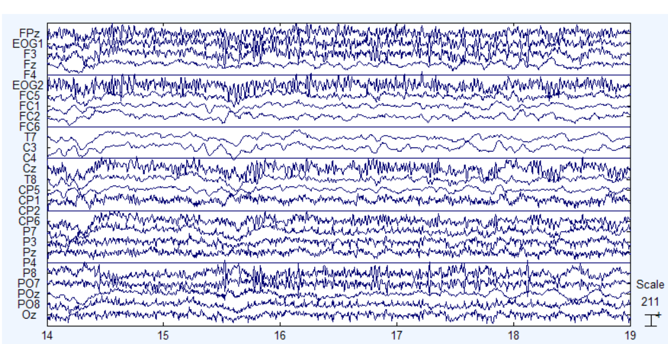

Fig. 3. Acquired EEG signals.

B. Independent Component Analysis (ICA)

In order to evaluate the spectra of the EEG, an ICA (Independent Component Analysis) was first performed on the given data. A rank of 21 was used for ICA in this experiment. ICA in EEG data is used to distinguish the particular regions of the brain contributing to robust EEG signals. The 2-D component maps of all the ICA components of non-seizure and seizure data are shown in Fig. 4 and Fig. 5 respectively.

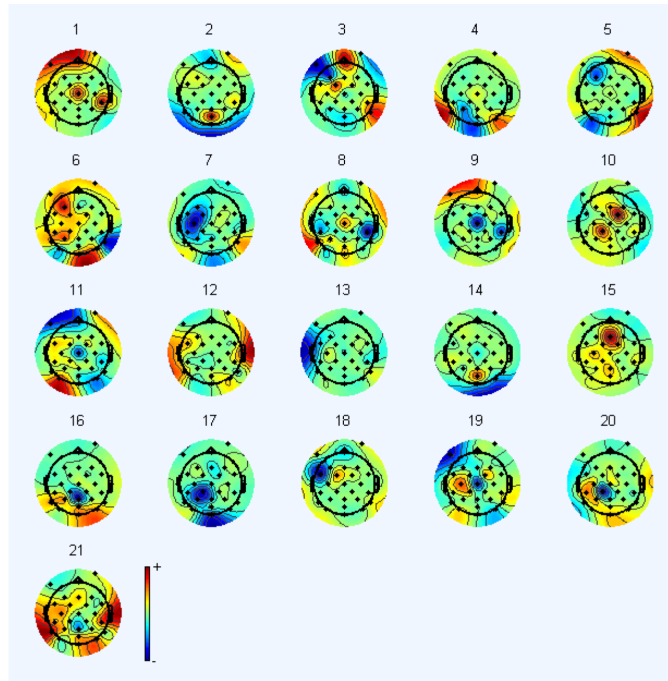

Fig. 4. 2-D Component plots of non-seizure data.

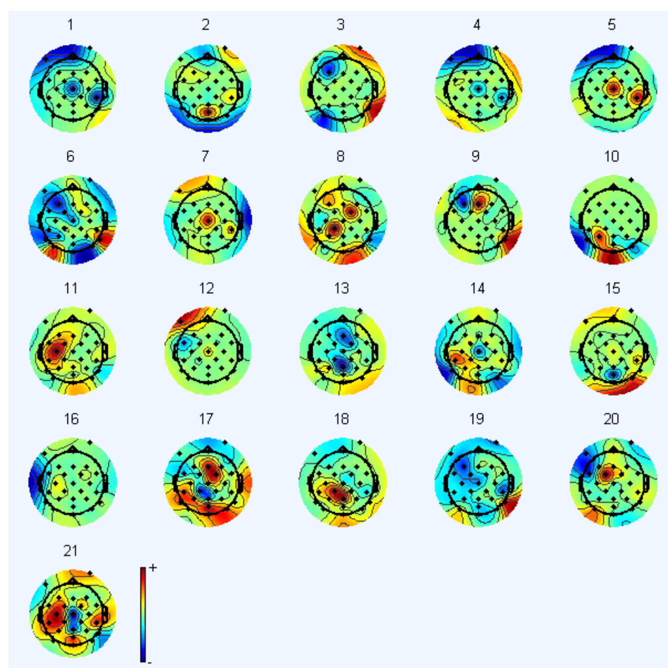

Fig. 5. 2-D Component plots of seizure data.

C. Channel Spectra

Once ICA has been performed, the spectrum of the EEG can be plotted to visualize the frequencies at which peaks are occurring and hence, quantitatively detect the possibility of seizures [18]. The channel spectrums for non-seizure and seizure data are shown in Fig. 6 and Fig. 7 respectively.

D. Activity Power Spectrum

The single channel activity power spectrum is then plotted for all the ICA components in both non-seizure and seizure data. Like the channel spectrum, the activity power spectrum also provides insights into information about peaks occurring in seizure and non-seizure data. One such activity power spectrum is shown in Fig. 8.

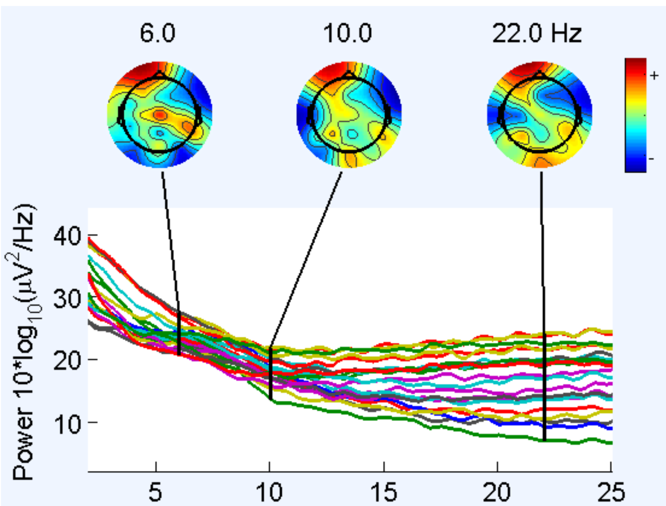

Fig. 6. Channel spectrum in non-seizure data.

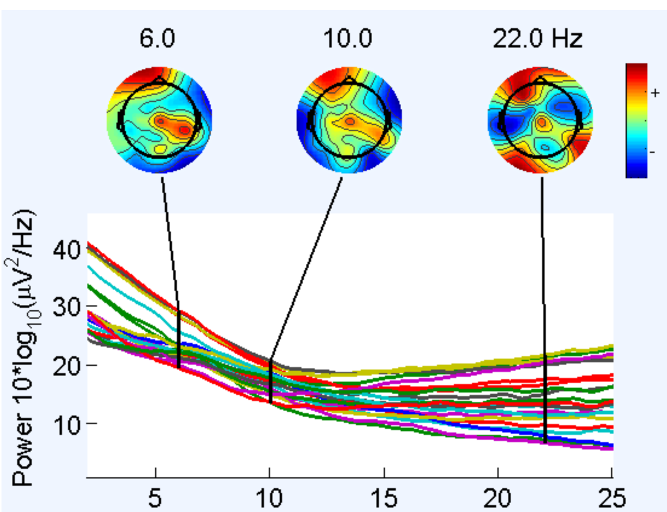

Fig. 7. Channel spectrum in seizure data.

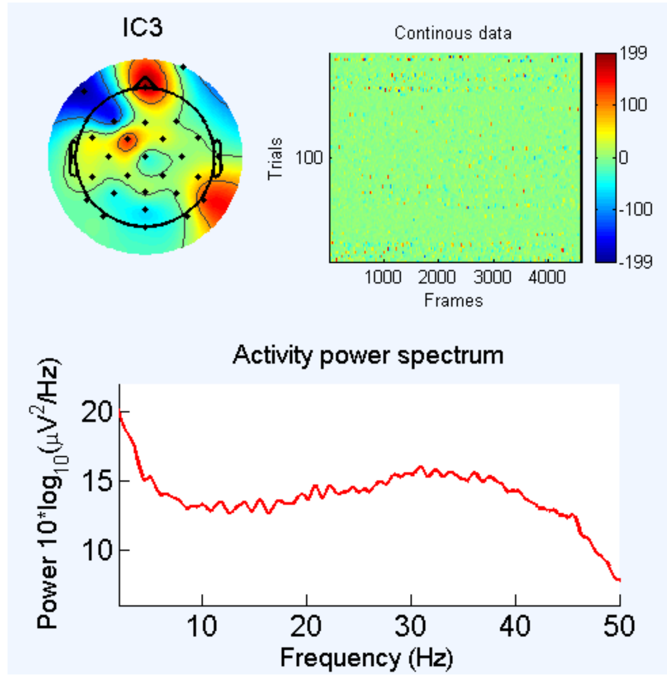

Fig. 8. Activity power spectrum for single component.

E. Artifact Rejection

Artifacts are unwanted signals due to eye blinking, heartbeat, muscle activity and so on that result in unwanted signals in EEG data. In order to retain only the brain signals, it is important to reject the artifacts using ICA. In this case, artifact rejection was done manually by visualizing each component.

F. Detection of Seizure Data

After the process of artifact rejection, only those components were retained that contributed to brain activities. From each graph, the peak and amplitude (peak-to-peak) was calculated. A separate set of data points were then obtained for non-seizure and seizure data. The points were then plotted as shown in Fig. 9 and a classification boundary (the line that was deemed best-fit) was set for detecting and separating seizure data from non-seizure data. This provides a suitable model for a particular subject (patient) and future prediction can be done based on the peak and amplitude.

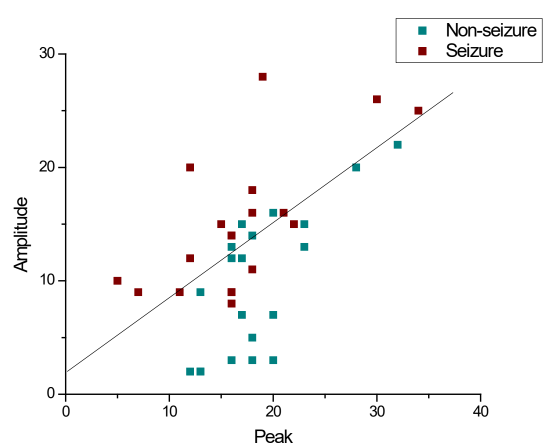

Fig. 9. Classification boundary for detection of seizure data.

An average classification accuracy of 90% and false positive rate of 9% was obtained using the proposed detection system. The proposed system performs at par with previously proposed systems having average accuracy 94.6% [7], detection rate 100% and false positive rate 9% [8], accuracy 91% and false negative rate 9% [10] efficiency 30% [11] and sensitivity 57% [13].

Hence, given any EEG sample, the proposed methodology can be followed and the detection of seizures can be carried out using its activity power spectrum and plotting its data point.

When seizures are detected, a focal cooling mechanism can be incorporated along with the mobile WSN EEG electrodes to cool the focal region in order to prevent impending seizures from arising.

V. Conclusion and Future Work

In this paper, an IoT-based system using wireless sensor networks has been proposed by incorporating machine learning for detection of seizures and a focal cooling mechanism for halting of seizures in epilepsy patients. This system is particularly helpful in the case of mobile EEG, especially in cases of patients with epilepsy who require monitoring even in ambulatory condition. The classification approach for detection of seizures has obtained 90% classification accuracy and 9% false positive rate, which is competent with the previous approaches.

Future approaches with regard to this work include enhancing the system with more advanced wireless electrodes and more advance machine learning algorithms.

References

[1] H. Alemdar and C. Ersoy, "Wireless sensor networks for healthcare: A survey," Comput. Networks, vol. 54, no. 15, pp. 2688–2710, 2010.

[2] R. S. Fisher, C. Acevedo, A. Arzimanoglou, A. Bogacz, J. H. Cross, C. Elger, et al., "ILAE Official Report: A practical clinical definition of epilepsy," Epilepsia, vol. 55, no. 4, pp. 475–482, 2014.

[3] M. Fujii, T. Inoue, S. Nomura, Y. Maruta, Y. He, H. Koizumi, et al., "Cooling of the epileptic focus suppresses seizures with minimal influence on neurologic functions," Epilepsia, vol. 53, no. 3, pp. 485–493, 2012.

[4] A. Lay-Ekuakille, P. Vergallo, A. Trabacca, M. De Rinaldis, F. Angelillo, F. Conversano, et al., "Low-frequency detection in ECG signals and joint EEG-Ergospirometric measurements for precautionary diagnosis," Meas. J. Int. Meas. Confed., vol. 46, no. 1, pp. 97–107, 2013.

[5] A. Lay-Ekuakille, P. Vergallo, D. Caratelli, F. Conversano, S. Casciaro, and A. Trabacca, "Multispectrum approach in quantitative EEG: Accuracy and physical effort," IEEE Sens. J., vol. 13, no. 9, pp. 3331–3340, 2013.

[6] S. Otoum, M. Ahmed, and H. T. Mouftah, "Sensor Medium Access Control (SMAC)-based epilepsy patients monitoring system," in Canadian Conference on Electrical and Computer Engineering, 2015, vol. 2015–June, no. June, pp. 1109–1114.

[7] S. Sareen, S. K. Sood, and S. K. Gupta, "An Automatic Prediction of Epileptic Seizures Using Cloud Computing and Wireless Sensor Networks," J. Med. Syst., vol. 40, no. 11, 2016.

[8] O. Salem, A. Naseem, and A. Mehaoua, "Epileptic seizure detection from EEG signal using Discrete Wavelet Transform and Ant Colony classifier," in Communications (ICC), 2014 IEEE International Conference on, 2014, pp. 3529–3534.

[9] G. T. Borujeny, M. Yazdi, A. Keshavarz-Haddad, and A. R. Borujeny, "Detection of epileptic seizure using wireless sensor networks.," J. Med. Signals Sens., vol. 3, no. 2, pp. 63–8, 2013.

[10] U. Kramer, S. Kipervasser, A. Shlitner, and R. Kuzniecky, "A Novel Portable Seizure Detection Alarm System: Preliminary Results," J. Clin. Neurophysiol., vol. 28, no. 1, pp. 36–38, 2011.

[11] J. Jeppesen, S. Beniczky, P. Johansen, P. Sidenius, and A. Fuglsang-Frederiksen, "Exploring the capability of wireless near infrared spectroscopy as a portable seizure detection device for epilepsy patients," Seizure, vol. 26, pp. 43–48, 2015.

[12] G. Yilmaz and C. Dehollain, "Single frequency wireless power transfer and full-duplex communication system for intracranial epilepsy monitoring," Microelectronics J., vol. 45, no. 12, pp. 1595–1602, 2014.

[13] I. Conradsen, S. Beniczky, P. Wolf, P. Jennum, and H. B. D. Sorensen, "Evaluation of novel algorithm embedded in a wearable sEMG device for seizure detection," in Proceedings of the Annual International Conference of the IEEE Engineering in Medicine and Biology Society, EMBS, 2012, pp. 2048–2051.

[14] M. El Menshawy, A. Benharref, and M. Serhani, "An automatic mobile-health based approach for EEG epileptic seizures detection," Expert Syst. Appl., vol. 42, no. 20, pp. 7157–7174, 2015.

[15] A. Delorme and S. Makeig, "EEGLAB: An open source toolbox for analysis of single-trial EEG dynamics including independent component analysis," J. Neurosci. Methods, vol. 134, no. 1, pp. 9–21, 2004.

[16] A. L. Goldberger et al., "PhysioBank, PhysioToolkit, and PhysioNet: Components of a New Research Resource for Complex Physiologic Signals," Circulation, vol. 101, no. 23, pp. e215–e220, 2000.

[17] A. Shoeb and J. Guttag, "Application of Machine Learning To Epileptic Seizure Detection," Seizure, pp. 975–982, 2010.

[18] A. S. M. D. S. Braga, B.D.R.R. Assis , J.T.R. Ribeiro, P.M.S. Polla, B.J.H. Pereira, R.G. Fonseca et al., "Quantitative EEG evaluation in patients with acute encephalopathy" Arq. Neuropsiquiatr., vol. 71, no. 12, pp. 937–42, 2013.

Research Issues in DFIG Based Wind Energy System

R. Rajasekaran and M. Mekala

Abstract—**Among different renewable energy sources, Wind energy is the most imperative energy source in power system. The development of grid connected wind energy conversion system expands, its grid connectivity issues has additionally been expanded. A portion of the issues are incorporates, for example, the regulation of voltage at Point of Common Coupling (PCC), reactive power absorption and injection, voltage sag and swell and etc. The Doubly Fed Induction Generator (DFIG) is most broadly utilized as a part of wind energy conversion system. DFIGs are extremely sensitive to grid voltage disturbances. With expanded entrance of wind energy as a renewable energy source the wind turbine should be connected to the grid during transient conditions like grid faults. The Fault Ride-Through (FRT) or Low Voltage Ride Through (LVRT) capability of wind turbines during grid faults is one of the core requirements to ensure stability in the power grid during transients and fault conditions. In this paper consists of various grid connectivity issues and research areas of wind energy conversion system and also the various control schemes for improving the LVRT system. These several techniques are used to improve the LVRT capability and limit the fault current to avoid the disconnection of DFIG from the grid under fault conditions for enhancement of stability and the performance of wind turbine.**

Index Terms—**Wind energy, Doubly Fed Induction Generator (DFIG), Fault Ride Through (FRT) or Low Voltage Ride Through (LVRT) capability, Grid Connectivity Technical Issues.**

Review Paper
DOI: 10.7251/ELS1822040R

I. Introduction

Renewable energy sources are including sun powered, wind, tidal, small Hydro, geothermal, denied determined fuel and fuel cell energies is supportable, reusable and earth benevolent and clean. With the expanding lack in petroleum products, and contamination issues renewable energy source has turned into an essential energy source on the planet [1]. The National Action Plan on Climate Change (NAPCC) was shaped in 2008 for environmental change control, has likewise considered part of renewable energy source in all out energy creation of India. NAPCC has additionally set an objective to expand the renewable energy source share in all out energy generation up to 15 percent till year 2020, which unmistakably demonstrates India‘s dedication towards a manageable improvement [2]. Under the Ministry of Non Renewable Energy (MNRE) program has done different alteration with respect to impetuses, plans and strategies for wind energy [3].

The Indian policy support for wind energy has driven India and it positioned fifth with biggest introduced wind power capacity. The aggregate introduced control limit was 19,565 MW on June 30, 2013 and now India is simply behind USA, China, Spain and Germany. Worldwide introduced wind control limit demonstrates India‘s better execution in wind energy. The aggregate introduced wind control limit in India had achieved 17.9 GW in August 2012.A fast development in wind control establishment has been estimated in southern and western states in India. A requirement for around 350-360 GW of aggregate energy age limit was accounted for by the Central Electricity Authority in its National Electricity Plan (2012) by the year 2022 [2],[3]. So among the different renewable energy sources wind energy is the quickest developing and most encouraging renewable energy source [4]-[11].

Wind Energy Conversion System (WECS) create power by utilizing the energy of wind to drive an electrical generator. The change of the kinetic energy of the approaching air stream into the electrical energy [12]. It happens in two stages: the extraction device, i.e., the wind turbine rotor catches the wind power movement by means of aerodynamically designed blades, and converts it into rotating mechanical energy, which drives the generator rotor. The electrical generator at that point changes over this rotating mechanical power into electrical power. A gear box might be utilized to coordinate the rotational speed of the wind turbine rotor with one that is fitting for the generator. The electrical power is then exchanged to the grid through a transformer. The association of the wind turbine to the system is conceivable at various levels of voltage [13] [14]. Power electronic converters can likewise be utilized for upgraded control extraction and variable speed operation of the wind turbine. The real parts of an average wind energy transformation system incorporate a wind turbine, generator, and interconnection mechanical assembly control systems.

II. Grid Code Requirements for Wind Turbines

The operation and grid connection requirements for wind turbines vary between utilities around the world, but some trends are common to most of them. A few of these requirements are summarized as follows [15], [16].

Manuscript received 18 December 2017. Received in revised form 19 April 2018 and 23 May 2018. Accepted for publication 5 June 2018.

R. Rajasekaran is with the Department of Electrical and Electronics Engineering, SNS College of Technology, Coimbatore, Tamilnadu, India (e-mail: rare457@gmail.com)

M. Mekala is with the Power Systems Engineering, SNS College of Technology, Coimbatore Tamilnadu, India (e-mail: mekalaeee1997@gmail.com)

A. Voltage and Frequency Operating Ranges

The wind turbines are required to stay connected to the grid and work within typical grid voltage and frequency ranges. Transmission level voltages are usually considered to be 115 kV and above. Lower voltages such as 66 kV and 33 kV are usually considered sub-transmission voltages. Voltages under33 kV are usually used for distribution. Voltages over 230 kV are viewed as additional high voltage and require diverse outlines contrasted with hardware utilized at bring down voltages.

The recurrence of the electrical system fluctuates by nation. The most electric power is produced at either 50 or 60 Hz. All the generating equipments in the electric system are designed to operate within very strict frequency margins. Grid codes specify that all generating plants should be able to operate continuously between a frequency range around the nominal frequency of the grid, usually between 49.5 to 50.5 Hz (for 50 Hz systems such as in Europe), and to operate for different periods of time when lower/higher frequencies down/up to a minimum/maximum limit, typically 47.5 and 52 Hz.

B. Reactive Power Control and Voltage Regulation

Wind farms are required to control their output reactive power in order to maintain the reactive power balance and the power factor at the Point Common Coupling (PCC) within the desired range. Grid codes additionally requires each wind turbine to control its own terminal voltage to steady an incentive by methods for an Automatic Voltage Regulator (AVR).

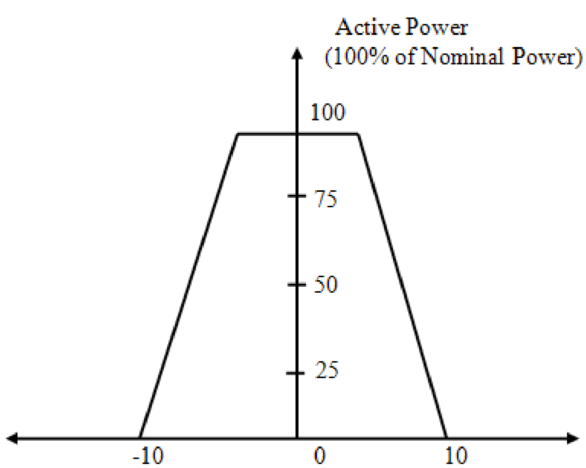

Fig.1. Typical reactive power limiting curve for wind generator.

The Voltage is closely related to the reactive power consequently wind turbines with the ability of controlling reactive power can support and regulate the PCC local system voltage.

C. Active Power and Frequency Control

Grid codes requires wind farms to provide a certain control of the output active power in order to ensure a stable frequency in the power system. Active power control requirements for supporting and stabilizing the system frequency refer to the ability of wind farms to regulate their power output to a defined level either by disconnecting turbines or by pitch control action for the case of variable speed wind turbines.

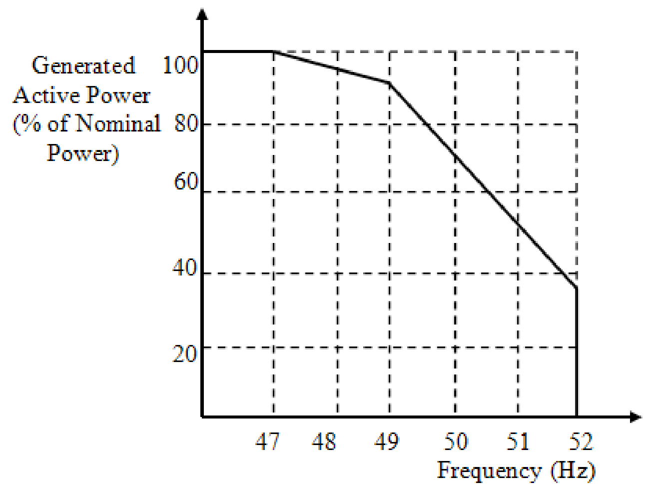

Fig. 2. Typical frequency controlled regulation of active power.

D. Low-Voltage Ride-Through (LVRT)

During grid faults, wind turbines are required to stay connected to the grid for a specific amount of time before being allowed to disconnect. Moreover, wind turbines are required to support the grid voltage during both symmetrical and asymmetrical grid voltage sags by means of reactive power compensation.

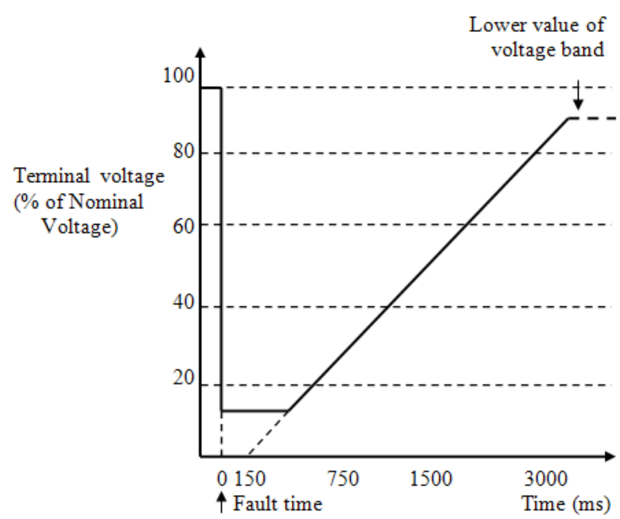

Fig. 3. Typical fault ride-through capability of a wind power generator.

The functional operation of LVRT is based on the comparison of the characteristic with that of the terminal voltage. The FRT requirements under voltage dip is one of the main focuses of the grid codes and also include fast active and reactive power restoration to the pre-fault values, after the system voltage returns to its normal operation levels.

E. High-Voltage Ride-Through (HVRT)

HVRT grid code states that wind turbines should be capable to stay connected to the power grid for a specific amount of time in the event the grid voltage goes above its upper limit value. With the rapid increase of large offshore wind farms, a new problem associated with the response of wind turbines to temporary overvoltage arises due to load shedding or unbalanced faults. Under this condition current may flow from the grid into dc link.

F. Power Quality Capability

Wind farms are required to deliver power with a desired quality by maintaining constant voltage or current harmonics within desired range. Flicker is another voltage quality issue on wind power generation associated with the electric grid. Fluctuations in the system voltage affect the power quality of grid connected wind turbine.

G. Wind Power Plants Modeling and Verification

Grid codes require that wind power plants must be modeled and controlled to meet the connection requirements. Wind farm owners/developers must provide models and system data to enable the system operator to investigate by simulations the interaction between the wind farm and the power system.

H. Communications and External Control

Grid codes require wind farm operators to provide the capability to connect and disconnect the wind turbines remotely. Furthermore, wind farm operators must provide signals corresponding to a number of parameters which are important for the system operators to enable proper operation of the power system. Communication and external control can be affected by harmonics. Harmonic disturbances are a phenomenon associated with the distortion of the fundamental sine wave and are produced by nonlinearity of electrical equipment.

III. Types of Generators Used in Wind Turbine System

Any types of three-phase generator can connect to with a wind turbine. Several different types of generators which are used in wind turbines are as follows. Asynchronous (induction) generator and synchronous generator. Squirrel cage induction generator (SCIG) and wound rotor induction generator (WRIG) are comes under asynchronous generators. Wound rotor generator (WRSG) and permanent magnet generator (PMSG) are comes under synchronous generator [17], [18].

A. Asynchronous Generator

a. *Squirrel Cage Induction Generator (SCIG)*

The fixed speed concept is used in this type of wind turbine. In this configuration the Squirrel Cage Induction Motor is directly connected to the wind through a transformer is shown in the Fig. 4. A capacitor bank is here for reactive power compensation and soft starter is used for smooth grid connection. The main disadvantage it does not support any speed control [17].

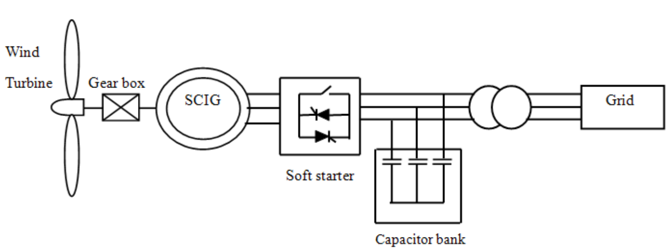

Fig. 4. SCIG wind turbine.

b. Wound rotor induction generator (WRIG)

The variable speed concept is used in this type .In this type of turbine Wound Rotor Induction Generator is directly connected to the grid as shown in Fig. 5.

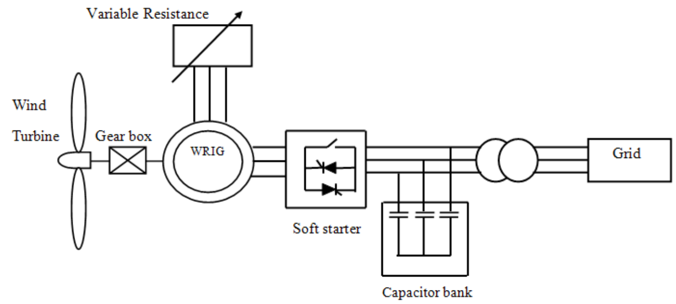

Fig. 5. WRIG wind turbine.

The variable rotor resistance is for controlling slip and power output of the generator. The soft starter used here for reduce inrush current and reactive power compensator is used to eliminate the reactive power demand. The disadvantages are speed range is limited, poor control of active and reactive power, the slip power is dissipated in the variable resistance as losses [18].

B. Synchronous Generator:

1) Wound Rotor Generator

Turbine with wound rotor connected to the grid is shown in figure 6.This configuration neither requires soft starter nor a reactive power comparator. The partial scale frequency converter used in this system will perform reactive power compensation as well as smooth grid connection. The wide range of dynamic speed control is depend on the size of frequency converter. The main disadvantage in the case of grid fault is it requires additional protection and uses slip rings, this makes electrical connection to the rotor.

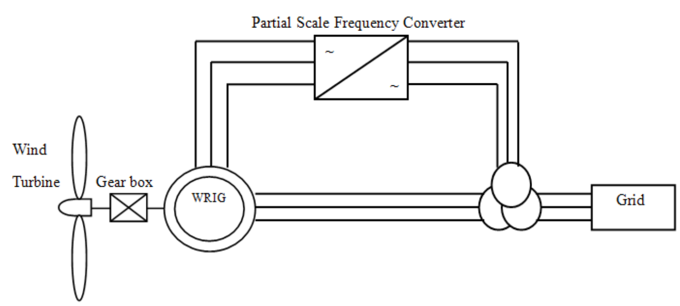

Fig. 6. WRIG wind turbine.

2) Permanent Magnet Generator

The generator is connected to the grid via full scale frequency converter. The frequency converter helps to control both the active and reactive power delivered by the generator to grid.

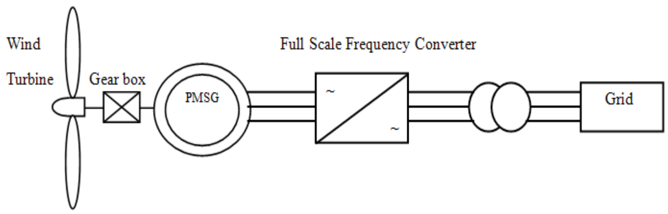

Fig. 7. PMSG wind turbine.

3) Doubly Fed Induction Generator

In order to satisfy the modern grid codes, the grid turbine system have the capability of reactive power support. Doubly fed induction generator based wind turbine system has more advantages than others [19]-[25].

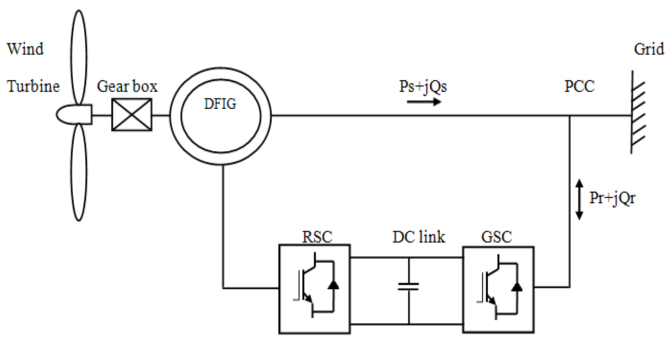

Fig. 8. Doubly Fed Induction Generator wind turbine.

DFIG wind turbine delivers power through the stator and rotor of the generator, the reactive power can be provided in two sides. Reactive power can be supported either through grid side converter or through rotor side converter. The stator part of the turbine is directly connected to the grid and the rotor is interfaced through a crowbar and a power converter [19]. The voltage to the stator part is applied from the grid and the voltage to the rotor is induced by the power converter. The doubly fed induction machine can be operated in generating mode in both sub-synchronous and super-synchronous modes [20].

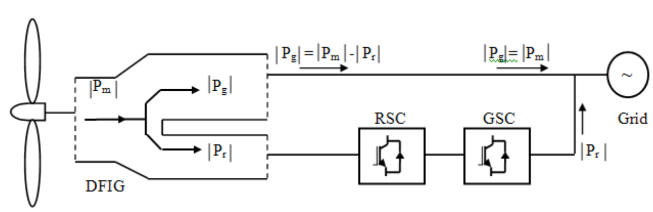

(a) Supersynchronous mode

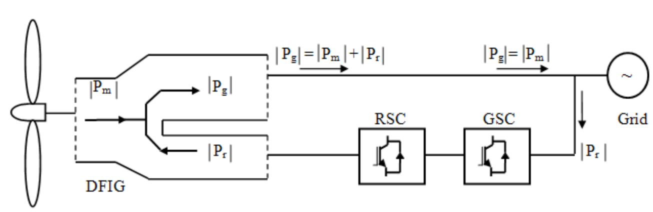

(b) Subsynchronous mode

Fig. 9. Operating modes of DFIG.

The power is delivered from the rotor through the power converter to the grid if the generator is operates above synchronous speed (super synchronous speed). If the generator is operates below synchronous speed (sub synchronous speed), then the power is delivered from the grid through the power converter to the rotor The power converter controls both the active and reactive power flow, the DC voltage of link capacitor between the grid and DFIG wind turbine by feeding the pulse width modules to the converters. A crowbar is implemented between the generator and converter to prevent short circuit in the wind energy system [19].Which may result in high current and high voltage. The RSC converter controls the flux of the DFIG wind turbine, which operates at the slip frequency that depends on the rotor speed of the generator. According to the maximum active and reactive power control capability of converter, the power rating of the RSC is determined. So DFIGs are widely used in modern WTs due to their power control capability, variable speed operation, low converter cost, and reduced power loss [20]-[25].

IV. Grid Connected Technical Issue on DFIG Based Wind Turbine

Doubly-Fed Induction Generator (DFIG) Wind Turbine (WT) can be affected by power system faults and requires crowbar protection. When the crowbar is triggered, the rotor is short circuited over the crowbar impedance, the DFIG operates as a Squirrel-cage Induction Generator (SCIG) that tends to drain large amount of reactive power from the grid during fault, potentially causing a voltage drop [26]. In this paper, the problem is many number of controllers are used that leads to the increase cost and complex design.

Novel active crowbar protection (NACB_P) system was designed to enhance the FRT capability. The problem in this is Capacitor is used in the protection circuit is to eliminate the ripples generated in the rotor current [27]. The problem is Overvoltage on DC link capacitor affect the converter during fault conditions.

The PI controller is used to enhance the low voltage ride through (LVRT) capability of doubly fed induction generator (DFIG) by means of STATCOM [28]. In this paper the problem is additional device needed for voltage sag compensation. STATCOM supports only for reactive power compensation.

A Fuzzy Logic Controlled Series Variable Resistor (FLC-SVR) used for transient stability enhancement of the grid co-nnected wind farms [29].The problem is when using of series variable resistor (SVR) it dissipates the large amount of energy that leads to losses.

Rotor Current-based Model Reference Adaptive System (MRAS) sensor less vector control provided for RSC. GTO-based thyristor controlled stator current limiter and dc chopper are used [30]. The problem is the control technique leads to complex design and also increase the installation cost.

Inductive and resistive Superconducting Fault Current Limiter(SFCL) are installed in series with the dc transmission line, and once the fault is detected, the current-limiting inductance or resistance will be activated to limit the fault current for Robustness improvement of a VSC-HVDC system with wind plants against DC fault [31]. The problem in this paper is it will leads to reactive power absorption and the fluctuations in the power.

Resistive-type Superconducting Fault Current Limiter (SFCL) connected in series with the DFIG rotor winding to limit the peak values of the fault rotor current, dc-link voltage [32]. It will leads to a complex design and it does not provide reactive power compensation are the problem associated in this paper.

A new controller approach for Unified Power Flow Controller (UPFC) is proposed to improve the LVRT capability. The shunt and series converters of the UPFC are controlled using a Hysteresis Current Controller (HCC) and Proportional Integral Controllers (PI) [33]. The major problem is: UPFC is a complex power electronic device developed to control and optimize the power flow in electrical power Transmission systems.

Study of the LVRT of grid-connected DFIG-based wind turbines including the crowbar. The back to back converter is used to control the reactive power from the power grid. The DFIG are very sensitive to grid faults and it will affect the converters [34]. It provides only about investigation of transient characteristics and the dynamic behavior of DFIG. The author does not consider about the problems generated in the DFIG based wind turbine system.

It proposes a modified flux-coupling-type Superconducting Fault Current Limiter (SFCL) is suggested to improve the Fault Ride-through (FRT) capability of DFIG [35]. Problem is the SFCL is used at different locations it increases the cost and produce switching harmonics.

The SFCL is used to limit the fault current, compensate the terminal voltage drop. The power fluctuation is suppressed by the Superconducting Magnetic Energy Storage (SMES) [36]. Problem is Combined operation of SFCL and SMES provide the Complex Controller design.

Improving the Fault Ride-Through Capability of DFIG Based Wind Turbine Using Superconducting Fault Current Limiter (SFCL). The SFCL is used to reduce fault current level at the stator side and to improve FRT capability of the system [37]. It does not limit the rotor short circuit current in the DFIG based wind turbine is one of the problem in the proposed method.

The wind turbine current controllers need to be designed to eliminate the impact of grid voltage harmonics, especially low-order harmonics. This paper proposes a stator current harmonic suppression method using a sixth-order resonant controller to eliminate negative sequence fifth- and positive sequence seventh-order current harmonics. A stator current harmonic control loop is added to the conventional rotor current control loop for harmonic suppression [38]. The author does not consider about the voltage compensation and reactive power compensation.

The studies on Doubly Fed Induction Generator (DFIG) based wind farm integrated with one superconducting fault current limiter (SFCL) based passive voltage compensator and one transient voltage control (TVC) based active voltage compensator is used for transient voltage stability improvement [39]. Problem is the resistive type of SFCL work is based on the choosing of resistance value.Due to large amount energy consumption affect the voltage compensation.

This describes an experimental investigation of an alternative FRT approach using a brake chopper circuit across the converter dc link to ensure that the dc-link voltage remains under control during a fault. DFIG systems employs a rotor circuit crowbar to protect the rotor converter during a fault [40]. The additional chopper circuit is used that leads to additional components and switching stress.

V. Role of Control Schemes in Performance of Wind Turbine

A. Control of Rotor Side Converter (RSC):

In normal operation, the control scheme of the RSC is illustrated in Fig. 10. In order to decouple the electromagnetic torque and the rotor excitation current, the induction generator is controlled in the stator-flux oriented reference frame, which is a Synchronously rotating reference frame, with its -axis oriented along the stator-flux vector position (the stator-flux vector is calculated using us) [41]. The typical proportional-integral (PI) controllers are used for regulation in the rotor speed and reactive power (outer) control loops as well as the rotor current (inner) control loops.

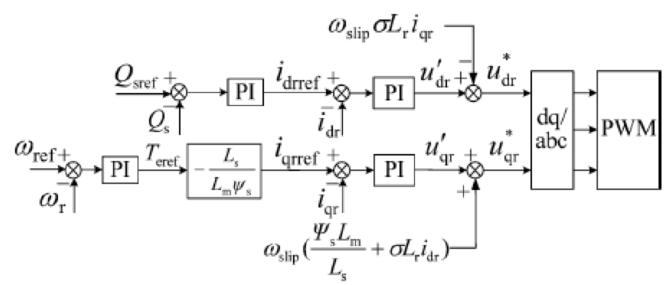

Fig. 10. Control scheme of the RSC during normal operation.

When a short-term low-voltage fault occurs, the incoming power from the wind and the power flowing into the grid are imbalanced instantaneously, resulting in the transient excessive currents in the rotor and stator circuits. Therefore from the energy balance point of view, the key point of suppressing the over-currents in the rotor and stator circuits is to reduce the imbalanced energy flowing through the DFIG WT system. When at least one of the monitored parameters, including the rotor current, stator current, DC-link voltage, and grid voltage, exceeds its respective protection setting due to the grid fault, LVRT control strategy will be triggered in [43]. With this control strategy, the rotor side controller will increase the generator rotor speed by reducing the generator torque to zero during the fault, in order to absorb and convert the incoming energy from the wind into the kinetic energy in the WT inertia. The increased kinetic energy can be transformed and released into the grid after the fault clearance. The control scheme of the RSC against grid faults is illustrated in Fig. 11.

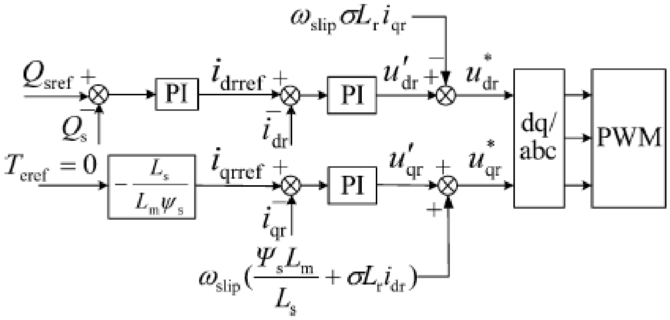

Fig. 11. Control scheme of the RSC during grid faults.

B. Control of Grid Side Converter (GSC)

In Fig. 12. shows the control scheme of the GSC in normal operation, where u_a and i_L are the grid-side converter voltage vector and the grid-side inductor current vector, respectively. In order to obtain the independent control of active and reactive power flowing between the grid and the GSC, the converter control operates in the grid-voltage oriented reference frame, which is a synchronously rotating reference frame, with its d-axis oriented along the grid-voltage vector position [41]. Similarly, the typical PI controllers are used for regulation in the DC-link voltage (outer) control loop and the grid side inductor current (inner) control loops.

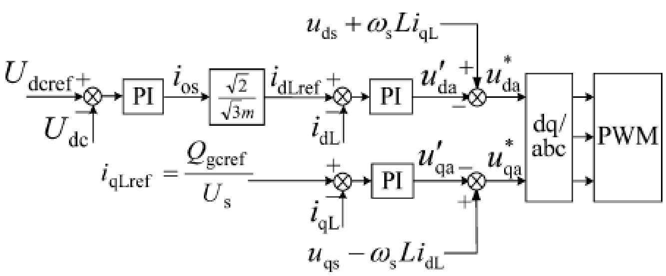

Fig. 12. Control diagram of the GSC in normal operation.

In normal operation, when the power flowing through the grid and rotor side converters is balanced i_{os} is equal to i_{or}, so the DC-link voltage is constant. When the grid voltage dips, i_{os} may not be equal to i_{od} due to the instantaneous unbalanced power flow between the grid and rotor side converters, and therefore the DC-link voltage may fluctuate. In order to reduce the fluctuation of the DC-link voltage, the item (P_r/u_{ds}) reflecting the instantaneous variation of the output power of the rotor side controller is directly set as the reference of the during the grid fault [42]. However, the stator voltage may reduce to zero during the grid fault. This will introduce an extremely high transient value of i_{dL}. The detailed control scheme of the GSC during the grid fault is shown in Fig. 13.

In this paper [43], when the rotor current, stator current, DC-link voltage, or grid voltage exceeds its respective relay setting due to the grid voltage dip, the term (P_r/U_{dc}) describing i_{or} is represented as a disturbance to compensate the instantaneous rotor power in the control scheme.

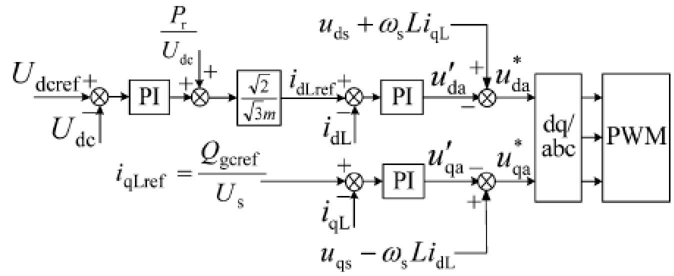

Fig. 13. Control scheme of the grid side converter during a grid fault.

VI. Possible Solutions

There are various possible solutions are available to avoid the problems in DFIG based wind turbine. These techniques can be splited into two categories by Adding external hardware to the conventional DFIG and using different control scheme with conventional DFIG.

A. Adding the Crowbar

The first solution to add LVRT capability to the DFIG is using crowbar resistance. In this solution, a set of three resistors are activated to be connected to the rotor upon the fault occurrence to bypass the RSC furthermore the gating signals for RSC and GSC are turned off. However, the control of the active and reactive powers is lost during the crowbar operation and the DFIG operates as a squirrel cage induction generator which absorbs reactive power from the grid leading to worst voltage dip situation. The position of the crowbar resistance is shown in Fig. 14.

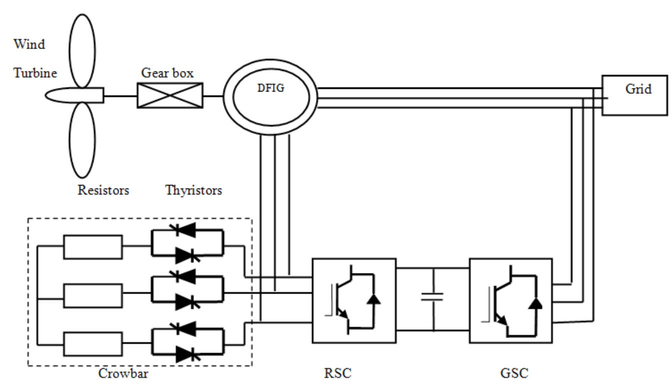

Fig. 14. DFIG with Crowbar.

B. Dynamic Voltage Restorer (DVR)

Another solution for adding LVRT capability for DFIG is using DVR in series with the DFIG to compensate the low voltage of the grid is shown in Fig. 15. The DVR consists of a battery, a three phase inverter, a filter and an injection transformer. The DVR has a great advantage of enabling DFIG to work in almost normal condition under symmetrical and asymmetrical faults.

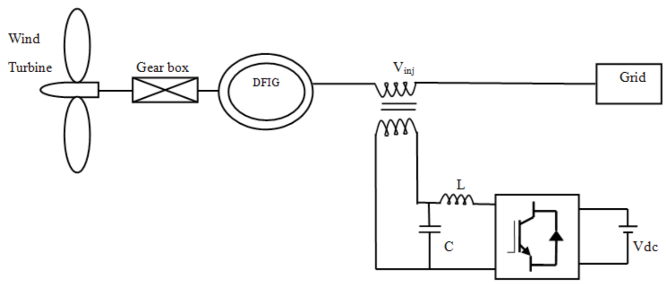

Fig. 15. Applying DVR to DFIG.

C. Superconducting Fault Current Limiter (SFCL) and Superconducting Magnetic Energy Storage (SMES)

Another solution is to connect a Superconducting Fault Current Limiter (SFCL) and Superconducting Magnetic Energy Storage (SMES) unit with the PCC to improve the dynamic performance of a wind energy conversion system equipped with DFIG during low voltage. The SMES circuit is composed of capacitor, DC chopper, and superconducting coil with inductance (LSC) shown in Fig 16. During the fault condition on stator side, SFCL is connected between the DFIG and grid to decrease the fault current and avoid the voltage drop. The SMES is connected in the DFIG based wind energy conversion system for avoiding the power fluctuations.

The SFCL is operates only if the current exceeds a threshold level. The SMES is used to eliminate the unbalanced kinetic energy after the operation of the SFCL, so that the remaining power fluctuation can be suppressed.

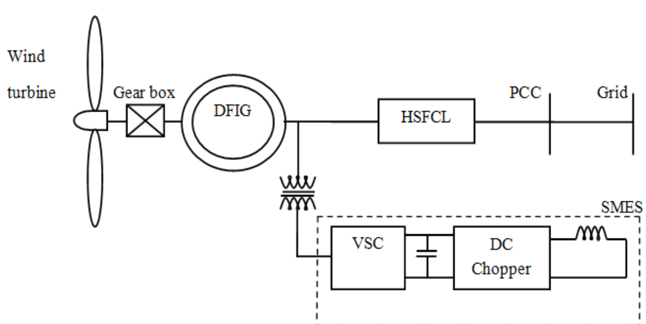

Fig. 16. Applying SMES to DFIG.

D. Chopper Circuit

Another solution controls the DC link voltage by adding a chopper circuit to the capacitor to release the excess energy from the capacitor besides overrating the diodes of the RSC to handle the high fault current.

E. Active and Passive Compensators

Another solution is using active and passive compensators are used. In this technique, a damping resistor in series with the stator (passive compensator) is used in addition to changing the mode of control of RSC to active ride-through compensator mode (active compensator). In active compensator mode the RSC uses the d and q components of the rotor currents to suppress the oscillations in the stator flux and limit the rotor current. Furthermore, a nonlinear control of the GSC has been used to contain the DC-link voltage within its safe limits.

VII. Conclusion

This paper has reviewed on major grid code requirements of DFIG based wind turbine. Among the various grid code requirements the Fault Ride-Through (FRT) or Low Voltage Ride Through (LVRT) capability of wind turbines is one of the core requirements to ensure stability in the power grid during transients and fault conditions. In this paper discussed about the various types of generators used in the wind energy conversion system. As a result DFIG has the better performance and has the more advantages compared to other generators. Then the literature review on various papers and the technical issues on DFIG based wind turbine system are provided.

References

[1] A. Kumar, “Dfig-Based Wind Power Conversion System Connected To Grid”, *International Journal of Technical Research and Applications*,Vol.1, Issue 3, PP. 15-24, (2013).

[2] S. Madhu and S. Payal, “A Review of Wind Energy Scenario in India”, International Research Journal of Environment Sciences, ISSN 2319–1414, Vol.3 (4),87-92, April (2014).

[3] R. Thresher, M. Robinson and P. Veers, “Wind Energy Technology: Current Status and R&D Future”, *National Renewable Energy Laboratory*, August(2008).

[4] S. Muller, M. Deicke and R. W. De Doncker, “Doubly fed induction generator systems for wind turbine,” *IEEE Industry Applications Magazine*, Vol.3, , pp. 26-33,(2002).

[5] R. Pena, J. C. Clare and G. M. Asher, “Doubly fed induction generator using back-to-back PWM converts and its application to variable speed wind-energy generation,” *IEE Proceedings Electrical Power Application*, Vol.143, pp. 231-241,(1996).

[6] Tapia, G. Tapia, J. X. Ostolaza and J. R. Saenz, “Modeling and control of a wind turbine driven doubly fed induction generator,” *IEEE Transactions on Energy Conversion*, Vol.18, pp. 194- 204,(2003).

[7] Y. Lei, A. Mullane, G. Lightbody, and R. Yacamini, “Modeling of the Wind Turbine With a Doubly Fed Induction Generator for Grid Integration Studies,” *IEEE Transactions on Energy Conversion*, Vol. 21(1), pp.257-264,(2006).

[8] V. Akhmatoy and H. Krudsen, “Modeling of windmill induction generator in dynamic simulation programs,” Proc. *IEEE Int. Conference on Power Technology*, Budapest, Hungary, paper No. 108,(1999).

[9] H. Li and Z.Chen, “Overview of generator topologies for wind turbines,” IET Proc. *Renewable Power Generation*, vol. 2, no. 2, pp. 123–138,(2008).

[10] L. Mihet-Popa, F. Blaabrierg, “Wind Turbine Generator Modeling and Simulation Where Rotational Speed is the Controlled Variable”, *IEEE Transactions on Industry Applications,* Vol. 40.No.1, (2004).

[11] B.H. Chowary, Srinivas Chellapilla, “Doubly-fed induction generator for variable speed wind power generation” *Transactions on Electric Power System Research*, Vol.76, pp. 786-800, (2006).

[12] A. Nouh And F. Mohamed, “Wind Energy Conversion Systems Classifications and Trends in Application”, *The fifth International Renewable Energy Congress (IREC)*, (2014).

[13] Z. Maira, X. David, B. Yuwen,“ Synchronous generator based wind energy conversion system (WECS) using multi-modular converters with autonomous controllers,” *IEEE, Electric Machines & Drives Conference (IEMDC)*, pp. 819 – 824, 2011.

[14] Y. Amirat, M. E. H. Benbouzid, B. Bensaker, R. Wamkeue, H. Mangel, “The State of the Art of Generators for Wind Energy Conversion Systems,” Hal-00527554, version 1, 19 Oct.(2010).

[15] W. Qiao and R.G. Harley, “Grid connection requirements and solutions

for DFIG wind turbines," Proc. *IEEE Energy 2030 Conference*, Atlanta, GA, pp. 1-8, (2008).

[16] C. Abbey and G. Joos, "Effect of low voltage ride through (LVRT) characteristic on voltage stability," Proc. *IEEE PES General Meeting*, San Francisco, CA, USA, June 12-16, , pp. 1901-1907,(2005).

[17] A. Kushwaha and I. Singh, "Literature review paper on doubly fed induction generator wind turbine technology", *International Journal of Enhanced Research in Science Technology & Engineering*, ISSN: 2319-7463, Vol. 2 Issue 9, pp: (44-50), September (2013).

[18] B. Babu1, Divya S, "Comparative study of different types of generators used in wind turbine and reactive power compensation", *IOSR Journal of Electrical and Electronics Engineering (IOSR-JEEE)* e-ISSN: 2278-1676, p-ISSN: 2320-3331, PP 95-99,(2015).

[19] S. O. Zain Elabideen, A. A. Helal, I. F. EI-Arabawy, "Low Voltage Ride Through Techniques For Dfig Based Wind Turbine", *International Journal of Electrical*, Computer, Energetic, Electronic and Communication Engirerering, Vol:10, No:7,(2016).

[20] W. L Kling, H. Polinder, J.G. Slootweg, "Dynamic modeling of a wind turbine with doubly fed induction generator." *Power engineering Society Summer Meeting*, Vancouver, Canada, July (2001).

[21] D. Zhou, F. Blaabjerg, T. Franke, M. Tonnes, and Mogens "Reduced Cost Of Reactive Power In Doubly Fed Induction Generator Wind Turbine System With Optimized Grid Filter", *IEEE Transactions On Power Electronics*, (2014).

[22] Z. Chen, J. M. Guerrero, F. Blaabjerg, "A review of the state of the art of power electronics for wind turbines," *IEEE Trans. Power Electronics*, vol.24,no.8,pp.1859-1875,(2009).

[23] R. Takahashi, H. Ichita, J. Tamura, M. Kimura, M. Ichinose, M. Futami, K. Ide, „Efficiency calculation of wind turbine generation system with doubly-fed induction generator," *International Conference on Electrical Machines* (ICEM)2010,PP.1-4,(2010).

[24] G. Abo-Khalil, H. Park, D. Lee, „Loss minimization control for doubly-fed induction generators in variable speed wind turbines," in Proc. of IECON 2007, pp. 1109-1114, (2007).

[25] Y. Lei, A. Mullane, and G. Lightbody, "Modeling of the wind turbine with a doubly fed induction generator for grid integration study," *IEEE Trans. Energy Conversion*, vol. 21, pp. 257-264,(2006).

[26] M. Q. Duong, F. Grimaccia, S. Leva, M. Mussetta, and K. Hung Le "A Hybrid Fuzzy-PI Cascade Controller for Transient Stability Improvement in DFIG Wind Generators", *IEEE conference publications*(2016).

[27] S. Swain and P. Kumar Ray "Ride-Through Capability Improvement of a Grid-Integrated DFIG based Wind Turbine System using a New Protection Design", *IEEEconference publications* (2016).

[28] P.K.Arunkumar, Dr.S.M.Kannan and I.Selvalakshmi "Low Voltage Ride Through Capability Improvement in a Grid Connected Wind Energy Conversion System using STATCOM", *IEEEconference publications* (2016).

[29] A B M Samsuzzamani Rabayet Sadnan and A.S.M. Jahid Hasan "Wind Farm Transient Stability improvement by Fuzzy Logic Controlled Series Variable Resistor", *9th International Conference on Electrical and Computer Engineering* (2016).

[30] S. K. Sahoo, A. K. Sinha and N. K. Kishore "Low Voltage Ride-Through of a Grid-Connected Doubly-Fed Induction Generator with Speed Sensorless Vector Control", *IEEE conference publications* (2016).

[31] L. Chen, H. Chen, Z. Shu, G. Zhang, T. Xia, and L. Ren, "Comparison of Inductive and Resistive SFCL to Robustness Improvement of a VSC-HVDC System With Wind Plants Against DC Fault", *IEEE TRANSACTIONS APPLIED SUPERCONDUCTIVITY,* VOL. 26, NO. 7, (2016).

[32] Z. CeZou, X. Y. Xiao, Y. F. Liu, Y. Zhang, and Y. H. Wang "Integrated Protection of DFIG-Based Wind Turbine With a Resistive-Type SFCL Under Symmetrical and Asymmetrical Faults", *IEEE Transactions On Applied Superconductivity* (2016).

[33] Yasser M. Alharbi andA. Abu-Siada "Application of UPFC to Improve the Low-Voltage-Ride-Through Capability of DFIG", *IEEE conference publications* (2015).

[34] Yazan M. Alsmadi, Longya Xu, Frede Blaabjerg, Alejandro Pina Ortega, and Aimeng Wang "Comprehensive Analysisof the Dynamic Behavior of Grid-Connected DFIG-Based Wind Turbines under LVRT Conditions" *IEEE conference publications* (2015).

[35] L. Chen, C. Deng, F. Zheng, S. Li, Y. Liu, and Y. Liao "Fault Ride-Through Capability Enhancement Of DFIG-Based Wind Turbine With a Flux-Coupling-Type SFCL Employed at Different Locations", *IEEE TRANSACTIONS ON APPLIED SUPERCONDUCTIVITY*, VOL. 25, NO. 3, (2015).

[36] I. Ngamroo and T. Karaipoom "Cooperative Control of SFCL and SMES for Enhancing Fault Ride Through Capability and Smoothing Power Fluctuation of DFIG Wind Farm", *IEEE Transactions On Applied Superconductivity* (2013).

[37] M. E. Elshiekh, D. Eldin A. M. Ahmed M. Azmy "Improving Fault Ride-Through Capability of DFIG Based Wind Turbine Using Superconducting Fault Current Limiter", *IEEEconference publications* (2012).

[38] C. Liu, F. Blaabjerg, W. Chen, and D. Xu, "Stator Current Harmonic Control With Resonant Controller for Doubly Fed Induction Generator", *IEEE TRANSACTIONS ON POWER ELECTRONICS*, VOL. 27, NO.7, (2012).

[39] R. Ou, X. Y. Xiao, Z. CeZou, Y. Zhang and Y. H. Wang "Cooperative Control of SFCL and Reactive Power for Improving the Transient Voltage Stability of Grid-Connected Wind Farm With DFIGs", *IEEE Transactions On Applied Superconductivity* (2016).

[40] G. Pannell, B. Zahawi, D. J. Atkinson, and P. Missailidis, "Evaluation of the Performance of a DC-Link Brake Chopper as a DFIG Low-Voltage Fault-Ride-Through Device", *IEEE TRANSACTIONS ON ENERGY CONVERSION*,(2012).

[41] R. Pena, J. C. Clare, and G. M. Asher, "Doubly fed induction generator using back-to-back PWM converters and its application to variable speed wind-energy generation," *Proc. Inst. Elect. Eng., Elect. Power Appl*., vol. 143, no. 3, pp. 231–241, May 1996.

[42] J. Yao, H. Li, Y. Liao, and Z. Chen, "An improved control strategy of limiting the DC-link voltage fluctuation for a doubly fed induction wind generator," *IEEE Trans. Power Electron*., vol. 23, no. 3, pp. 1205–1213,May 2008.

[43] L. Yang, Z. Xu, J. Østergaard, Z. Yang Dong, and K. P. Wong "Advanced Control Strategy of DFIG Wind Turbines for Power System Fault Ride Through" *IEEE TRANSACTIONS ON POWER SYSTEMS,* VOL. 27, NO. 2, MAY 2012.

A Collaborative Framework for Avoiding Interference Between Zigbee and WiFi for Effective Smart Metering Applications

Vikram. K. and Sarat Kumar Sahoo

***Abstract*—Energy management is one of the foremost priorities of research in many countries across the world. The introduction of modern information and communication technologies (ICT) are transforming the existing power grid, towards a more distributed and flexible "Smart Grid" (SG). The wireless sensor networks (WSN) are considered for data communication and are generally, incorporated with actuators to implement the control actions remotely. The wireless technologies like ZigBee (for automation), WiFi (for internet) and Bluetooth (entertainment) work in the 2.4GHz band. The coexistence of different wireless technologies working in the common area is unavoidable. Hence, this phenomenon degrades the performance of each other, due to the interference phenomenon. The wireless nodes with high energy had a great influence on the performance of the nodes working with low energy. Under the influence of interference, the low-power nodes experience the uncertain sleep-wake scheduling and increased delays in channel occupation. Interference also results in, high packet error rates (PER), decreased throughput, and high energy consumption. Hence for overcoming the above problems, A collaborative framework for an effective interference management and its avoidance is proposed in this paper. The framework proposed assures the effective ZigBee communication by systematic channel scheduling operating even under the influence of Wi-Fi. The work proposed performs better even under extreme interference conditions and the results obtained shows enriched performance.**

***Index Terms*—Advanced data communications, Home area networks, Interference, Smart meter, The 2.4GHz frequency band, Wi-Fi, ZigBee.**

Original Research Paper
DOI: 10.7251/ELS1822048V

Manuscript received 18 December 2017. Received in revised form 28 April 2018 and 1 June 2018. Accepted for publication 5 June 2018.

The authors would like to acknowledge the financial support from the Department of Science and Technology (DST), Government of India, Project no. DST/TSG/NTS/2013/59. This work has been carried out in School of Electrical Engineering, VIT University, Vellore, India.

Vikram K. is with the School of Electrical Engineering, VIT University, Vellore, TamilNadu, India. (phone: +91-9952566338; e-mail: vikram.k2014@vit.ac.in).

Sarat Kumar Sahoo is with School of Electrical Engineering, VIT University, Vellore, TamilNadu, India. 632014 (e-mail: sksahoo@vit.ac.in).

I. Introduction

The energy management using advanced metering infrastructure (AMI) employs WSN for monitoring the power usage of the end-user [1]. The monitoring and control areas for smart grid applications is an important research area. Smart meters will allow the consumers to interact with the utility companies and allow to monitor the power consumption on an hourly basis towards consumer side. Thus, with the introduction of Smart metering, every building should become smart and should adapt the better communication system for transmitting the data. The Internet of Things (IoT) plays a prominent role in the information transfer and controlling the load. This allows the consumer to decrease electricity usage bills and on the utility side, they can properly assess the load supply the demand [2]. There is need for research in terms of collaborative communication between different networks so as to form network of networks and SG communication system demands this integration of networks [3]. The implementation of IoT is based on IEEE 802.15.4 standard [4]. The networks operating in same frequency band (2.4GHz unlicensed) effects each other's performance. The networks with different standards like IEEE 802.15.4 (IoT based on ZigBee communication) and IEEE 802.11(WiFi) need to coexist with each other and the issue is addressed in this paper.

In many applications of SG, the WSN has already replaced wired data communication systems [5]. WSN, in general, refers to the wireless network based on ZigBee nodes effectively employed for data communication. The important characteristics of the WSN include low cost, ease of deployment. WSN supports the smart grid in decision making through the remote management, data collection, querying abilities [6]. The wireless technologies like ZigBee, WiFi, and Bluetooth operate in the 2.4GHz unlicensed frequency band is shown in figure 1 below. The channel operating in 2.4GHz is distributed between frequencies 2400MHz to 2483.5MHz. The ZigBee operation is defined by IEEE 802.15.4 standard. The ZigBee technology consists of 27 channels for data communications. Among the available channels, one channel operates in the 868MHz frequency band, 10 channels operated in the 915MHz band and remaining 16 channels (channel 11 to channel 26) operates in the 2.4GHz frequency band [7]. The WiFi (Wireless Fidelity) operates based on the IEEE 802.11 standard in the 2.4GHz band. The WiFi generally has 11 channels (in the USA), 13 channels (in Europe) and 14 channels (in Japan). But among the available, only channels 1, 6 and 11 are useful for data communication [8]. The WiFi access points and clients (Laptop's) are usually very near to continuous power supply and shall maintain high link strength a with high data speed. Because of high link strength the channel 1 of WiFi overlaps with the channels 11, 12, 13 and 14 of ZigBee, channel 6 of WiFi overlaps the channels 16, 17, 18, and 19 of ZigBee, and finally, channel 11 of WiFi overlaps the channels 21, 22, 23, and 24 of ZigBee. Though channels 15, 20, 25 and 26 of ZigBee node are affected partially or remains unaffected (free from interference) the network programmer cannot opt for these channels [9].

The Bluetooth technology operates based on IEEE 802.15.1 technology. The Bluetooth has 79 channels operating in the 2.4GHz band. But the data communication using this technology will not be much affected because of the interference. It is because data communication is based on Frequency hopping spread spectrum (FHSS) technology. As soon the data transmission is initiated it keeps on changing the frequencies until it reaches the destination [10]. Hence it has fewer effects of interference from WiFi. But disadvantage Bluetooth is it consumes more energy and covers less distance when compared to ZigBee nodes [11].

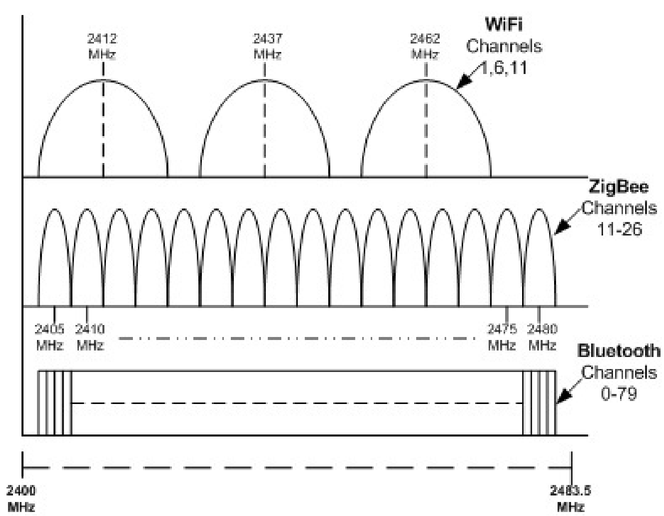

Fig. 1. Channel distribution of different technologies in 2.4GHz frequency band.

Though ZigBee is considered as a prominent technology for modern automation applications including IoT, it has certain difficulties in the coexistence mediums and research must be done to overcome the problems [12] [13]. The domestic applications like microwave ovens and cordless phones also emanate the electromagnetic radiation in the 2.4GHz band [14]. The coexistence of different wireless technologies in the vicinity of each other and working in the same frequency band affects the performance of each other. The performance of ZigBee in terms of packet delivery gets highly affected under the influence of WiFi when compared to Bluetooth. The electromagnetic radiation from the Microwave oven when switched ON will affect almost all the channels of ZigBee [15].

One of the best and emerging applications of WSN is monitoring the power system assets aimed at increasing the reliability of smart grid [16]. The prototype was developed for smart homes for monitoring the power usage and controlling purposes based on ZigBee communication [17]. The SecureHAN is based on ZigBee [18], employed for data communication about power usage between the appliance and the smart meter. Secure HAN emphasizes and addresses the complications raised due to the coexistence environment.

The Section II shows the background of the related works. Section III presents the mathematical model and algorithms. The mathematical results are presented in Section IV and the conclusion is given in Section V.

II. Related Works

The CCS algorithm is proposed for improving the performance of ZigBee operating under the influence of WiFi (IEEE 802.11b) operating in a 2.4GHz frequency [19]. The CCS comprises a scheduler to coordinate the signaling with temporary channel hopping for ZigBee data transformation operating in the vicinity of WiFi. The successive interference cancellation (SIC) to avoid the interference at physical layer level and improves the packet reception at the receiver side of ZigBee. In addition to SIC, the work also proposes the optimization model for the identification of accurate channel [20].

The advanced multichannel clustering algorithm aims for determining the interference and avoids it substantially. The algorithm proposed is aimed at improving the performance of ZigBee based cluster tree networks affected by WLAN access points (AP) and resolves the issues of channel utilization within the cluster [21]. The effects of interference on ZigBee communication in the coexistence model is based on the transmitter and receiver distance. The experimental setup based on distance and variation of distance for decreasing the interference has decreased the effect considerably [22]. The channel selection is a very significant parameter for better network performance. The algorithm ReSIST [23] is aimed for better channel selection and decreases the packet error rate (PER) significantly. The experimental evaluation of interference on IEEE 802.15.4 (ZigBee) in [24] by corresponding 2.4GHz frequency-based technologies like WLAN (IEEE 802.11b), Bluetooth (IEEE 802.15.1) and Microwave oven and the cordless phone is evaluated. It is discovered that the effect of Bluetooth on Zigbee results in PER of around 4%. The impact of WLAN on Zigbee can be avoided by better channel selection strategies and can limit the PER<10% can be achievable. Based on station assessment and determination of spectrum utility near cordless phone can only reduce the interference effects on ZigBee. Microwave oven radiation on 2.4 GHz WSN can be avoided by safer channel selection. The PER can be expected around 8% if the Zigbee node is placed at least 1.5m away from Microwave oven.

The work in [25] assessed the ZigBee propagation under WiFi interference for the applications of the smart grid. ZigBee may be to a great degree interfered by WiFi but if an "Ensured Distance" and "Safe Offset Frequency" is identified then it can be a better solution. It is exhibited that 8 meters between ZigBee and WiFi is considered as "secured" partition that can guarantee the better throughput for ZigBee. A multi-channel architecture in [26] was proposed for defeating the issue of concealed hubs and WLAN interference with the point of expanding packet delivery ratio (PDR). The Multi-Channel Cluster Tree (MCCT) convention with Adaptive Channel Access (ACA) calculation was proposed to decrease the effects of interference. Every sensor hub inside the system continuously examines each of the 16 channels by performing PDR measurements with a specific end goal to decide their inhabitance level. The facilitator performs counts for every channel to assure that every hub adds to the determination of the ideal channel as per set up needs.

The smart grid requirement for monitoring and control [27] have defined the necessity of the wireless sensors and actuator networks (WSAN). The WSAN is used for regulating the smart grid assets and calls for the prioritization of critical data. Two MAC layer-based algorithms were proposed. Firstly, delay aware cross layer algorithm (DRX) deals with delay estimation and prioritization of data. Secondly, the FDRX introduces the fairness into DRX and avoids few dominating nodes from occupying the communication channel. The work in [28] evaluates the performance of ZigBee based IoT aimed for smart homes under the close proximity of WLAN it is observed that because of coexistence the response time is getting affected. Hence the work carried will guarantee the delay experienced by ZigBee while maintaining the data rate of WLAN. The cross- layer multichannel MAC protocol was introduced in [29] for interference avoidance between WiFi and ZigBee operating in the 2.4GHz frequency band. Based on the present state interference calculation, the forthcoming interference is estimated based on hidden Markov model and based on the estimation the channel with low interference is assigned. Then when the packet reaches near the destination it will be processed by CMCMAC-FEC algorithm to recover the data lost because of collisions occurred during the transmission process.

III. Proposed Work

In our previous works, we have proposed a WSN protocol CMCMAC, aiming for strengthening the wireless data communication keeping in the view for smart metering applications [13]. The CMCMAC works efficiently for external interference and assures improved performance of IEEE 802.15.4 based network working in the vicinity of IEEE 802.11b. Initially, it estimates the delay and Received signal strength indicator (RSSI) values for all the possible linkages between the nodes in the network. After obtaining the initial values, the Hidden Markov Model (HMM) based prediction is employed for anticipating the channel with no interference. Then, clear channel assessment (CCA) period was adjusted to obtain the specified channel with in stipulated time based on the estimation from HMM. The fairness offered was obtained by adjusting CCA that was again dependent on MAC layer and Physical (PHY) layer regulations. In [27] a new forward error correction algorithm was added to the above work (FEC-CMCMAC). This algorithm mainly aims to improve the performance of above work so as to restore the collided data (partially lost) due to the data collision occurred because of external interference or internal interference. Though it notices the interference systematically, the channel shifting process is not practical and hence consuming a substantial amount of delay. Hence, for surpassing the above problem in 2.4GHz ISM band, the PSOLACES (Particle swarm optimization-based load aware channel estimation and channel scheduling for Zigbee networks under the influence of WiFi) was proposed [9]. The PSOLACES based collision-free multichannel super frame scheduling was employed to communicate the data without any collision. The channel with best energy function was selected for data transmission.

A. *The Collaborative Framework for Avoiding Interference between Zigbee and WiFi networks.*

A collaborative framework for avoiding the interference (CFAI) between the ZigBee and the WiFi nodes is proposed in this paper. The efficient and improved ZigBee communication under the interference conditions from WiFi is an important research problem considered in this paper. When compared to our previous works, in this paper we have proposed an improved mathematical analysis for avoiding interference. The block diagram of proposed work is pictorially represented in figure 2.

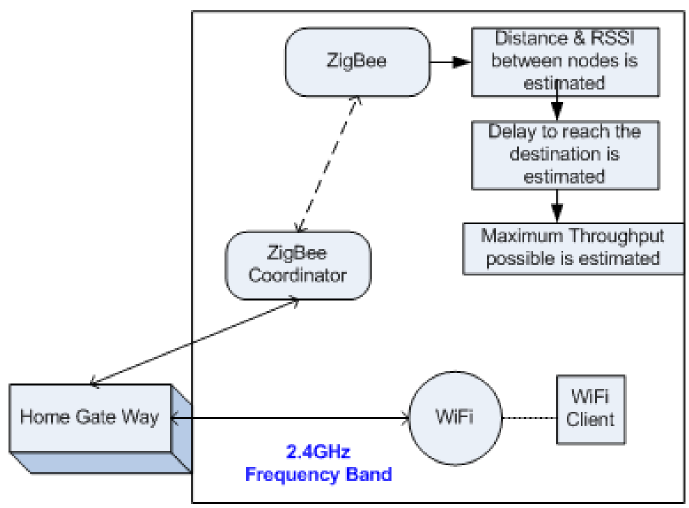

Fig. 2. Block diagram of the proposed work.

The architecture considered for the implementation of CFAI is as shown in figure 3. The modern smart home considering ZigBee for automation, WiFi for accessing internet and Home Gate Way (H\GW) acts as Smart meter for SG based energy management. The figure 3, consists of 4 ZigBee coordinators, connected through a wireless connection to about 17 ZigBee nodes. Where Each ZigBee coordinator is connected to about 4 to 5 ZigBee nodes. There are 4 WiFi access points (AP) and about 5 WiFi clients, each AP is connected to 1 to 2 WiFi clients. The position of all the nodes is assumed and placed such that they fall under each other's influence. The Zigbee coordinator and WiFi access points are connected to Home Gate-Way

(HGW) through wired network as shown in the figure. The HGW can be considered as Smart Meter.

CFAI helps in finding the best channel, based on minimized delay, and assures high throughput by effective channel utilization by maintaining good link strength. The CFAI allots ranking for the channels based on the chances for effective bandwidth utilization. When source node (ZigBee) is ready for data transmission, it estimates the quality of the channel for effective communication in the coexisting environments. Based on the quality of channel it transmits the information as early as possible. All the communication between ZigBee sensors and HGW is accomplished through the ZigBee coordinator. The CFAI is based on the arrangement as shown in the Fig. 2. CFAI reduces the interference based on the realization of distance and (RSSI) between two nodes, delay estimation, and throughput estimation. Initially, when the WSN node is ready for data communication to the destination (ZigBee coordinator), the source node estimates the distance and RSSI parameters for understanding the link strength.

1) Realization of the Distance and RSSI

Consider the reference node (WLAN) $b_n = (b_{n1}, b_{n2} \dots b_{nN})$ is focusing on path loss that can be expressed as a function of distance

$$P_L(\bar{d}_{hi}) = P_L(d_0) + 10n \log\left(\frac{\bar{d}_{hi}}{d_0}\right) \quad (1)$$

Where $\bar{d}_{hi}$ is the distance among the node *h* and anonymous node *i*, d_0 is the reference distance (for ZigBee typically the value of d_0 is taken to below 10m), *n* is considered as path loss exponent (the rate at which the signal/decay). The RSSI value P^r at a distance $\bar{d}_{hi}$ is

$$\mathrm{P}^r(\bar{d}_{hi}) = p^t - P_L(\bar{d}_{hi}) \quad (2)$$

For each pair of *nodes (h, i)* which is in transmission range(*r*), we can measure the received signal strength (P_{hi}^r). The set of such pair is as follows.

$$\Psi = \{(P_{hi}^r, \bar{d}_{hi}) : \|S_k - S_i\|^2 < r\} \quad (3)$$

The activity of AP in a node *i* and *h* can be represented by. It describes the activity of the node S_i seen by the node S_k that means distance, RSSI and path loss of the nodes. It depends on the transmission activity of node S_k and S_i. The activity of $A_{k,i}$ is a relative value between one and zero.

$$A_{k,i} = t_i(|Channel(S_k) - Channel(S_i)|) \quad (4)$$

Where t_i is the time that node S_i is active (measured between one and zero).

The arithmetic means of the transmission time of busy slots, denoted by *T*

$$T = (T_s \times (1 - P_c)) + (T_f \times P_c) \quad (5)$$

where P_c is the probability of unsuccessful transmission because of the collision.

The slot admittance probability of a node *i,* to the adjacent node *h,* computed at the position of node *k* and it represented by $\tau_i^{(k)}$. The arithmetic means of channel utilization of a node *i* from $\tau_i^{(h)}$ denoted by U_h, that is not disturbed by changes of neighboring nodes, U_h can be expressed as,

$$\mathrm{U}_h = \frac{c_n T(t)}{t} \quad (6)$$

where c_n is the number of occupied slots and *T(t)* is the average broadcast time of *node i* for the duration of *t*.

Let S_i be the set of all the nodes near to node *i.* The average busy slot size of node S_i is T_i. The average channel utilization of set S_i denoted by U_{Si}

$$U_{S_i} = \frac{(1 - \prod_{i \in S_i}(1 - \tau_i^{(h)}))T_i}{P_i^{(t)} T + P_n \sigma} \quad (7)$$

Since, $P_i^{(T)} : \tau_i^{(h)} = U_{S_i} : U_t$, we get $\tau_i^{(h)}$ with equation (6)

$$\tau_i^{(h)} = U_h \frac{P_i^{(T)} T_i + P_n \sigma}{T_i},$$

$$\tau_i^{(h)} = \frac{U_h \sigma}{(1 - U_{S_i})T_i + U_{S_i}\sigma} \quad (8)$$

In the steeped condition, slot admission probability is extended. From [9], we can achieve the comprehensive value of $\tau_i^{(h)}$ measured at its location as

$$max(\tau_i^{(h)}) = \frac{2(1 - 2P_{hi}^{(f)})}{(1 - 2P_{hi}^{(f)})(W' + 1) + P_{hi}^{(f)} W'(1 - (2P_{hi}^{(f)})^{BF})} \quad (9)$$

Where, W' is initial window size, *BF* is maximum back off stage, $P_{hi}^{(f)}$ be the probability of communication failure caused by the packet collisions is given by,

$$P_{hi}^{(f)} = 1 - (1 - P_{hi}^{(I)})(1 - P_{hi}^{(C)}) \quad (10)$$

The probability of communication failure initiated by interference and data packet collisions, indicated by $P_{hi}^{(I)}$ and $P_{hi}^{(C)}$, is given by

$$P_{hi}^{(I)} = 1 - \prod_{i \in S_i}(1 - \tau_i^{(h)}) \quad (11)$$

$$P_{hi}^{(C)} = 1 - e^{(-\gamma/\lambda k)} \quad (12)$$

where, γ be the collision period and λk be the average packet arrival rate of the *node k* in the set of *AP's.* Equation (13) demonstrates the throughput of node *i* once correlated with an *AP* is denoted as

$$T(S_k) \mid A_{h,i} = \frac{\mathrm{P}^r(\bar{d}_{hi})}{T_i} \sum_{i \in S_i} (1 - P_{hi}^{(f)}) U_{S_i} \quad (13)$$

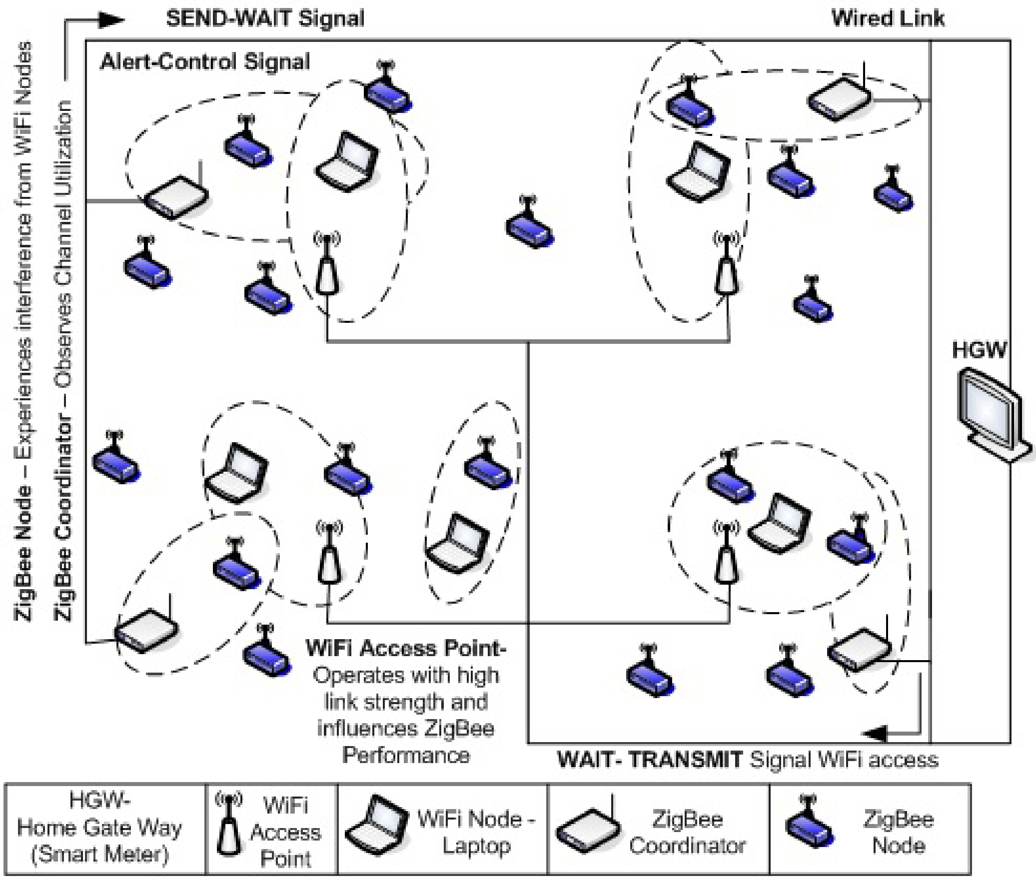

Fig. 3. The architecture of smart home environment.

After the distance and RSSI values are estimated then the delay is estimated for increasing the fairness for assuring the data communication within the time.

2) Delay Estimation

Let $Z = (z_{1a}, z_{1b})$ denotes the coordinates of ZigBee nodes that experience interference from the WiFi node. The arithmetic means of interference strength accepted at the ZigBee coordinator, *z* is

$$P_{z,i}^{\text{int}} = \frac{\sum_{i \in S_z} \tau_i^{(z)} T_i P_{z.i}}{U_z} \tag{14}$$

Where, $P_{z.i}$ is the beacon power obtained by the Zigbee coordinator, z.

The small difference in the delay may introduce the errors in the data due to the collision at the receiver side, because of the interference, the estimation of the Bit error rate (BER) value for the ZigBee sensor is as given below,

$$BER_{z,s}^{(k)}(P_{z,i}) = \frac{1}{2} - \phi\left(\sqrt{\frac{2P_{z,i}}{P_z^{(n)} + P_{z,i}}}\right) \tag{15}$$

Where, $\phi(\gamma) = \frac{1}{\sqrt{2\pi}} \int_0^{\gamma} e^{\left(-\frac{u^2}{2}\right)} du$ is the standard distribution function. from (14), the PER for the packet communicated from the ZigBee sensor, *s* to the Zigbee coordinator, *z* is given as

$$P_{s,z}^{(e)} = (1 - BER_{z,s}^{(k)}(0))^{L_p(1-U_c)} (1 - BER_{z,s}^{(k)}(P_{z,i}^{\text{int}}))^{L_p U_z} \tag{16}$$

where, L_p be an average size of a ZigBee packet and U_z is the WLAN channel utilization detected at the coordinator, z.

In (16), $BER_{z,s}^{(k)}$ is the 'zero' if WiFi is ideal, doesn't communicate but ZigBee sensor *s* is ready to communicate a packet to coordinator *z*.

Let S_z be the group of ZigBee sensors that are within transmission range of the coordinator, z. Using (16), we discover the PER of the coordinator, z as

$$P_z^{(e,s)} = \frac{\sum_{s \in S_z} \varphi_s P_{s,z}^{(e)}}{\sum_{s \in S_z} \varphi_s} \tag{17}$$

where, φ_s be the average packet arrival rate from WiFi node

$$U_z = \frac{T_i}{T_i + a\sigma} \tag{18}$$

Where, *a* is the number of empty slots between WiFi packet transmissions.

By means of (18), the probability that any WLAN packet is not communicated in the empty time slots is given as

$$P_a = 1 - \frac{T_i + 2T_{slot}}{T_i + a\sigma}, \quad P_a = 1 - U_z - 2U_z \frac{T_{slot}}{T_i} \tag{19}$$

Let BF and R denote the max. a permissible number of Back-Off stages and the highest number of retransmissions allowable just after a communication failure. Then, we have the frame failure probability due to collisions with the WLAN packets $P_z^{(f)}$ as follows:

$$P_z^{(f)} = 1 - (1 - c_z^{(f)})^R \tag{20}$$

Where is the probability that the only packet communicated by the Zigbee node which is given by

$$c_z^{(f)} = (1 - P_n)^{BF} + (1 - (1 - P_n)^{BF}) P_z^{(e,s)} \tag{21}$$

Using (19) and (20), $\overline{A}_{BF}$ can be expressed as

$$\overline{A}_{BF} = P_a \frac{W' + 1}{2} + \sum_{S_i = 1}^{BF} (2(1 - P_n)) S_i \frac{W' + 1}{2} \tag{22}$$

The arithmetic mean delay for a single transmission attempt $[D]_s$ is a combination of [sleep period, Back-Off, and frame communication time]**,**

$$[D]_s = \frac{\overline{A}_{BF}}{N_{SF}} (T_{bi} - T_{sf}) + \overline{A}_{BF} T_{slot} + \{1 - \left(U_z + 2U_z \frac{T_{slot}}{T_i} \right)^{BF} \tag{23}$$

where, T_{bi} is beacon interval and T_{sf} denote the superframe duration, in the ZigBee network, and N_{SF} is the no. of slots in a superframe.

From Eq. (23), the average successful transmission delay for a ZigBee packet is obtained as:

$$Delay, D = \frac{1 - (P_z^{(f)})^R}{1 - (P_z^{(f)})} [D]_s \tag{24}$$

3) Throughput Estimation

In WSN, let us consider the set of sensor nodes S_k, where $k=1, 2, 3\ldots, n$ with known and unknown positions in the area considered, expressed as m-dimensional coordinates. Let, T_s and T_f be the mean time duration of successful and unsuccessful transmissions correspondingly is given as below,

$$T_s = H_{phy} + \frac{H_{mac} + \mathrm{P_r}}{d} + SIFS + ACK + DIFS \tag{25}$$

$$T_f = H_{phy} + \frac{H_{mac}}{d} + ACK_{timeout} + DIFS \tag{26}$$

Where P_r is the signal strength of the data frame, H_{PHY} & H_{MAC} is the PHY and MAC header respectively and d is the distance between the nodes.

The probability of collision due to transmissions by any one of n active nodes and other nodes is given by,

$$P_c = \tau'(1 - (1 - \tau)^n) \tag{27}$$

Where, τ and τ*'* denoted as transmission probabilities of slot per n active nodes and other nodes.

The average slot duration is given by,

$$T_{slot} = P_s T_s + P_f T_f + P_{idle}\sigma - P_c \min(T_f) \tag{28}$$

where P_s be the probability of successful transmission appears in a slot for n^{th} active node. P_f is the probability of unsuccessful transmission occurs in a slot for n^{th} active node. σ is the duration of empty slots*,* P_c is the probability of collision among nodes. P_{idle} is the probability that a slot is idle, which is given by $P_{idle} = (1 - \tau')(1 - \tau)^n$.

Let us consider node j is interferer with h retrieves the channel at the location of node i transmits.

Let $P_i^{(t)}$ denote the probability of transmission for estimating the interference that at least one among the available nodes can interfere with node i. The probability is given

$$P_i^{(t)} = 1 - \prod_{h \in S_i} (1 - \tau_i^{(h)})^{n_i} \tag{29}$$

where is the set of all the i number of nodes and n_i is the active nodes among set S_i. The transmission probability $\tau_i^{(h)}$ of channel at h retrieves the node i through the particular AP. The value of the distance and received signal strength and channel quality of each node at the allocated time slot are derived in (1) and (2).

The probability that the node in a set S_k transmits in the considered slot for the particular AP

$$P_s = \sum_{S_i \in S_k} \tau_{S_i} \sum_{i \in S_i, i \neq h} (1 - \tau_i^{(h)}) \tag{30}$$

The probability that no node in a set S_i communicates in the considered slot (idle),

$$P_n = 1 - P_i^{(t)} \tag{31}$$

IV. Performance Evaluation

The ns 2.34 simulation tool is enhanced for simulation results by extending the libraries of IEEE 802.15.4 and IEEE 802.11 based on the requirements, by analyzing the interference between the ZigBee and WiFi networks. The area considered is 500*500 sq. meters. The parameters considered for simulation are considered in Table I.

TABLE I
Parameters and values for simulation

Parameters	Values
ZigBee protocol	IEEE 802.15.4
WiFi	IEEE 802.11b
HGW (Server)	1
WiFi Access Points	4
WiFi clients	5
ZigBee Coordinator	4
ZigBee Sensors	17
Simulation time	300 secs
Routing Protocol	AODV
Bit rate	250 Kbps
ZigBee Node Energy	10 J
ZigBee Tx Power	0.5mW
ZigBee Rx Power	0.3mW

The proposed is architecture is carried based on the smart home architecture proposed in Fig. 3. The typical network is considered consists of 17 ZigBee nodes, 4 ZigBee coordinators, working the in the influence of the 4 WiFi AP's, and about 5 WiFi clients. The CFAI model proposed in this paper aims for controlling the traffic of WLAN which tolerate continuous transformation of ZigBee and the highest tolerable delay is avoided as a result of the WLAN interference. The CFAI assures the efficient ZigBee based operation, by the assessment of distance between source and distance based on the RSSI parameter. Then CFAI assures for Channel availability based on the delay and channel weight (T_S, T_F & P_s) calculations. The evaluation of CFAI is carried based on the comparison to the following works. The K. Hong et al. [28] have proposed the algorithm for the efficient operation of the ZigBee working under the influence of WiFi. The authors have focused on the channel utilization but have not considered the traffic generated in the network due to the overhead and this has a serious impact on the network life time. The work proposed in [9] was for the indoor environment based on Wireless HAN having ZigBee and WiFi that are coexisting in the same area. This work has considered the load scheduling effectively but have not considered the Channel utilization parameter. The CMCMAC-FEC [29] was proposed for coexisting mechanism environment and have considered efficient packet delivery towards receiver side and also arrangement was there for finding the low interference effected channel. But could not assess the channel utilization effectively. The CFMSS [30] have proposed a systematic algorithm for assuring the efficient ZigBee performance. But the authors have not considered the coexisting environment with WiFi nodes

The CFAI model proposed in this paper aims for controlling the traffic of WLAN which tolerate continuous transformation of ZigBee and the highest tolerable delay is avoided as a result of the WLAN interference. The CFAI assures the efficient ZigBee based operation, by the assessment of distance between source and distance based on the RSSI parameter. Then CFAI assures for Channel availability based on the delay and channel weight (T_S, T_F & P_s) calculations. The evaluation of CFAI is carried based on the comparison to the following works. The K. Hong et al. [28] have proposed the algorithm for the efficient operation of the ZigBee working under the influence of WiFi. The authors have focused on the channel utilization but have not considered the traffic generated in the network due to the overhead and this has a serious impact on the network life time. The work proposed in [9] was for the indoor environment based on Wireless HAN having ZigBee and WiFi that are coexisting in the same area. This work has considered the load scheduling effectively but have not considered the Channel utilization parameter. The CMCMAC-FEC [29] was proposed for coexisting mechanism environment and have considered efficient packet delivery towards receiver side and also arrangement was there for finding the low interference effected channel. But could not assess the channel utilization effectively. The CFMSS [30] have proposed a systematic algorithm for assuring the efficient ZigBee performance. But the authors have not considered the coexisting environment with WiFi nodes.

The information from WiFi (AP) is downloaded from each node of WiFi. For each and every WiFi node, the packet entry follows a neighbor strategy along with a mean value. The ZigBee network works with constant bit rate (CBR) runs at the data rate of 27Kbps for every second. WiFi node receives the data from the AP. The WiFi node receives the data at a maximum rate up to 12Mbps for every second. The simulation runs for 300sec. The ZigBee node has to wait, until Back-off period to occupy the channel for the transmission of the data, when interference occurs this is considered as delay (D). The value of '*D'* is Considered by taking the two scenarios 10ms and 50ms. The simulation is carried for channel utilization by considering different data delays like D=10ms in Fig. 4 and D=50ms in Fig. 5 for evaluation of CFAI.

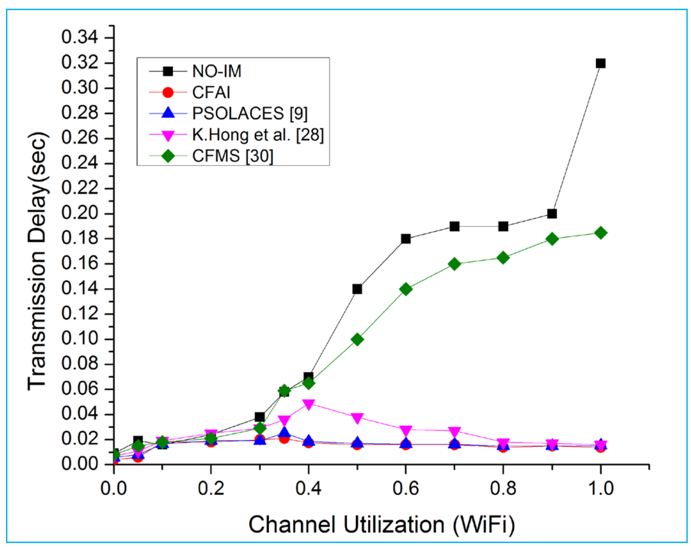

Fig. 4. Transmission delay in Zigbee network. (Delay D=10ms).

From the Fig. 4 and Fig. 5, it can be inferred that the ZigBee network works better considering CFAI methodology when the volume of data transmission from WiFi is increased. CFAI performs better compared to the existing method as in [28], [9], [30] and when there is no interference mitigation methodology (NO-IM). Fig. 4 delay D is considered as 10ms and in Fig. 5 delay D is considered as 50ms.

The Fig. 6 evaluates the performance of CFAI in terms of an average number of packets generated per second when different number of nodes is considered. The CFAI performance is compared to the existing works like [9], [28]-[30]. The average number of packets generated by ZigBee network based on CFAI is very economical compared to the others. The ZigBee network performance is also evaluated for 4 nodes, 8 nodes, 12 nodes and finally 17 nodes based on network sizes. In all the scenarios for various network sizes, the CFAI performance is very better compared to the other works.

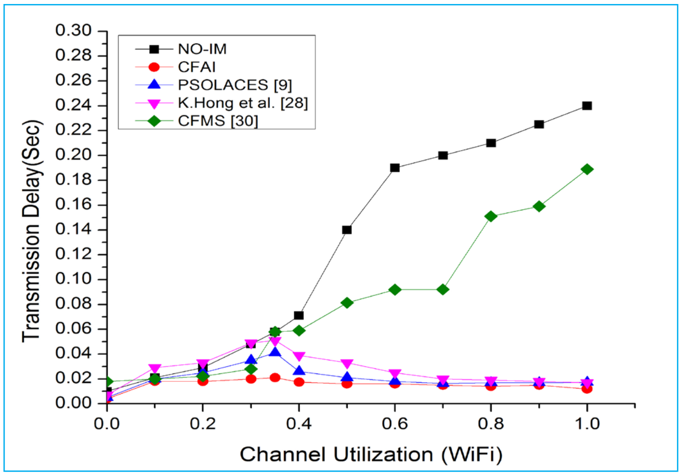

Fig. 5. Transmission delay in Zigbee network. (Delay D=50ms).

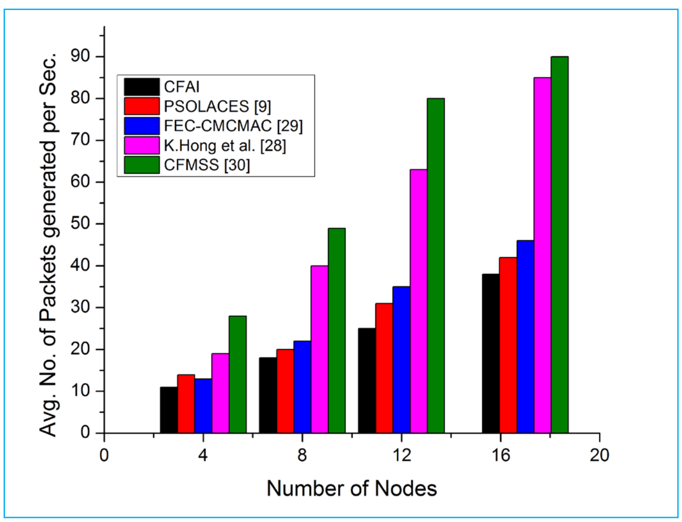

Fig. 6. Average Number of Packets Generated per Second.

The Fig. 7 below represents the number of acknowledgements received by the respective source nodes that have generated packets transmitted to the destination. In this scenario the ZigBee network varied by 4, 8, 12, and 17 nodes respectively. From the graph above it can be inferred as the CFAI methodology works better when compares to other works considered [9], [28]-[30]. The number of acknowledgement messages received by ZigBee nodes shows 100 percent when network size is 4 and 8. The number of Acknowledgement messages received when network size with 12 and 17 nodes considered is above 90 percent. The results obtained in various scenarios strengthens the CFAI model as the most suitable for the Coexisting environment.

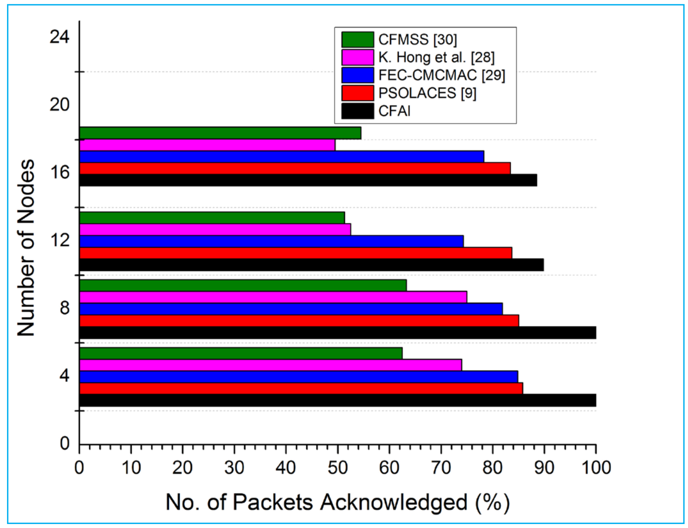

Fig. 7. Number of Acknowledgements received by Source Nodes.

Based on the above results when compared to other works CFAI is working much better and has improved the performance of ZigBee network working under the influence of the WiFi.

V. Conclusion

The employment of wireless networks like Zigbee and WiFi for data communication in the HAN premises is unavoidable. Both the networks considered are operating in 2.4GHz frequency band. It is considered as no radio is immune to the occurrence of interference. This interference occurs is because of overlapping of the frequency channels in the same band and it exactly occurs when ZigBee node and WiFi desires to transmit at the same instance. In general, the WiFi node with high energy shall occupy the channel. To carry out the efficient operation of IEEE 802.15.4 based ZigBee network there is a need for a coexisting mechanism for managing the operation of low-power network in particular. In this paper, CFAI methodology is proposed for improving the performance of ZigBee network which is operating in the vicinity of WiFi. From the results obtained it can be inferred that CFAI performs better when compared the existing methodologies like PSOLACES [7], K. Hong et al. [26], FEC-CMCMAC [27] and CFMSS [28]. and when no interference mitigation is present. The CFAI based ZigBee network shows better channel occupancy, and other network parameters considered as shown in the results and also assures better data rate with good throughput even under the coexistence of WiFi.

References

[1] A. Faruqui, K. Arritt, S. Sergici, "The impact of advanced metering infrastructure on energy conservation: A case study of two utilities," *The Electricity Journal*, Volume 30, Issue 3, 2017, Pages 56-63, https://doi.org/10.1016/j.tej.2017.03.006.

[2] S. Sofana Reka, T. Dragicevic, "Future effectual role of energy delivery: A comprehensive review of Internet of Things and smart grid," *Renewable and Sustainable Energy Reviews*, Volume 91, Pages 90-108, 2018.

[3] M. Kuzlu, M. Pipattanasomporn, S. Rahman, "Communication network requirements for major smart grid applications in HAN, NAN and WAN," *Computer Networks-Elsevier*, Volume 67, 2014, Pages 74-88.

[4] L. Davoli, L. Belli, A. Cilfone and G. Ferrari, "From Micro to Macro IoT: Challenges and Solutions in the Integration of IEEE 802.15.4/802.11 and Sub-GHz Technologies." *IEEE Internet of Things Journal,* vol. 5, no. 2, pp. 784-793, April 2018.

[5] E. Fadel, V.C. Gungor, L. Nassef, N. Akkari, M.G. Abbas Malik, S. Almasri, I. F. Akyildiz, "A survey on wireless sensor networks for the smart grid," *Computer Communications*, Volume 71, 1 November 2015, Pages 22-33

[6] Vikram K., Yuvaraj. P., V. L. Narayana K., "A Survey on Wireless Sensor Networks for Smart Grid," *Sensors & Transducers Journal*, Vol. 186, Issue 3, March 2015, pp. 18-24.

[7] IEEE Standard for Local and metropolitan area networks--Part 15.4: Low-Rate Wireless Personal Area Networks (LR-WPANs) Amendment 1: MAC sublayer," in IEEE Std 802.15.4e-2012 (Amendment to IEEE Std 802.15.4-2011), vol., no., pp.1-225, April 16, 2012

[8] IEEE Std 802.11-2016, IEEE Standard for Information Technology Telecommunications and information exchange between systems Local and metropolitan area networks Specific Requirements Part 11: Wireless LAN Medium Access Control (MAC) and Physical Layer (PHY) Specifications.

[9] Vikram K. and S. K. Sahoo, "Load Aware Channel Estimation and Channel Scheduling for 2.4GHz Frequency Band Based Wireless Networks for Smart Grid Applications", *International Journal on Smart Sensing and Intelligent Syatems*, Vol.10, No.4, PP: 879-902, Dec. 2017.

[10] IEEE Std 802.15.1-2002, IEEE Standard for Information Technology Telecommunications, Part 15.1: Wireless Medium Access Control (MAC) and Physical Layer (PHY) Specifications for Wireless Personal Area Networks (WPANs).

[11] S. M. Iftekharul Alam and S. Fahmy. "Energy-efficient provenance transmission in large-scale wireless sensor networks". In Proceedings of the 2011 IEEE International Symposium on a World of Wireless, Mobile and Multimedia Networks (WOWMOM '11). *IEEE Computer Society*, Washington, DC, USA, 2011, 1-6.

[12] V. Namboodiri, V. Aravinthan, S. N. Mohapatra, B. Karimi and W. Jewell, "Toward a Secure Wireless-Based Home Area Network for Metering in Smart Grids," in *IEEE Systems Journal*, vol. 8, no. 2, June 2014, pp. 509-520.

[13] J. Kakarla, B. Majhi, and R. B. Battula, "IAMMAC: an interference-aware multi-channel MAC protocol for the wireless sensor–actor networks", *International Journal of Communication systems*, 2015, pp. 801–822.

[14] C. A. Boano, T. Voigt, C. Noda, K. Romer, and M. Zuniga, "JamLab: Augmenting sensornet testbeds with realistic and controlled interference generation," Proc. 10th ACM/IEEE Int. Conf. Inf. Process. Sens. Networks, pp. 175–186, 2011.

[15] K. Vikram and K. V. L. Narayana, "Cross-layer multi-channel MAC protocol for interference mitigation," 2016 *IEEE Annual India Conference* (INDICON), Bangalore, 2016, pp. 1-6.

[16] I. Al-Anbagi, M. Erol-Kantarci and H. T. Mouftah, "Delay-Aware Medium Access Schemes for WSN-Based Partial Discharge Measurement," in *IEEE Transactions on Instrumentation and Measurement*, vol. 63, no. 12, pp. 3045-3057, Dec. 2014.

[17] N. K. Suryadevara, S. C. Mukhopadhyay, S. D. T. Kelly and S. P. S. Gill, "WSN-Based Smart Sensors and Actuator for Power Management in Intelligent Buildings," in *IEEE/ASME Transactions on Mechatronics*, vol. 20, no. 2, pp. 564-571, April 2015.

[18] V. Namboodiri, V. Aravinthan, S. N. Mohapatra, B. Karimi and W. Jewell, "Toward a Secure Wireless-Based Home Area Network for Metering in Smart Grids," in *IEEE Systems Journal*, vol. 8, no. 2, pp. 509-520, June 2014.

[19] X. Zhang and K. G. Shin, "Cooperative Carrier Signaling: Harmonizing Coexisting WPAN and WLAN Devices," in *IEEE/ACM Transactions on Networking*, vol. 21, no. 2, pp. 426-439, April 2013.

[20] X. Wang, H. Shen, S. Lv, and X. Zhou, "A Genetic Approach for Joint Link Scheduling and Power Control in SIC-enable Wireless Networks", *KSII Transactions on Internet and Information Systems* Vol. 10, No. 4, pp. 1679-1691, Apr. 2016.

[21] M. S. Kang, J. W. Chong, H. Hyun, S. M. Kim, B. H. Jung and D. K. Sung, "Adaptive Interference-Aware Multi-Channel Clustering Algorithm in a ZigBee Network in the Presence of WLAN Interference," 2007 *2nd International Symposium on Wireless Pervasive Computing*, San Juan, 2007.

[22] W. Guo, W. M. Healy and M. Zhou, "An experimental study of interference impacts on ZigBee-based wireless communication inside buildings," 2010 *IEEE International Conference on Mechatronics and Automation*, Xi'an, 2010, pp. 1982-1987.

[23] L. Tytgat, O. Yaron, S. Pollin, I. Moerman, and P. Demeester, "Analysis and Experimental Verification of Frequency-Based Interference Avoidance Mechanisms in IEEE 802.15.4", *IEEE/ACM Transactions on Networking*, 2014.

[24] Hong-wei HUO, You-zhi XU, Gidlund Mikael, Hong-ke ZHANG, Coexistence of 2.4 GHz sensor networks in a home environment, *The Journal of China Universities of Posts and Telecommunications*, Volume 17, Issue 1, Pages 9-18, 2010.

[25] P. Yi; Iwayemi, A.; C. Zhou, "Developing ZigBee Deployment Guideline Under Wi-Fi Interference for Smart Grid Applications,", in *IEEE Transactions on Smart Grid*, vol.2, no.1, pp.110-120, March 2011.

[26] C. H. Cheng, C. C. Ho, Implementation of multi-channel technology in *ZigBee wireless sensor networks, Computers & Electrical Engineering*, Volume 56, Pages 498-508, 2016.

[27] I. Al-Anbagi, M. Erol-Kantarci and H. T. Mouftah, "Priority- and Delay-Aware Medium Access for Wireless Sensor Networks in the Smart Grid," in *IEEE Systems Journal*, vol. 8, no. 2, pp. 608-618, June 2014.

[28] K. Hong, S. Kyoung Lee, K. Lee, Performance improvement in ZigBee-based home networks with coexisting WLANs, *Pervasive and Mobile Computing*, Volume 19, Pages 156-16, May 2015.

[29] K Vikram, S. K. Sahoo, K. Venkata Lakshmi Narayana, "Forward Error Correction based Encoding Technique for Cross-layer Multi Channel MAC protocol", *Energy Procedia*, Volume 117, 2017, Pages 847-854.

[30] X. Jin, Q. Zhang, P. Zeng, F. Kong and Y. Xiao, "Collision-free multichannel superframe scheduling for IEEE 802.15.4 cluster-tree networks", Int. J. *Sensor Networks*, Vol-15, No.4, 2014.

Preparation of Papers for Electronics (September 2011)

First A. Author, Second B. Author, and Third C. Author

***Abstract*—These instructions give you guidelines for preparing papers for ELECTRONICS journal. Use this document as a template if you are using Microsoft *Word* 6.0 or later. Otherwise, use this document as an instruction set. The electronic file of your paper will be formatted further. Define all symbols used in the abstract. Do not cite references in the abstract. Do not delete the blank line immediately above the abstract; it sets the footnote at the bottom of this column.**

***Index Terms*—About four key words or phrases in alphabetical order, separated by commas.**

Paper Classification
DOI: 10.7251/ELSxxxxxxxx

I. Introduction

THIS document is a template for Microsoft *Word* versions 6.0 or later.

When you open the file, select "Page Layout" from the "View" menu in the menu bar (View | Page Layout), which allows you to see the footnotes. Then, type over sections of file or cut and paste from another document and use markup styles. The pull-down style menu is at the left of the Formatting Toolbar at the top of your *Word* window (for example, the style at this point in the document is "Text"). Highlight a section that you want to designate with a certain style, then select the appropriate name on the style menu. The style will adjust your fonts and line spacing. **Do not change the font sizes or line spacing to squeeze more text into a limited number of pages.** Use italics for emphasis; do not underline. The length of the manuscript is limited to the maximum of 15 pages.

To insert images in *Word,* position the cursor at the insertion point and either use Insert | Picture | From File or copy the image to the Windows clipboard and then Edit | Paste Special | Picture (with "float over text" unchecked).

We will do the final formatting of your paper.

II. Procedure for Paper Submission

A. Review Stage

The manuscripts are to be submitted using the Electronics Journal online submission system – accessible from Journal's homepage. Prepare it in two-column format as shown in this template. Place all figures and tables at the end of the paper (after the references) on separate page(s). Figures and tables must have the same caption names as referenced in the text. Only PDF format of the manuscript is allowed at the review stage. Please, check if all fonts are embedded and subset and that the quality of diagrams, illustrations, and graphics is satisfactory. Failing to provide above listed requirements is a valid reason for rejection.

B. Final Stage

When you submit your final version (after your paper has been accepted), prepare it in two-column format, including figures and tables in accordance with this template. Pack all of your files (manuscript source file in *Word*, figures, and manuscript PDF form) within one archive file (you may use any of the available file compression tools: *WinZip*, *WinRAR*, *7-Zip*, etc.). Do not forget to provide the manuscript converted in PDF format that will be used as a reference for final formatting of your paper. Figures should be named as referenced in the manuscript (e.g. *fig1.eps*, *fig2.tif*, etc.)

C. Figures and Tables

Format and save your graphic images using a suitable graphics processing program and adjusts the resolution settings. We accept images in the following formats: PS, EPS, TIFF, GIF, and PNG. Additionally, it is allowed to use images generated by using one of the following software tools: Microsoft Word, Microsoft PowerPoint, or Microsoft Excel. The resolution of a RGB color file should be 400 dpi. Please note that JPG and other lossy-compressed image formats are not allowed. Use available software tools to convert these images to appropriate format.

Image quality is very important to how yours graphics will reproduce. Even though we can accept graphics in many formats, we cannot improve your graphics if they are poor quality when we receive them. If your graphic looks low in

Manuscript received 15 September 2011 (write the date when you have first sent the manuscript for review). Received in revised form 20 October 2011 (write the date when you have sent the manuscript in its revised form if revisions required for your paper after review).

(Place here any sponsor and financial support acknowledgments).

F. A. Author is with the Faculty of Electrical Engineering, University of Banja Luka, Banja Luka, Bosnia and Herzegovina (corresponding author to provide phone: +387-51-222-333; fax: +387-51-111-222; e-mail: author@etfbl.net).

S. B. Author was with Faculty of Technical Sciences, University of Novi Sad, Novi Sad, Serbia. He is now with the Institute "Mihailo Pupin", Belgrade, Serbia (e-mail: author@pupin.rs).

T. C. Author is with the School of Electrical Engineering, University of Belgrade, Belgrade, Serbia, on leave from the Faculty of Electronic Engineering, University of Niš, Niš, Serbia (e-mail: author@elfak.ni.ac.rs).

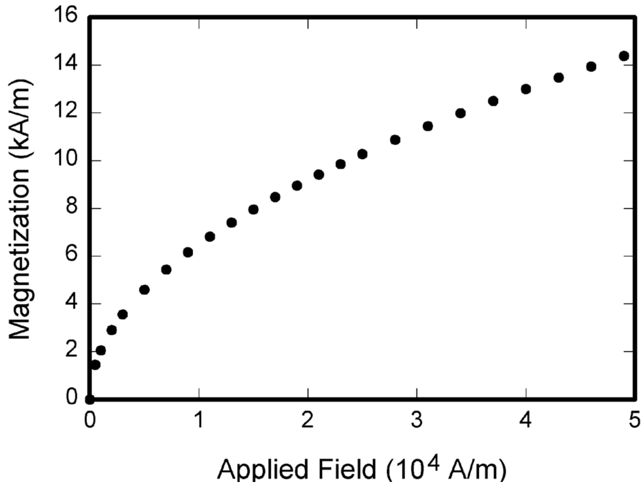

Fig. 1. Magnetization as a function of applied field. Note that "Fig." is abbreviated. There is a period after the figure number, followed by two spaces. It is good practice to explain the significance of the figure in the caption.

quality on your printer or monitor, please keep in mind that cannot improve the quality after submission.

If you are importing your graphics into this Word template, please use the following steps:

Under the option EDIT select PASTE SPECIAL. A dialog box will open, select paste picture, then click OK. Your figure should now be in the Word Document.

If you are preparing images in TIFF, EPS, or PS format, note the following. High-contrast line figures and tables should be prepared with 600 dpi resolution and saved with no compression, 1 bit per pixel (monochrome).

Photographs and grayscale figures should be prepared with 300 dpi resolution and saved with no compression, 8 bits per pixel (grayscale).

Most charts graphs and tables are one column wide (3 1/2 inches or 21 picas) or two-column width (7 1/16 inches, 43 picas wide). We recommend that you avoid sizing figures less than one column wide, as extreme enlargements may distort your images and result in poor reproduction. Therefore, it is better if the image is slightly larger, as a minor reduction in size should not have an adverse affect the quality of the image.

III. Math

If you are using *Word,* use either the Microsoft Equation Editor or the *MathType* add-on (http://www.mathtype.com) for equations in your paper (Insert | Object | Create New | Microsoft Equation *or* MathType Equation). "Float over text" should *not* be selected.

IV. Units

Use either SI (MKS) or CGS as primary units. (SI units are strongly encouraged.) English units may be used as secondary units (in parentheses). **This applies to papers in data storage.** For example, write "15 Gb/cm^2 (100 Gb/in^2)." An exception

TABLE I
Units for Magnetic Properties

Symbol	Quantity	Conversion from Gaussian and CGS EMU to SI [a]
Φ	magnetic flux	1 Mx $\rightarrow 10^{-8}$ Wb $= 10^{-8}$ V·s
B	magnetic flux density, magnetic induction	1 G $\rightarrow 10^{-4}$ T $= 10^{-4}$ Wb/m^2
H	magnetic field strength	1 Oe $\rightarrow 10^3/(4\pi)$ A/m
m	magnetic moment	1 erg/G = 1 emu $\rightarrow 10^{-3}$ A·m^2 $= 10^{-3}$ J/T
M	magnetization	1 erg/(G·cm^3) = 1 emu/cm^3 $\rightarrow 10^3$ A/m
$4\pi M$	magnetization	1 G $\rightarrow 10^3/(4\pi)$ A/m
σ	specific magnetization	1 erg/(G·g) = 1 emu/g $\rightarrow$ 1 A·m^2/kg
j	magnetic dipole moment	1 erg/G = 1 emu $\rightarrow 4\pi \times 10^{-10}$ Wb·m
J	magnetic polarization	1 erg/(G·cm^3) = 1 emu/cm^3 $\rightarrow 4\pi \times 10^{-4}$ T
χ, κ	susceptibility	$1 \rightarrow 4\pi$
χ_ρ	mass susceptibility	1 cm^3/g $\rightarrow 4\pi \times 10^{-3}$ m^3/kg
μ	permeability	$1 \rightarrow 4\pi \times 10^{-7}$ H/m $= 4\pi \times 10^{-7}$ Wb/(A·m)
μ_r	relative permeability	$\mu \rightarrow \mu_r$
w, W	energy density	1 erg/cm^3 $\rightarrow 10^{-1}$ J/m^3
N, D	demagnetizing factor	$1 \rightarrow 1/(4\pi)$

Vertical lines are optional in tables. Statements that serve as captions for the entire table do not need footnote letters.

[a]Gaussian units are the same as cgs emu for magnetostatics; Mx = maxwell, G = gauss, Oe = oersted; Wb = weber, V = volt, s = second, T = tesla, m = meter, A = ampere, J = joule, kg = kilogram, H = henry.

is when English units are used as identifiers in trade, such as "3½-in disk drive." Avoid combining SI and CGS units, such as current in amperes and magnetic field in oersteds. This often leads to confusion because equations do not balance dimensionally. If you must use mixed units, clearly state the units for each quantity in an equation.

The SI unit for magnetic field strength H is A/m. However, if you wish to use units of T, either refer to magnetic flux density B or magnetic field strength symbolized as $\mu_0 H$. Use the center dot to separate compound units, e.g., "A·m^2."

V. Helpful Hints

A. Figures and Tables

Because we will do the final formatting of your paper, you do not need to position figures and tables at the top and bottom of each column. In fact, all figures, figure captions, and tables can be at the end of the paper. Large figures and tables may span both columns. Place figure captions below the figures; place table titles above the tables. If your figure has two parts, include the labels "(a)" and "(b)" as part of the artwork. Please verify that the figures and tables you mention in the text actually exist. **Please do not include captions as part of the figures. Do not put captions in "text boxes" linked to the figures. Do not put borders around the outside of your figures.** Use the abbreviation "Fig." even at the beginning of a sentence. Do not abbreviate "Table." Tables are numbered with Roman numerals.

Color printing of figures is not available Do not use color unless it is necessary for the proper interpretation of your figures.

Figure axis labels are often a source of confusion. Use words rather than symbols. As an example, write the quantity "Magnetization," or "Magnetization *M*," not just "*M*." Put units in parentheses. Do not label axes only with units. As in Fig. 1, for example, write "Magnetization (A/m)" or "Magnetization ($A \cdot m^{-1}$)," not just "A/m." Do not label axes with a ratio of quantities and units. For example, write "Temperature (K)," not "Temperature/K."

Multipliers can be especially confusing. Write "Magnetization (kA/m)" or "Magnetization (10^3 A/m)." Do not write "Magnetization (A/m) x 1000" because the reader would not know whether the top axis label in Fig. 1 meant 16000 A/m or 0.016 A/m. Figure labels should be legible, approximately 8 to 12 point type.

B. References

Number citations consecutively in square brackets [1]. The sentence punctuation follows the brackets [2]. Multiple references [2], [3] are each numbered with separate brackets [1]–[3]. When citing a section in a book, please give the relevant page numbers [2]. In sentences, refer simply to the reference number, as in [3]. Do not use "Ref. [3]" or "reference [3]" except at the beginning of a sentence: "Reference [3] shows ... ." Please do not use automatic endnotes in *Word*, rather, type the reference list at the end of the paper using the "References" style.

Number footnotes separately in superscripts (Insert | Footnote).[1] Place the actual footnote at the bottom of the column in which it is cited; do not put footnotes in the reference list (endnotes). Use letters for table footnotes (see Table I).

Please note that the references at the end of this document are in the preferred referencing style. Give all authors' names; do not use "*et al*." unless there are six authors or more. Use a space after authors' initials. Papers that have not been published should be cited as "unpublished" [4]. Papers that have been accepted for publication, but not yet specified for an issue should be cited as "to be published" [5]. Papers that have been submitted for publication should be cited as "submitted for publication" [6]. Please give affiliations and addresses for private communications [7].

Capitalize only the first word in a paper title, except for proper nouns and element symbols. For papers published in translation journals, please give the English citation first, followed by the original foreign-language citation [8]. All references **must be** written in Roman alphabet.

C. Abbreviations and Acronyms

Define abbreviations and acronyms the first time they are used in the text, even after they have already been defined in the abstract. Abbreviations such as IEEE, SI, ac, and dc do not have to be defined. Abbreviations that incorporate periods should not have spaces: write "C.N.R.S.," not "C. N. R. S." Do not use abbreviations in the title unless they are unavoidable (for example, "IEEE" in the title of this article).

D. Equations

Number equations consecutively with equation numbers in parentheses flush with the right margin, as in (1). First use the equation editor to create the equation. Then select the "Equation" markup style. Press the tab key and write the equation number in parentheses. To make your equations more compact, you may use the solidus (/), the exp function, or appropriate exponents. Use parentheses to avoid ambiguities in denominators. Punctuate equations when they are part of a sentence, as in

$$\begin{aligned}\int_0^{r_2} F(r,\varphi)\, dr\, d\varphi = [\sigma r_2 / (2\mu_0)] \\ \cdot \int_0^{\infty} \exp(-\lambda |z_j - z_i|)\, \lambda^{-1} J_1(\lambda r_2)\, J_0(\lambda r_i)\, d\lambda .\end{aligned} \tag{1}$$

Be sure that the symbols in your equation have been defined before the equation appears or immediately following. Italicize symbols (*T* might refer to temperature, but T is the unit tesla). Refer to "(1)," not "Eq. (1)" or "equation (1)," except at the beginning of a sentence: "Equation (1) is ... ."

E. Other Recommendations

Use one space after periods and colons. Hyphenate complex modifiers: "zero-field-cooled magnetization." Avoid dangling participles, such as, "Using (1), the potential was calculated." [It is not clear who or what used (1).] Write instead, "The potential was calculated by using (1)," or "Using (1), we calculated the potential."

Use a zero before decimal points: "0.25," not ".25." Use "cm^3," not "cc." Indicate sample dimensions as "0.1 cm x 0.2 cm," not "0.1 x 0.2 cm^2." The abbreviation for "seconds" is "s," not "sec." Do not mix complete spellings and abbreviations of units: use "Wb/m^2" or "webers per square meter," not "webers/m^2." When expressing a range of values, write "7 to 9" or "7-9," not "7~9."

A parenthetical statement at the end of a sentence is punctuated outside of the closing parenthesis (like this). (A parenthetical sentence is punctuated within the parentheses.) In American English, periods and commas are within quotation marks, like "this period." Other punctuation is "outside"! Avoid contractions; for example, write "do not" instead of "don't." The serial comma is preferred: "A, B, and C" instead of "A, B and C."

If you wish, you may write in the first person singular or plural and use the active voice ("I observed that ..." or "We observed that ..." instead of "It was observed that ..."). Remember to check spelling. If your native language is not English, please get a native English-speaking colleague to carefully proofread your paper.

[1] It is recommended that footnotes be avoided (except for the unnumbered footnote with the receipt date and authors' affiliations on the first page). Instead, try to integrate the footnote information into the text.

VI. Some Common Mistakes

The word "data" is plural, not singular. The subscript for the permeability of vacuum μ_0 is zero, not a lowercase letter "o." The term for residual magnetization is "remanence"; the adjective is "remanent"; do not write "remnance" or "remnant." Use the word "micrometer" instead of "micron." A graph within a graph is an "inset," not an "insert." The word "alternatively" is preferred to the word "alternately" (unless you really mean something that alternates). Use the word "whereas" instead of "while" (unless you are referring to simultaneous events). Do not use the word "essentially" to mean "approximately" or "effectively." Do not use the word "issue" as a euphemism for "problem." When compositions are not specified, separate chemical symbols by en-dashes; for example, "NiMn" indicates the intermetallic compound $Ni_{0.5}Mn_{0.5}$ whereas "Ni–Mn" indicates an alloy of some composition Ni_xMn_{1-x}.

Be aware of the different meanings of the homophones "affect" (usually a verb) and "effect" (usually a noun), "complement" and "compliment," "discreet" and "discrete," "principal" (e.g., "principal investigator") and "principle" (e.g., "principle of measurement"). Do not confuse "imply" and "infer."

Prefixes such as "non," "sub," "micro," "multi," and "ultra" are not independent words; they should be joined to the words they modify, usually without a hyphen. There is no period after the "et" in the Latin abbreviation "*et al.*" (it is also italicized). The abbreviation "i.e.," means "that is," and the abbreviation "e.g.," means "for example" (these abbreviations are not italicized).

An excellent style manual and source of information for science writers is [9].

VII. Editorial Policy

Each manuscript submitted is subjected to the following review procedure:

- It is reviewed by the editor for general suitability for this publication
- If it is judged suitable, two reviewers are selected and a single-blinded review process takes place
- Based on the recommendations of the reviewers, the editor then decides whether the particular paper should be accepted as is, revised or rejected.

Do not submit a paper you have submitted or published elsewhere. Do not publish "preliminary" data or results. The submitting author is responsible for obtaining agreement of all coauthors and any consent required from sponsors before submitting a paper. It is the obligation of the authors to cite relevant prior work.

Every paper submitted to "Electronics" journal are single-blind reviewed. For conference-related papers, the decision to accept or reject a paper is made by the conference editors and publications committee; the recommendations of the referees are advisory only. Undecipherable English is a valid reason for rejection.

VIII. Publication Principles

The contents of "Electronics" are peer-reviewed and archival. The "Electronics" publishes scholarly articles of archival value as well as tutorial expositions and critical reviews of classical subjects and topics of current interest.

Authors should consider the following points:

1) Technical papers submitted for publication must advance the state of knowledge and must cite relevant prior work.
2) The length of a submitted paper should be commensurate with the importance, or appropriate to the complexity, of the work. For example, an obvious extension of previously published work might not be appropriate for publication or might be adequately treated in just a few pages.
3) Authors must convince both peer reviewers and the editors of the scientific and technical merit of a paper; the standards of proof are higher when extraordinary or unexpected results are reported.
4) Because replication is required for scientific progress, papers submitted for publication must provide sufficient information to allow readers to perform similar experiments or calculations and use the reported results. Although not everything need be disclosed, a paper must contain new, useable, and fully described information. For example, a specimen's chemical composition need not be reported if the main purpose of a paper is to introduce a new measurement technique. Authors should expect to be challenged by reviewers if the results are not supported by adequate data and critical details.
5) Papers that describe ongoing work or announce the latest technical achievement, which are suitable for presentation at a professional conference, may not be appropriate for publication in "Electronics".

IX. Conclusion

A conclusion section is not required. Although a conclusion may review the main points of the paper, do not replicate the abstract as the conclusion. A conclusion might elaborate on the importance of the work or suggest applications and extensions.

Appendix

Appendixes, if needed, appear before the acknowledgment.

Acknowledgment

The preferred spelling of the word "acknowledgment" in American English is without an "e" after the "g." Use the singular heading even if you have many acknowledgments. Avoid expressions such as "One of us (S.B.A.) would like to thank ... ." Instead, write "F. A. Author thanks ... ." **Sponsor and financial support acknowledgments are placed in the unnumbered footnote on the first page, not here.**

References

[1] G. O. Young, "Synthetic structure of industrial plastics (Book style with paper title and editor)," in *Plastics*, 2nd ed. vol. 3, J. Peters, Ed. New York: McGraw-Hill, 1964, pp. 15–64.

[2] W.-K. Chen, *Linear Networks and Systems* (Book style). Belmont, CA: Wadsworth, 1993, pp. 123–135.

[3] H. Poor, *An Introduction to Signal Detection and Estimation*. New York: Springer-Verlag, 1985, ch. 4.

[4] B. Smith, "An approach to graphs of linear forms (Unpublished work style)," unpublished.

[5] E. H. Miller, "A note on reflector arrays (Periodical style—Accepted for publication)," *IEEE Trans. Antennas Propagat.*, to be published.

[6] J. Wang, "Fundamentals of erbium-doped fiber amplifiers arrays (Periodical style—Submitted for publication)," *IEEE J. Quantum Electron.*, submitted for publication.

[7] C. J. Kaufman, Rocky Mountain Research Lab., Boulder, CO, private communication, May 1995.

[8] Y. Yorozu, M. Hirano, K. Oka, and Y. Tagawa, "Electron spectroscopy studies on magneto-optical media and plastic substrate interfaces (Translation Journals style)," *IEEE Transl. J. Magn.Jpn.*, vol. 2, Aug. 1987, pp. 740–741 [*Dig. 9th Annu. Conf. Magnetics* Japan, 1982, p. 301].

[9] M. Young, *The Techincal Writers Handbook.* Mill Valley, CA: University Science, 1989.

[10] J. U. Duncombe, "Infrared navigation—Part I: An assessment of feasibility (Periodical style)," *IEEE Trans. Electron Devices*, vol. ED-11, pp. 34–39, Jan. 1959.

[11] S. Chen, B. Mulgrew, and P. M. Grant, "A clustering technique for digital communications channel equalization using radial basis function networks," *IEEE Trans. Neural Networks*, vol. 4, pp. 570–578, Jul. 1993.

[12] R. W. Lucky, "Automatic equalization for digital communication," *Bell Syst. Tech. J.*, vol. 44, no. 4, pp. 547–588, Apr. 1965.

[13] S. P. Bingulac, "On the compatibility of adaptive controllers (Published Conference Proceedings style)," in *Proc. 4th Annu. Allerton Conf. Circuits and Systems Theory*, New York, 1994, pp. 8–16.

[14] G. R. Faulhaber, "Design of service systems with priority reservation," in *Conf. Rec. 1995 IEEE Int. Conf. Communications,* pp. 3–8.

[15] W. D. Doyle, "Magnetization reversal in films with biaxial anisotropy," in *1987 Proc. INTERMAG Conf.*, pp. 2.2-1–2.2-6.

[16] G. W. Juette and L. E. Zeffanella, "Radio noise currents n short sections on bundle conductors (Presented Conference Paper style)," presented at the IEEE Summer power Meeting, Dallas, TX, Jun. 22–27, 1990, Paper 90 SM 690-0 PWRS.

[17] J. G. Kreifeldt, "An analysis of surface-detected EMG as an amplitude-modulated noise," presented at the 1989 Int. Conf. Medicine and Biological Engineering, Chicago, IL.

[18] J. Williams, "Narrow-band analyzer (Thesis or Dissertation style)," Ph.D. dissertation, Dept. Elect. Eng., Harvard Univ., Cambridge, MA, 1993.

[19] N. Kawasaki, "Parametric study of thermal and chemical nonequilibrium nozzle flow," M.S. thesis, Dept. Electron. Eng., Osaka Univ., Osaka, Japan, 1993.

[20] J. P. Wilkinson, "Nonlinear resonant circuit devices (Patent style)," U.S. Patent 3 624 12, July 16, 1990.

[21] IEEE Criteria for Class IE Electric Systems (Standards style)*,* IEEE Standard 308, 1969.

[22] Letter Symbols for Quantities, ANSI Standard Y10.5-1968.

[23] R. E. Haskell and C. T. Case, "Transient signal propagation in lossless isotropic plasmas (Report style)," USAF Cambridge Res. Lab., Cambridge, MA Rep. ARCRL-66-234 (II), 1994, vol. 2.

[24] E. E. Reber, R. L. Michell, and C. J. Carter, "Oxygen absorption in the Earth's atmosphere," Aerospace Corp., Los Angeles, CA, Tech. Rep. TR-0200 (420-46)-3, Nov. 1988.

[25] (Handbook style) *Transmission Systems for Communications,* 3rd ed., Western Electric Co., Winston-Salem, NC, 1985, pp. 44–60.

[26] *Motorola Semiconductor Data Manual,* Motorola Semiconductor Products Inc., Phoenix, AZ, 1989.

[27] (Basic Book/Monograph Online Sources) J. K. Author. (year, month, day). *Title* (edition) [Type of medium]. Volume (issue). Available: http://www.(URL)

[28] J. Jones. (1991, May 10). Networks (2nd ed.) [Online]. Available: http://www.atm.com

[29] (Journal Online Sources style) K. Author. (year, month). Title. *Journal* [Type of medium]. Volume(issue), paging if given. Available: http://www.(URL)

[30] R. J. Vidmar. (1992, August). On the use of atmospheric plasmas as electromagnetic reflectors. *IEEE Trans. Plasma Sci.* [Online]. *21(3).* pp. 876–880. Available: http://www.halcyon.com/pub/journals/21ps03-vidmar

Information for Authors

Editorial objectives

In the journal "Electronics", the scientific papers from different fields of electronics and electrical engineering in the broadest sense are published. Main topics are electronics, automatics, telecommunications, computer techniques, power engineering, nuclear and medical electronics, analysis and synthesis of electronic circuits and systems, new technologies and materials in electronics etc. The main emphasis of papers should be on methods and new techniques, or the application of existing techniques in a novel way.

The reviewing process

Each manuscript submitted is subjected to the following review procedures:

- It is reviewed by the editor for general suitability for this publication;
- If it is judged suitable, two reviewers are selected and a double-blind review process takes place;
- Based on the recommendations of the reviewers, the editor then decides whether the particular paper should be accepted as it is, revised or rejected.

Submissions Process

The manuscripts are to be submitted using the Electronics Journal online submission system – accessible from Journal's homepage.

Manuscripts have to be prepared in accordance with the instructions given in the template for paper preparation that can be found on the journal's web page (www.els-journal.etf.unibl.org).

Authors should note that proofs are not supplied prior to publication and ensure that the paper submitted is complete and in its final form.

Copyright

Articles submitted to the journal should be original contributions and should not be under consideration for any other publication at the same time. Authors submitting articles for publication warrant that the work is not an infringement of any existing copyright and will indemnify the publisher against any breach of such warranty. For ease of dissemination and to ensure proper policing of use, papers and contributions become the legal copyright of the publisher unless otherwise agreed.

ELECTRONICS, VOL. 22, NO. 1, JUNE 2018

ISSN 1450-5843
UDK 621.38